

THE PHOTORECEPTORS OF THE ATLANTIC DEEP SEA  
SCALLOP, PLACOPECTEN MAGELLANICUS (GMELIN  
1791) (BIVALVIA:PTEROCONCHIDA)

CENTRE FOR NEWFOUNDLAND STUDIES

TOTAL OF 10 PAGES ONLY  
MAY BE XEROXED

(Without Author's Permission)

CATHERINE VONNIE LORETTA POWELL, B.Sc., M.Sc.







The Photoreceptors Of The Atlantic Deep Sea Scallop,

Placopecten magellanicus (Gmelin 1791)

(Bivalvia:Pteroconchida)

BY

©Catherine Vonnie Loretta Powell, B.Sc., M.Sc.

A thesis submitted to the School of Graduate  
Studies in partial fulfillment of the  
requirements for the degree of  
Doctor of Philosophy

Department of Biology  
Memorial University of Newfoundland  
January 1990

St. John's

Newfoundland

"....the most beautiful feature of this animal (scallop)..is a row of minute circular points, of high refractive power, possessing all the brilliancy of precious stones. They look indeed like diamonds of the first water, each set in a ring or socket of black substance, which greatly enhances their beauty. They are about half as numerous again as the radiating grooves of the shell; but are not set with perfect regularity. They are still less uniform in size, some having a diameter twice as great as others. These are believed to be eyes, and they are well placed for enabling the animal to watch the world around it."

Philip Henry Gosse

(taken from Rees, 1957)

## ABSTRACT

The morphology and development of the pallial eyes and larval photoreceptors of the Atlantic Deep Sea Scallop, Placopecten magellanicus (Gmelin 1791) were investigated, for the first time, by the correlative techniques of light and electron microscopy.

The structure of the pallial eye in Placopecten magellanicus is similar to that of other scallops. Each eye is borne on an optic tentacle whose outer columnar epithelium is modified into a pigmented iris and transparent cornea. Beneath the cornea are located a cellular lens, a two-layered retina, a reflecting argentea and a pigmented tapetum. P. magellanicus eyes differ from those of other scallops in that the distal retina has fewer receptor cells than the proximal retina and a common optic nerve is not present. The absence of synapses within the retinae is confirmed and the three-dimensional structure of the photoreceptive cilia on the distal retinal receptor cells is elucidated. The presence of cilia and associated structures in the proximal retinal receptor cells is established and the implications of this are discussed.

The development of the pallial eye of Placopecten magellanicus is described. The presence of a papilla-like prospective optic tentacle containing the retinal anlage and

components of the tapetum and argentea is conventional.

However, the sequence of appearance of the optical components differs from that reported for other scallops.

Morphogenesis of the pallial eye of P. magellanicus proceeds from the collective differentiation of the tapetum, argentea and proximal retina to the formation of the distal retina, proximal optic nerve, iris, lens, distal optic nerve and cornea. Aspects of the formation of certain optical structures (ie. rhabdomeric microvilli, photoreceptive cilia, nerves) within the pallial eye are described and their relationship and significance to specific differentiation events is discussed. The mode of synthesis of the reflecting crystals in the developing argentea cells is described. Cells are added to the differentiating retinae from the peripheral anlage and mitosis does not occur in the retinae or in the differentiating lens. The possible role subserved by the short cilia and their extensive root systems in the differentiating proximal receptor cells is discussed in relation to existing theories. The mesodermal origin of prospective lens cells is confirmed and the presence of rudimentary cilia in prospective lens cells is established.

The fine structure of the photoreceptors in the pediveliger larvae of Placopecten magellanicus is described. Each ocellus consists of a single pigmented cell with long microvilli at the distal end forming a rhabdomere and a presumptive axon at the base, and non-pigmented cells which

bear at least 3 cilia, each with a  $9 \times 2+2$  axoneme pattern. The pigmented cell forms a cup that sheaths the photosensory organelles. A lens is absent. A ciliary component in the form of a basal body is located in the distal cytoplasm of the pigmented cell and its significance is discussed. Arguments that the pigmented cell is the photosensory cell are presented. Morphological comparisons are made between the photoreceptors in the scallop pediveliger and ocelli found in other invertebrates and protochordates. The possible function of the larval scallop's photoreceptors is discussed.

v  
ACKNOWLEDGEMENTS

I would like to express my sincere appreciation to all those who rendered invaluable assistance and gave generously of their time and talent during the course of this investigation.

Dr. Vernon C. Barber for his role as my PhD program supervisor, for his guidance and invaluable council, for critically editing the manuscript and whose preliminary work on bivalve photoreceptors laid the foundation for this research project. Dr. Pat Dabinett who acted as my thesis supervisor during the final months of my program and whose encouragement, humor and perserverance to the task at hand were unsurpassed. Dr. Dabinett and Dr. Fred Aldrich for acting on the supervisory committee, who read through drafts of the manuscript and offered useful criticisms and suggestions. I am grateful to them for sharing their expertise and experience.

I would like to acknowledge the several people who provided scallop specimens. These include Mr. Sundraj Naidu and Mr. Frank Cahill, Department of Fisheries and Oceans, St. John's, NF; Mr. Neil Farrel, Little Bay, NF; Mr. Cyr Couturier, Department of Biology, Dalhousie University, Halifax, NS; Marine Sciences Research Laboratory (MSRL) diving staff; Dr. P. Dabinett, Mrs. Barb Dooley and summer students of the MSRL pilot scallop hatchery.

My thanks are also due to Mr. Roy Ficken and Mr. Graham

Hillier for photographic services and to Dr. Eric Henry and Mrs. Carolyn Emerson whose scientific expertise and technical help during the course of this investigation proved invaluable.

To Dr. Don Deibel whose enthusiasm and fraternization constantly provided encouragement, countless thanks.

The text was typed by Miss B.A. Powell. Her skill at promptly converting the manuscript into well-laid out error-free sheets was a major factor in converting the final stages of this dissertation.

I would like to acknowledge the Director, Marine Sciences Research Laboratory and the Head, Department of Biology, Memorial University for use of facilities. Thanks are also due to Dr. I.A. Meinertzhagen, Dalhousie University, Halifax, NS, the Chief of Service, Saint John Regional Hospital, Saint John, NB, and the Department of Biology, University of New Brunswick, Fredericton, NB for facilities and space.

Financial support was mainly provided by a graduate scholarship and bursary from Memorial University, by funds from a Whitehall Foundation grant to V.C. Barber and by the Department of Biology, Memorial University.

I dedicate this work to my parents, Frank and Annabelle Powell, whose continued love, support and forbearance have made this and all of my other efforts possible, and, more importantly, worthwhile. To them I owe a debt of gratitude.

## TABLE OF CONTENTS

ABSTRACT	ii
ACKNOWLEDGEMENTS	v
LIST OF TABLES	ix
LIST OF FIGURES	x
LIST OF ABBREVIATIONS	xvii
1. INTRODUCTION	1
1.1. General	1
1.2. The Pallial Eye	3
1.2.1. History	3
1.2.2. Eye Structure	4
1.2.3. Behaviour and Electrophysiology	12
1.2.4. Function	15
1.2.5. Objectives	17
1.3. Eye Development	18
1.3.1. Objectives	22
1.4. The Larval Photoreceptors	23
1.4.1. Objectives	24
2. MATERIALS AND METHODS	25
2.1. Collection and Maintenance of Adult Scallops	25
2.2. Pallial Eye	28
2.3. Whole Tissues	29
2.4. Initial Preparation for Microscopy	29
2.5. LM and TEM of Pallial Eye	30
2.6. SEM of Pallial Eye	32
2.7. Collection and Maintenance of Scallop Larvae	33
2.8. TEM of Larval Photoreceptors	34
2.9. Morphological Analysis	34
2.10. Statistics	35
3. RESULTS	36
THE PALLIAL EYE	36
3.1. The Iris	44
3.2. The Cornea	50
3.3. The Lens	53
3.4. The Retina	55
3.4.1. The Distal Retina	56
3.4.2. The Proximal Retina	71
3.5. The Argentea	85
3.6. The Tapetum	88
4. DISCUSSION	94
THE PALLIAL EYE	94
5. RESULTS	107
PALLIAL EYE DEVELOPMENT	107
5.1. Formation of The Tapetum and Argentea	108
5.2. Formation of The Proximal Retina	114
5.3. Formation of The Distal Retina	131
5.4. Formation of The Iris	144
5.5. Formation of The Lens	146
5.6. Formation of The Cornea	159

6. DISCUSSION	163
PALLIAL EYE DEVELOPMENT	163
7. RESULTS	186
LARVAL PHOTORECEPTORS	186
8. DISCUSSION	199
LARVAL PHOTORECEPTORS	199
9. GENERAL CONCLUSIONS	211
10. BIBLIOGRAPHY	215
11. APPENDICES	248
APPENDIX A	248
11.1. Data: Scallop Characteristics	248
APPENDIX B	251
11.2. Statistical Data	251

## LIST OF TABLES

Table A-1:	Parameters recorded for individual scallops.	248
Table B-1:	Statistics for regressions of the total number of eyes against shell height.	251
Table B-2:	Statistics for t-test for paired observations for the differences in the number of eyes between the upper and lower mantle lobes.	251
Table B-3:	Statistics for t-test for the differences between the sex of the scallop and the total number of eyes.	251

## LIST OF FIGURES

## THE PALLIAL EYE

FIG. 1: Schematic diagram showing the position of the optic tentacle on the mantle edge.	5,6
FIG. 2: Schematic diagram of the anatomy of the pallial eye of <i>Pecten</i> .	8,9
FIG. 3: Map showing location of scallop collecting sites.	26,27
FIG. 4: Photograph of adult <i>Placopecten magellanicus</i> .	37,38
FIG. 5: Photograph of pallial eyes of <i>Placopecten magellanicus</i> projecting among tentacles.	37,38
FIG. 6A: Graph showing the relationship between size in shell height and the total number of eyes per scallop.	39,40
FIG. 6B: Graph showing the relationship between size in shell height and the number of eyes on the upper and lower mantle lobes.	39,40
FIG. 7: Color photograph of a pallial eye showing iridescence of the argentea.	42,43
FIG. 8: SEM of a pallial eye.	42,43
FIG. 9: LM longitudinal section of a pallial eye showing eye components.	42,43
FIG. 10: SEM of freeze-fractured pallial eye showing eye components.	42,43
FIG. 11: TEM oblique section of epithelial cells of eyestalk.	45,46
FIG. 12: SEM of eyestalk epithelium.	45,46
FIG. 13: TEM cross section of cilia from eyestalk epithelial cells.	45,46
FIG. 14: LM longitudinal section of the iris.	45,46
FIG. 15: High magnification LM longitudinal section of the iris.	45,46
FIG. 16: SEM of iris epithelium.	45,46
FIG. 17: Photograph of a pallial eye showing aberration in iris pigmentation.	48,49
FIG. 18: TEM longitudinal section showing pigmented and non-pigmented iris cells.	48,49
FIG. 19: TEM of apex of pigmented iris cells showing membrane-bounded inclusions containing granular material.	48,49
FIG. 20: TEM of apex of pigmented iris cells showing membrane-bounded inclusions containing flocculent material.	48,49
FIG. 21: TEM of apex of pigmented iris cells showing membrane-bounded pigment granules.	51,52
FIG. 22: SEM of iris epithelium showing mucous coat.	51,52
FIG. 23: SEM freeze-fractured iris epithelium.	51,52
FIG. 24: High magnification SEM of freeze-fractured iris cells.	51,52

FIG. 25: TEM longitudinal section of ciliated iris cells.	51,52
FIG. 26: TEM of non-pigmented iris cell cilia.	54,55
FIG. 27: LM longitudinal section of cornea epithelium.	54,55
FIG. 28: TEM longitudinal section of cornea cells.	54,55
FIG. 29: TEM of cornea cells showing elaborate interdigitations between adjacent cells.	54,55
FIG. 30: TEM longitudinal section of cornea cells showing vacuoles containing flocculent material.	54,55
FIG. 31: SEM of a pallial eye showing the cornea and iris.	54,55
FIG. 32: SEM of a ciliary bundle on the cornea.	57,58
FIG. 33: LM longitudinal section of a pallial eye showing the lens.	57,58
FIG. 34: LM of lens cells.	57,58
FIG. 35: TEM of lens cells.	57,58
FIG. 36: TEM of elongated lens cells.	57,58
FIG. 37: SEM of freeze-fractured lens cells.	57,58
FIG. 38: High magnification SEM of freeze-fractured lens cells.	60,61
FIG. 39: TEM showing the nucleus of a lens cell.	60,61
FIG. 40: SEM of freeze-fractured eye showing relationship between retinae, lens, argentea and tapetum.	60,61
FIG. 41: LM longitudinal section showing ciliary whorls of the distal retinal receptor cells.	60,61
FIG. 42: TEM oblique section of distal retinal receptor cells.	62,63
FIG. 43: TEM longitudinal section of distal retinal receptor cells.	62,63
FIG. 44: TEM tangential section showing distal retinal receptor cell cilia.	65,66
FIG. 45: TEM oblique section through the apical end of a distal retinal receptor cell.	65,66
FIG. 46: TEM tangential section of distal retinal receptor cell cilia showing basal feet.	65,66
FIG. 47: SEM of ciliary whorls.	65,66
FIG. 48: Schematic diagram of a distal retinal receptor cell cilium.	65,66
FIG. 49: TEM oblique section of distal retinal receptor cell cilia.	65,66
FIG. 50: TEM oblique section through the apical region of a distal retinal receptor cell.	69,70
FIG. 51: TEM longitudinal section of the base of a distal retinal receptor cell cilium.	69,70
FIG. 52: TEM cross section of distal retinal receptor cell cilia.	69,70
FIG. 53: TEM of distal retinal receptor cell mitochondria.	69,70
FIG. 54: TEM of intramitochondrial particles.	69,70
FIG. 55: TEM of ciliary whorls.	69,70

FIG. 56: LM longitudinal section of a pallial eye showing the distal optic nerve.	69,70
FIG. 57: SEM transverse section of freeze-fractured distal optic nerve.	72,73
FIG. 58: LM longitudinal section of a pallial eye showing separate proximal and distal optic nerves.	72,73
FIG. 59: TEM of axons in the distal optic nerve.	72,73
FIG. 60: TEM longitudinal section of rhabdomeric photoreceptive cells.	74,75
FIG. 61: Schematic diagram of a proximal retinal receptor cell.	77,78
FIG. 62: LM longitudinal section of a pallial eye showing the location of the proximal retina in relation to other eye components.	77,78
FIG. 63: TEM oblique section of the proximal retina showing proximal retinal receptor cells and supporting cells.	77,78
FIG. 64: TEM of rhabdomeric microvilli in straight arrays.	80,81
FIG. 65: TEM oblique section through rhabdomere showing cytoplasmic vesicles in microvilli.	80,81
FIG. 66: Oblique section through rhabdomeric microvilli.	80,81
FIG. 67: Tangential section of proximal retinal receptor cell cilia.	80,81
FIG. 68: Longitudinal section of a proximal retinal receptor cell cilium.	80,81
FIG. 69: TEM longitudinal section of the root system in a conical process of a proximal retinal receptor cell.	83,84
FIG. 70: Oblique section of a supporting cell.	83,84
FIG. 71: TEM of an axon of a proximal retinal receptor cell.	83,84
FIG. 72: TEM oblique section through the edge of the retina showing axons of proximal retinal receptor cells.	83,84
FIG. 73: SEM transverse section of freeze-fractured proximal optic nerve.	86,87
FIG. 74: LM transverse section of the proximal optic nerve.	86,87
FIG. 75: TEM transverse section of the proximal optic nerve.	86,87
FIG. 76: LM longitudinal section of a pallial eye showing the proximal optic nerve.	86,87
FIG. 77: TEM of axons in the proximal optic nerve.	86,87
FIG. 78: TEM of a glial cell in the proximal optic nerve.	86,87
FIG. 79: TEM of a synaptic-like profile between axons in the proximal optic nerve.	89,90
FIG. 80: TEM of a synaptic-like profile between axons in the proximal optic nerve.	89,90

FIG. 81:	SEM of freeze-fractured argentea showing layers of crystals.	89,90
FIG. 82:	TEM oblique section of the argentea showing layers of crystals.	89,90
FIG. 83:	SEM of the distal surface of the argentea.	89,90
FIG. 84:	SEM of freeze-fractured pallial eye showing the tapetum and argentea.	89,90
FIG. 85:	TEM oblique section of pigment-containing cells at the edge of the tapetum.	91,92
FIG. 86:	TEM oblique section of tapetal cells located near the optic axis of the eye.	91,92
 PALLIAL EYE DEVELOPMENT		
FIG. 87:	LM longitudinal section through a papilla-like prospective optic tentacle.	110,111
FIG. 88:	High magnification LM longitudinal section of a papilla-like prospective optic tentacle.	110,111
FIG. 89:	TEM of tapetum cells.	110,111
FIG. 90:	High magnification TEM of tapetum pigment granules.	110,111
FIG. 91:	TEM of membranous lamellae.	110,111
FIG. 92:	TEM of a fibrillary inclusion in a tapetum cell nucleus.	110,111
FIG. 93:	TEM of a circular body in a differentiating argentea cell.	115,116
FIG. 94:	TEM of a circular body showing a system of internal membranes.	115,116
FIG. 95:	TEM showing layers of oblong compartments in a differentiating argentea cell.	115,116
FIG. 96:	TEM showing oblong compartments aligned in rows.	115,116
FIG. 97:	TEM of an argentea cell at an intermediate stage of differentiation.	115,116
FIG. 98:	TEM of pigment granules containing crystals.	115,116
FIG. 99:	TEM of a differentiating argentea.	115,116
FIG. 100:	TEM of cells in the retinal anlage.	118,119
FIG. 101:	TEM of an early differentiating proximal retinal receptor cell.	118,119
FIG. 102:	TEM transverse section c° inclusion-bodies in a prospective proximal retinal receptor cell.	118,119
FIG. 103:	TEM oblique section showing a basal body in a differentiating proximal retinal receptor cell.	118,119
FIG. 104:	TEM longitudinal section of a prospective proximal retinal receptor cell showing the appearance of the apical conical process.	120,121
FIG. 105:	TEM longitudinal section through the distal end of a differentiating proximal	120,121

retinal receptor cell.	
FIG. 106: TEM transverse section through the distal end of a differentiating proximal retinal receptor cell.	120, 121
FIG. 107: TEM transverse section through a differentiating apical conical process.	120, 121
FIG. 108: TEM transverse section through a differentiating apical conical process.	123, 124
FIG. 109: TEM transverse section through a differentiating apical conical process.	123, 124
FIG. 110: TEM of a cilium at the apex of an apical conical process.	123, 124
FIG. 111: TEM of a group of cilia on the apical conical process.	123, 124
FIG. 112: TEM of cilia showing bifurcating, striated roots.	123, 124
FIG. 113: TEM longitudinal section of a proximal retinal receptor cell at a late stage of differentiation.	125, 126
FIG. 114: TEM of the proximal end of an apical conical process showing a complex array of microvilli.	128, 129
FIG. 115: TEM tangential section of an apical conical process at a late stage of development.	128, 129
FIG. 116: TEM tangential section through axons of proximal retinal receptor cells.	128, 129
FIG. 117: TEM oblique section through the proximal optic nerve.	128, 129
FIG. 118: LM oblique section through a papilla-like prospective optic tentacle.	133, 134
FIG. 119: TEM oblique section through the differentiating retina.	133, 134
FIG. 120: TEM longitudinal section of a young distal retinal receptor cell showing centriolar elements.	133, 134
FIG. 121: TEM of a young distal retinal receptor cell showing fiber-like structures at the base of the basal body.	133, 134
FIG. 122: TEM of a vesicle located over the basal body.	133, 134
FIG. 123: TEM showing an expanded vesicle above the basal body.	133, 134
FIG. 124: TEM showing basal body microtubules extending into the vesicle.	133, 134
FIG. 125: TEM of a ciliary bud.	133, 134
FIG. 126: TEM showing a ciliary shaft beneath the vesicle.	133, 134
FIG. 127: TEM showing a rudimentary cilium.	133, 134
FIG. 128: TEM longitudinal section of a prospective distal retinal receptor cell.	137, 138
FIG. 129: TEM of whorls of cilia.	137, 138

FIG. 130: TEM oblique section through the apical region of a developing distal retinal receptor cell at the time of lens formation.	137, 138
FIG. 131: TEM oblique section showing cilia at different stages of formation.	137, 138
FIG. 132: TEM longitudinal section through a developing distal retinal receptor cell showing a newly formed axon.	139, 140
FIG. 133: TEM showing axons from several distal retinal receptor cells joining to form the distal optic nerve.	139, 140
FIG. 134: TEM oblique section showing the prospective distal optic nerve at the edge of the retinae.	139, 140
FIG. 135: TEM transverse section of the young nerve bundle.	142, 143
FIG. 136: TEM longitudinal section of the prospective distal optic nerve.	142, 143
FIG. 137: TEM longitudinal section of the prospective distal optic nerve entering the mantle.	142, 143
FIG. 138: TEM longitudinal section of a supporting cell below the distal retinal receptor cells.	142, 143
FIG. 139: TEM longitudinal section showing undifferentiated epithelium of iris.	147, 148
FIG. 140: TEM oblique section of stages of pigment formation in a prospective iris cell.	147, 148
FIG. 141: TEM oblique section of an iris cell at an intermediate stage of differentiation.	147, 148
FIG. 142: TEM oblique section showing pigment granules in prospective iris cells.	147, 148
FIG. 143: TEM oblique section of iris epithelium.	147, 148
FIG. 144: Composite; TEM longitudinal sections of differentiating pallial eye.	149, 150
FIG. 145: TEM of developing lens.	152, 153
FIG. 146: TEM oblique section of a lens precursor cell.	152, 153
FIG. 147: TEM oblique section showing a cilium of a lens precursor cell.	152, 153
FIG. 148: TEM oblique section showing a cilium of a lens precursor cell.	155, 156
FIG. 149: TEM longitudinal section showing fibrous material in an intermediate-type lens cell.	155, 156
FIG. 150: TEM showing distended cisternae of RER.	155, 156
FIG. 151: TEM showing consolidated particulate material liberated from RER cisternae.	155, 156
FIG. 152: TEM showing dispersed granular material.	155, 156
FIG. 153: TEM of an intermediate lens cell at a late stage of differentiation.	155, 156

FIG. 154: TEM oblique section of an intermediate lens cell at a late stage of development.	157, 158
FIG. 155: TEM longitudinal section of a lens cell.	157, 158
FIG. 156: TEM oblique section of a cornea precursor cell.	161, 162
FIG. 157: TEM oblique section of cornea epithelium.	161, 162
 LARVAL PHOTORECEPTORS	
FIG. 158: Schematic diagram of a pediveliger larva of <i>Placoplecten magellanicus</i> .	187, 188
FIG. 159: Photograph of a fixed veliger larva of <i>Placoplecten magellanicus</i> .	187, 188
FIG. 160: Schematic diagram of the larval photoreceptor of <i>Placoplecten magellanicus</i> .	187, 188
FIG. 161: TEM oblique section of the larval ocellus showing the U-shaped pigment cup.	190, 191
FIG. 162: TEM of pigment granules.	190, 191
FIG. 163: TEM normal section of microvilli in the ocellar cavity.	190, 191
FIG. 164: TEM cross section of pigmented cell microvilli.	190, 191
FIG. 165: TEM cross section of pigmented cell microvilli extending beyond the ocellar cavity.	190, 191
FIG. 166: High magnification TEM of pigmented cell microvilli in cross section.	190, 191
FIG. 167: TEM oblique section of the apical region of a pigmented cell and ocellar cavity.	193, 194
FIG. 168: TEM of the nucleus of a pigmented cell.	193, 194
FIG. 169: TEM oblique section of a multilamellar body and microvilli of a non-pigmented cell.	193, 194
FIG. 170: TEM cross section of a presumptive axon of a pigmented cell.	193, 194
FIG. 171: TEM of the cerebral ganglion and cerebral-pleural-visceral commissure.	193, 194
FIG. 172: TEM of a larval photoreceptor.	193, 194
FIG. 173: TEM oblique section of a non-pigmented cell projecting into the ocellar cavity.	196, 197
FIG. 174: TEM cross section of basal bodies in a non-pigmented cell.	196, 197
FIG. 175: TEM cross section showing a cilium of a non-pigmented cell in the ocellar cavity.	196, 197
FIG. 176: TEM oblique section showing cilia of a non-pigmented cell in the ocellar cavity.	196, 197
FIG. 177: TEM of a cilium of a non-pigmented cell.	196, 197
FIG. 178: TEM of the cerebral ganglion.	196, 197

xvii  
LIST OF ABBREVIATIONS

a,A	argentea
aa	anterior adductor muscle
acp	apical conical process
ax	axon
bb	basal body
bf	basal foot
bl	basal lamina
bpon	branch of proximal optic nerve
c	cilia
cb	ciliary bud
CG	cerebral ganglion
co	cornea
cp	clear process
CPVC	cerebral-pleural-visceral commissure
cr	ciliary root
cs	circumciliary space
cz	cortical-like zone
d	desmosome
db	dense body
don	distal optic nerve
dr	distal retina
DRC	distal retinal receptor cell
e	eye
es	extracellular space
f	foot

fi	fibrillary inclusion
G	Golgi
g	gill
gc	gill cavity
gl	glial cell
glp	glial cell process
i	iris
ilc	intermediate lens cell
l,L	lens
lc	lens cell
LM	light microscopy/microscope/micrograph
lpc	lens precursor cell
lt	long tentacle
m	mitochondria
ma	mantle
mc	mucous coat
mf	microfilaments
mlb	multilamellar body
mt	microtubules
mv	microvilli
mvb	multivesicular body
mz	medullar zone
N	nucleus
nf	neurofilaments
NPC	non-pigmented cell
nt	neurotubules
o	ocelli

oc	ocellar cavity
on	optic nerve
OT	optic tentacle
pa	posterior adductor muscle
pb	peripheral band
PC	pigmented cell
pdon	prospective distal optic nerve
PDRC	prospective distal retinal receptor cell
PG	pigment granule
PG	pedal ganglion
pon	proximal optic nerve
POT	prospective optic tentacle
pr	proximal retina
PRC	proximal retinal receptor cell
r	retina
RA	retinal anlage
RER	rough endoplasmic reticulum
rh	rhabdom
sc	sheath cell
scp	supporting cell process
SEM	scanning electron microscopy/microscope/

micrograph

SER	smooth endoplasmic reticulum
SF	shell fold
SPC	supporting cell
st	short tentacle
sy	synapse

xx

t	tapetum
TEM	transmission electron microscopy/microscope/ micrograph
tf	tonofilaments
v	vesicles
V	vacuole
ve	velum
VF	velar fold
VG	visceral ganglion
wc	whorl of cilia
za	zonula adhaerens
zo	zonula occludens

## CHAPTER ONE

## INTRODUCTION

## 1.1.

## General

This study is concerned primarily with the structure of the photoreceptive organs of the Atlantic Deepsea Scallop, Placopecten magellanicus (Gmelin 1791). Techniques of light and electron microscopy were employed to examine the gross anatomy, morphology and ultrastructure of the visual organs. The investigation is presented in three parts. The aim of the research in the first part was to describe the structure of the pallial eye of adult P. magellanicus in order to complement existing data on bivalve visual organs. Emphasis is given to the interrelationship of features of the photoreceptive apparatus and their implications for existing studies of behaviour, electrophysiology and function. For comparison, eyes of other species of scallops are discussed.

The objective of the second part of this study was to augment previous studies by documenting the development of the eye. The literature on the development of the pallial eye is sparse and restricted to light microscopical observations. Descriptions are principally concerned with

the order of appearance of eye structures and with the origin and patterns of development.

The third part of this study involves a documentation of the morphology of the photoreceptors (termed ocelli) of pediveliger larvae in order to secure a better understanding of the function of these visual organs during the early life of the scallop. The observations on their structure are compared with findings in larvae in other invertebrate phyla.

## 1.2.

## The Pallial Eye

## 1.2.1. History

Photoreception is phylogenetically very old (Autrum 1979). As a result of past selection pressure, there has been a wide variety of adaptations by animals for intercepting light energy and securing information about the environment. It is therefore not surprising to find that organs of vision are among the most specialized receptors known in invertebrates.

The reduction of the head in the Bivalvia has been accompanied by a great decrease in the occurrence of cephalic eyes (Messenger 1981), although mantle or 'pallial' eyes do occur.

The scallops alone of the Bivalvia possess numerous highly developed single lens eyes along the mantle edge. Poli (1795), working on Ostrea (Pecten) jacobaeus, was the first to mention the eyes and name some external structures associated with these organs, but it was another forty years before Garner (1837) suggested that their principal function was vision. Classical investigations on the anatomy of the pallial eyes are those by Krohn (1840), Hensen (1865), Hickson (1880, 1882), Sharp (1884), Carrière (1885, 1889), Patten (1886, 1887), Rawitz (1888), Schreiner (1896), Hesse

(1900, 1902, 1908, 1916), Hyde (1903), Drew (1906), Dakin (1910a,b, 1928) and Küpfer (1916). Collectively, these pioneer researchers provided such explicit details on eye morphology that the bulk of their observations remain of great value to this day.

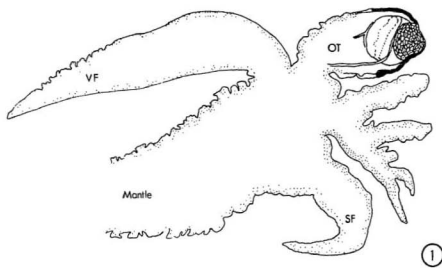
Most anatomical studies have been carried out on eyes of one genus of scallop--Pecten. The eye is supported by a short stalk, the optic tentacle, which is borne on the middle fold of the mantle margin (Fig. 1). The number of eyes varies with age (Drew 1906) and with species.

Typically, there are more eyes on the upper mantle lobe than on the lower (Carrière 1885; Patten 1886, 1887; Rawitz 1888; Schreiner 1896; Dakin 1910a,b; Butcher 1930; Gutsell 1930; White 1937; Wilkens 1981) and the eyes vary in size within a single individual. White (1937) noted a regular arrangement of large and small eyes around the mantle margin. However, Patten (1886) and Rawitz (1888) reported that the eyes on the lower lobe of Pecten jacobaeus are much smaller than those of the upper lobe.

#### 1.2.2. Eye Structure

Many of the early workers recognized a similarity between the pallial eye of the scallop and the eye of vertebrates. This resemblance led scientists to consider the eye of scallops deserving of the term 'Wirbelthieraugen' (Semper 1877; Hickson 1880) and to apply names as assigned

FIG. 1 Schematic diagram illustrating position of optic tentacle (OT) on mantle edge of the scallop (redrawn from Drew 1906). SF, shell fold; VF, velar fold.



to vertebrate structural features.

Thus, the scallop eye (Fig. 2) is described as consisting of seven major structures: cornea, iris, lens, two-layered retina, optic nerve, argentea (reflecting mirror), and pigmented tapetum.

The surface layer of the eyestalk consists of columnar epithelium in direct continuation with the mantle epithelium and is modified into a cornea and an iris. The cornea lies at the summit of the optic tentacle and is transparent. The iris, as it was termed by Patten (1886), is, with one exception, highly pigmented. The iris circumscribes the cornea and extends down the optic tentacle where the pigmented cells gradually increase in height (Dakin 1910b). Schreiner (1896) reported that Pecten abyssorum possessed no pigment in the iris cells.

The lens lies immediately beneath the cornea. It is composed of many transparent cells of irregular shape. The shape of the lens was the subject of much dispute. Krohn (1840) and Keferstein (1863) believed it to be spherical, Hickson (1880) considered it to be elliptical, Hensen (1865), Sharp (1884), and Dakin (1910b) described it as being biconvex with the proximal surface having greater curvature, and Butcher (1930) reported the lens as being oval. More recently, Land (1965) suggested that the lens was in the shape of a Cartesian oval.

The lens is mucoid and non-refractile, and its focal point lies far behind the eye (Land 1964, 1968). Therefore,

FIG. 2 Schematic diagram illustrating anatomy of the pallial eye of Pecten (redrawn from Dakin 1910b).  
a, argentea; co, cornea; dr, distal retina;  
i, iris; l, lens; on, optic nerve; pr, proximal  
retina; t, tapetum.



the lens does not focus an image on the retinae.

The complex retina is separated into two layers, the distal retina and the proximal retina, each containing approximately 5000 receptor cells (Land 1968, 1978, 1984). The photoreceptive cells of the distal retina are of the ciliary type (ie. the photosensitive membranes are formed from modified cilia; Eakin 1963, 1965). Hesse (1900) and Dakin (1910a) noted cilium-like appendages arising from photoreceptive cells of the distal retina and Hesse (1908) proposed a photoreceptive function for them. The cilia extend towards the lens as either whorls of lamellae derived from the ciliary membrane (Miller 1958, 1960), or as straight flattened sacs (Barber *et al.* 1967). The cilia, as many as 100 per cell, have a 9x2+0 arrangement of microtubule doublets (Barber *et al.* 1967). Microvilli are also present along the distal edge of the receptor cells (Barber *et al.* 1967).

Photoreceptor cells of the proximal retina are of the rhabdometric type (ie. the photosensitive membranes are formed from microvilli; Eakin 1963, 1965), characterized by irregular arrays of microvilli extending from the proximal end of the cell body (Miller 1960; Bell 1966; Barber *et al.* 1967). Cilia, 1 or 2 per cell (Barber *et al.* 1967), are also present. A system of striated roots extending from the cilia of the proximal retinal receptor cells has been described for Pecten irradians (Miller 1960), but is absent in Pecten maximus (Barber *et al.* 1967).

The two retinae of the Pecten eye are inverted (Dakin 1910), ie. nerves enter the distal end of the cells, so light must pass through the axons before reaching the photoreceptive organelles. Axons of the distal retinal receptor cells arise adjacent to the cilia, extend distally, and pass laterally along the inner surface of the lens to form the distal branch of the optic nerve (Barber et al. 1967). Axons of the proximal retinal receptor cells arise from the opposite end of the cell relative to the receptor organelles, and pass to the sides of the retina to form the proximal branch of the optic nerve. The two branches join at the back of the eye to form the common optic nerve which subsequently connects with the circum pallial nerve and then with the pallial nerves (Sharp 1884; Dakin 1910a,b; Wilkens 1981). In turn the pallial nerves pass to the parietovisceral ganglion (Dakin 1910a; Wilkens 1981; Spagnolia & Wilkens 1983).

The argentea, first noted by Krohn (1840) and named by Patten (1886), lies below the retina. This highly reflecting layer, which is accurately spherical (Land 1965), is thickest at the optic axis of the eye and becomes thin in the peripheral regions (Dakin 1910b). The mirror consists of 30-40 layers (Barber et al. 1967) of  $1 \mu\text{m}^2$  guanine crystals separated by cytoplasm (Land 1965, 1966a,b, 1972) and acts as a 1/4 wavelength reflector, producing the iridescence of the eye (Land 1966b).

The pallia's eyes of scallops are the only kind known

among the Mollusca which form an image by reflection from the argentea. Patten (1887) concluded that the lens formed the image and the argentea reflected it back to the retina. Land (1965, 1966a,b) demonstrated that the argentea functions as an interference reflector, and that it both reflects and focuses an image onto the cilia of the distal retinal receptor cells. The lens is thought to function solely to provide correction for spherical aberration (Land 1968).

Located directly beneath the argentea is the pigmented tapetum. Hickson (1880) thought it was a fluid layer with no cellular elements. More recently, it has been demonstrated that the pigmented tapetum consists of a single layer of cells (Barber et al. 1967), or sometimes two layers (Schreiner 1896; Dakin 1910b), containing red pigment granules (Hickson 1882; Sharp 1884; Dahlgren & Kepner 1928).

#### 1.2.3. Behaviour and Electrophysiology

Aristotle, almost 2500 years ago first noted the vigorous shadow reaction of the scallop (Curtis 1966). Since then, it has been demonstrated many times that a scallop reacts to a shadow cast on the eyes by closing its valves (Rawitz 1888; Drew 1906; Dakin 1910a,b, 1928; von Uexküll 1912; Wenrich 1916; Gutsell 1930; Hartline 1938; von Buddenbrock & Möller-Racke 1953; Land 1966a). Although Rawitz (1888) and Dakin (1910a) found that several eyes must

be affected by a shadow to initiate a reaction, Wenrich (1916) found that a decrease in light intensity on only two eyes was sufficient to cause a response.

Other visual behaviours known to exist in scallops include escape reactions mediated by the perception of movement (Drew 1906; von Uexküll 1912; Wenrich 1916; Gutsell 1930; Land 1966a, 1968, 1978) and orientation postures occurring as a result of sensitivity to contrast (von Buddenbrock & Moller-Racke 1953; Land 1966a, 1968; Spagnolia & Wilkens 1983). Such behaviour is due, in great part, to the number and location of eyes around the mantle edge (Messenger 1981).

In Pecten, the receptor function of the eyes has been well documented. Electrophysiological studies have shown that the photoreceptive cells of the two retinae respond independently to light. Axons of photoreceptive cells in the distal retina produce a discharge of impulses to the cessation of light (ie. 'off' responses) (Bell 1966; Land 1966a,b; Toyoda & Shapley 1967), whereas those of the proximal retina respond to the onset of illumination (ie. 'on' responses) (Bell 1966; Toyoda & Shapley 1967; Land 1968; Gorman & McReynolds 1969, 1978; McReynolds & Gorman 1970a,b).

Hartline (1938) demonstrated that the 'off' and 'on' responses from single fibers in the distal and proximal branches of the optic nerve of Pecten irradians resulted from hyperpolarizing and depolarizing potentials,

respectively. Land (1966a), studying Pecten maximus, confirmed Hartline's findings. Toyoda & Shapley (1967) and McReynolds & Gorman (1970a,b) made intracellular recordings in the scallop retina and showed that the ciliary type photoreceptors responded to a cessation of illumination and the rhabdometric type photoreceptors responded during illumination. In both types of cells, the response was an increase in plasma membrane conductance or permeability (Toyoda & Shapley 1967; McReynolds & Gorman 1970b; Gorman & McReynolds 1978).

In the proximal retinal receptor cells, the increase in conductance results in a  $\text{Na}^+$  influx (McReynolds & Gorman 1974). Hyperpolarization in the distal retinal receptor cells is associated with a  $\text{K}^+$  efflux (Gorman & McReynolds 1974, 1978; McReynolds & Gorman 1974; Gorman & Cornwall 1976). Calcium ions are also involved in distal retinal receptor cell hyperpolarization (Gorman & McReynolds 1974, 1978; Cornwall & Gorman 1979).

Hartline (1938) believed that the photoreceptive cells of the distal retina might be second order neurons and that the 'off' responses occurred as a result of synaptic inhibition mediated by the proximal retinal receptor cells. The question of whether primary inhibition exists has been placed in doubt by subsequent researchers. Miller (1958) concluded from morphological investigation that the ciliary type photoreceptors were primary sense cells. Other morphological studies have shown that axons of the

photoreceptive cells of each layer give rise to a separate branch of the optic nerve without synapsing (Land 1966a; Barber *et al.* 1967). Moreover, Thrum (1969) and McReynolds & Gorman (1970a) reported evidence that the hyperpolarizations of the distal retinal receptor cells were not synaptic potentials produced via the nerve impulses of the proximal cells. Each receptor layer also lacks ocular interneurons and lateral interaction between cells of the same layer (see Laverack 1968).

It has been proposed that optic fibers from the scallop pallial eye terminate in the paired lateral lobes of the parietovisceral ganglion (Dakin 1910a,b; Bullock & Horridge 1965; Wilkens 1981). Wilkens & Ache (1977) recorded electrical responses in the pallial nerve and the lateral lobe of the parietovisceral ganglion in Pecten ziczac. Exclusively 'on' responses were obtained from the ganglion at the onset of illumination, but both 'on' and 'off' responses were obtained from the nerve. Spagnolia & Wilkens (1979) suggested that the glomerular and subcellular neuropil areas of the lateral lobe were associated with photoreceptor axons projecting from the mantle eyes. This was later confirmed by light microscope autoradiography (Wilkens & Spagnolia 1979; Spagnolia & Wilkens 1983).

#### 1.2.4. Function

A number of different functions have been ascribed to

the eye of the scallop. Hickson (1880) argued that the eye is of little value in prey avoidance on the grounds that it is unlikely that the eye can receive a focused image. He suggested instead, that the eyes are used to monitor changes in light intensity, which allow the scallop to avoid being stranded by the ebbing tide. Butcher (1930) agreed with this latter statement. Sharp (1884) discounted Hickson's theory on eye function but agreed with Henson (1865) that the cells of the iris detect changes in light intensity. Further, Sharp (1884) concurs with Schmidt's (1882) hypothesis that the 'so-called eyes' function as phosphorescent organs. Dakin (1910b) found no evidence to uphold the belief that the eyes of Pecten emit light and he, too, doubted the efficacy of the eye in receiving a focused image (Dakin 1928). Patten's (1886) theory that scallop eyes are 'haliophags' designed for the reception of light energy to be utilized for metabolic purposes, met with a storm of criticism (Anonymous 1886; Dakin 1910b) and was short-lived.

The extensive behavioural experiments performed on Pecten by Wenrich (1916) produced evidence showing that the eye is capable of forming an image. Detailed optical, behavioural and electrophysiological studies by Land (1965, 1966a) showed that the eye of Pecten is able to form an image of reasonable quality. The large number of photoreceptive cells in the distal retina, with their abilities to resolve an image from the argentea and to react

to dimming of light, are responsible for the detection of movement (Land 1966a, 1978, 1984). Among other things this is vitally important in the avoidance of predators. Furthermore, the distal retinal receptor cells also possess the capacity for detecting the position and the direction of movement (Land 1966a, 1978). Land (1978) provided electrophysiological evidence suggesting that photoreceptive cells of the proximal retina are responsible for phototoxic behavior. Further, he believes that the receptor cells of the proximal retina function in monitoring environmental light intensity (Land 1978), and that they may act as directional light intensity sensors (Land 1984).

#### 1.2.5. Objectives

The literature on scallop eyes, from an optical, physiological and behavioural standpoint, is extensive. It is, therefore, surprising that although the structure of the scallop eye has been widely investigated at the light microscope level, only one complete study (that of Barber et al. 1967) has been made of its fine structure. A thorough knowledge of the morphology of the eye is a prerequisite in order to obtain information critical to our understanding of the physiology and behavioural events. The initial objective of this study is to document the structure of the pallial eye of Placopecten magellanicus in order to complement existing studies on the comparative anatomy of

bivalve pallial eyes and to compare the structural characteristics with those of other molluscs.

## 1.3.

## Eye Development

Few studies have been made of the development of the pallial eyes in molluscs. Patten (1886, 1887) made reference to eye formation in Pecten opercularis, but his description was superficial and incomplete. The most definitive account was that of Kämpfer (1916) whose descriptions on eye development in Pecten testae laid the foundation for present understanding of the organogenesis of the eye. Very few changes have been made to the literature on eye development since that time, although Butcher (1930) noted certain differences in his studies of the development and regeneration of the eye of Pecten gibbus borealis. No work has since been published on the formation of pallial eyes in bivalve molluscs.

Patten (1886) and Rawitz (1888) reported that no new eyes develop once a scallop obtains a size of 2 cm. However, the observation that large scallops bear more eyes than small individuals of the same species (Dakin 1910b; Butcher 1930) implies that new eyes appear throughout the life history (Dakin 1910b; Kämpfer 1916). Butcher (1930) indicated that the number of eyes in large individuals remains constant.

It is generally agreed that the eyes begin to form at the base of the ophthalmic fold (Patten 1886, 1887; Dakin 1910b; K  pfer 1916; Butcher 1930). The eye first appears as an oval thickening (Patten 1886), or downgrowth (Butcher 1930), which invaginates from the surface epithelium (Dakin 1910b; Butcher 1930), pinches free and forms a closed 'optic vesicle' (Patten 1887, Dakin 1910b; Butcher 1930). K  pfer (1916) saw no sign of invagination, but described the appearance of an 'eye papilla' derived from the mantle epithelium and connective tissue.

Cell proliferation at the area of the optic vesicle which lies farthest from the shell (K  pfer 1916) (=furthest from the light (Butcher 1930)) results in the appearance of several layers. Patten (1886) and Butcher (1930) agree that the more central of these become the visual cells (=proximal retina) while the more distally peripheral layer forms the ganglionic cells (=distal retina).

Little is known about the formation and organization of the photoreceptive apparatus. K  pfer (1916) published data suggesting that the anlage of the retina arises through migrations of the ectodermal cells from the surface epithelium. Within the anlage, the distal ciliary photoreceptors differentiate first, the proximal rhabdomeric ones later (K  pfer 1916). Cells from the annular edges of the retinal anlage are added to the developing distal retina (K  pfer 1916). The proximal retina is believed to form from an accumulation of cells contributed from the anlage lying

on either side of the developing distal retina.

It is still uncertain if the rhabdomeric photoreceptors are produced by migration from the anlage followed by proliferation in situ or by proliferation within the anlage followed by displacement from it (I.A. Meinertzhagen, personal communication). The proximal retinal receptor cells are initially aligned orthogonally to the radius of the eye (Küpfer 1916), gradually pushing more centrally towards the optic axis of the eye (Patten 1887; Küpfer 1916). Although the origin of the supporting cells is unclear, they are first apparent in the distal retina and eventually spread by cell division to the proximal retina (Küpfer 1916).

Meanwhile, the argentea and pigmented tapetum develop from a single layer of cells above the wall of the optic vesicle next to the shell (Patten 1887; Dakin 1910b) (=closest to the light; Butcher 1930). These structures are derived from cells that migrated from the connective tissue, and are thus mesodermal in origin (Küpfer 1916). Initially, the pigmented tapetum contains colorless granules (Patten 1887; Butcher 1930). As the eye develops, the cells acquire a red or brown pigment (Patten 1887; Dakin 1910b; Butcher 1930) and become irregular in shape (Dakin 1910b).

The formation of the argentea has been the subject of much confusion. Patten (1887) believed that the argentea was formed by the transformation of cells into superimposed plated membranes. The cells originally contain nuclei, but

as development progresses, the nuclei decrease in size and eventually disappear. Dakin (1910b) thought that the argentea was formed either by the underlying pigment containing cells, or by other cells which eventually disappear. Butcher (1930) reported that the argentea was derived from cells of the innermost part of the pigmented tapetum. Nothing is known about the mode of formation of the argentea.

When formation of the retina has commenced, a cellular anlage condenses adjacent to it, both from cells which have migrated from the connective tissue (Patten 1886, 1887; Küpfer 1916; Butcher 1930) and from mitosis *in situ* (Küpfer 1916). This aggregation of mesodermal cells gives rise to the lens. Küpfer (1916) produced evidence showing that the cortex of the lens remains embryonic. New cells are added at the junction of the lens and the cornea until late in development. These findings merit closer examination.

As the eye reaches maturity, the cornea and iris are differentiated. The cornea is formed by the loss of pigmentation in the cells of the epithelium above the lens. The epithelial cells lying adjacent to the edges of the lens become highly pigmented and form the iris (Butcher 1930).

During development the eye pushes out on a stalk, and rotates so that there is a shift in the optic axis from an orientation in parallel with the mantle edge, to a position perpendicular to it (Küpfer 1916; Butcher 1930). This rotation occurs after the nerves have grown out from the

retinae (Butcher 1930) to form the branches of the optic nerve. This gradual shift in the optic axis accounts for the separation of the distal from the proximal optic nerve (Patten 1887; K  pfer 1916).

Butcher's (1930) elaborate regeneration experiments on the eye of Pecten gibbus borealis provided evidence that the eyes were self-differentiating and could regenerate, under his experimental conditions, in about 40 days. Furthermore, the nervous system has little effect on the ability of an eye to develop or regenerate. Butcher (1930) believed that the epithelium of the ophthalmic groove possessed the potential to form eyes and that the ability was evenly distributed. He also advocated that the potential for initiating eye development was gradually lost with age.

#### 1.3.1. Objectives

There is much to be learned about the interactions leading to the formation of these remarkable eyes. The complexity of eye development is apparent, but clearly more information is needed. It is appropriate to make a comparative study of the development of the pallial eye to augment existing data, to clarify the developmental process this unique visual organ undergoes, to determine if there is a consistent developmental pattern for the eyes of scallops, and also to relate these findings, where appropriate, to the functioning of the fully formed eye.

## 1.4.

## The Larval Photoreceptors

The structure of the larval eyespot in bivalve molluscs is virtually unknown. Light microscopic studies include Erdmann (1935), Cole (1938), and Hickman & Gruffydd (1971) with Ostrea edulis, Prytherch (1934) with Ostrea virginica, and Hodgson & Burke (1988) with Chlamys hastata. The only ultrastructural investigation is a scanning electron microscope study by Waller (1981) describing the external features of the ocelli of O. edulis. Ultrastructural data on the internal morphology of larval bivalve photoreceptors are non-existent.

The photoreceptors (=ocelli) are paired structures innervated by the cerebral ganglion. Generally each eyespot is positioned at the center of the valve, immediately below the shell and consists of a U-shaped pigment cup surrounding a primitive lens. Hickman & Gruffydd (1971) reported that ocelli of Ostrea edulis consisted of several pigmented cells surrounding a lens. Hodgson & Burke (1988) noted that the ocelli of the spiny scallop Chlamys hastata were comprised of two cells, one cup-shaped pigmented cell and a second unpigmented cell located within the lumen of the cup. Direct evidence of the type of photoreceptive cells contained in these ocelli is unavailable.

The appearance of the larval eyespot varies

considerably in different bivalves, ranging in scallops, from 23 or 24 days (Culliney 1974; Hodgson & Burke 1988) to 36 days (Gruffydd & Beaumont 1972). Hickmann & Gruffydd (1971) presented evidence showing that the eyespots in O. edulis are retained for as long as six days after metamorphosis, but they are less prominent than in 48-hour old spat.

#### 1.4.1. Objectives

This section of the study describes the morphology of the ocellus of larval Placopecten magellanicus to complement existing light microscope studies on larval bivalve photoreceptors, and to compare its structure with findings in other invertebrate phyla.

## CHAPTER TWO

## MATERIALS AND METHODS

## 2.1. Collection and Maintenance of Adult Scallops

Adult male and female Placopecten magellanicus, 2 to 8 years old, were obtained from shellfish aquaculture farms at Little Bay (Burin Peninsula) and Spencer's Cove (Merasheen Island) in Placentia Bay, Newfoundland, Canada (Fig. 3) during the spring and summer of 1982 to 1984. Additional specimens were collected by SCUBA divers in depths of less than 15 meters from Colinet, St. Mary's Bay and from Sunnyside, Trinity Bay (Fig. 3). All scallops were transported the same day by truck, in polyethylene tanks containing seawater cooled with sea ice, and subsequently held at the Marine Sciences Research Laboratory (MSRL) of Memorial University of Newfoundland at Logy Bay (Fig. 3). The scallops were maintained in shallow wet-benches supplied with a continuous flow of unfiltered seawater at ambient ocean temperature and salinity.

FIG. 3 A map of southeastern Newfoundland, Canada showing location of collecting sites; 1. Little Bay ( $47^{\circ}10' N$ ,  $55^{\circ}09' W$ ) 2. Spencers Cove ( $46^{\circ}39' N$ ,  $54^{\circ}05' W$ ) 3. Colinet ( $47^{\circ}10' N$ ,  $53^{\circ}36' W$ ) 4. Sunnyside ( $47^{\circ}51' N$ ,  $53^{\circ}55' W$ ). Asterisk marks the location of Logy Bay.



## 2.2. Pallial Eye

All samples of eyes were obtained in the following manner: shell valves were wedged apart and held open with a cork bung (allowing full view of the centrally located posterior adductor muscle); the muscle was then cut with a scalpel at its attachment to the inner surface of the upper (left) valve, the upper valve was removed and its height and length measured to the nearest 0.5 mm; the sex of each scallop was recorded; the upper and lower lobes of the mantle were separated from each other and a strip, approximately 1 cm in width, was dissected along the entire margin of each mantle lobe, extending from the anterior side near the ears of the valves, around the periphery of the mantle lobe to the posterior side.

The tissue was placed in a shallow petri dish of chilled seawater and examined at 25X magnification using a dissecting microscope equipped with a transparent glass base plate. Light, provided by a 6V incandescent lamp, was reflected by a mirror located beneath the glass base plate. The number of eyes borne on each mantle lobe was counted. Individual eyes were removed by carefully dissecting a small portion of the middle mantle fold bearing the optic tentacle. Eyes were excised from a number of different positions on the mantle edge.

### 2.3. Whole Tissues

Entire mantle lobes were dissected from living scallops, placed in petri dishes of chilled seawater, and examined with bright and dark field with a Wild M420 stereomicroscope equipped with a Schott swan-neck fiber optic light source and a Wild MPS51 35mm film magazine. Photomicrographs were obtained with a Wild Photoautomat MPS55 and recorded on Kodak Plus-X (125 ASA) print film and Kodak Ektachrome (200 ASA) slide film.

### 2.4. Initial Preparation for Microscopy

All eyes to be examined by microscopy were processed within 48 h of the time of animal collection. Eyes excised from scallops were immersed immediately in ice-cold 2% glutaraldehyde (Sabatini *et al.* 1963), pH 7.2, buffered with 0.1M Sorensen's phosphate buffer for 2-3 h. After initial fixation, eyes were rinsed in three changes of Sorensen's phosphate buffer for 15 min each and osmicated (for 1 h) on ice in 1% osmium tetroxide buffered with 0.1M Sorensen's phosphate buffer (Dawes 1971). The rinse time was kept to a minimum as a precaution against the possible reversal of the glutaraldehyde fixation (Hayat 1981; Ockleford 1975). The osmolarity of the fixatives and rinse solutions was adjusted to 1100 mOsm/kg by addition of sucrose (Maser *et al.* 1967).

After postfixation, at room temperature, the eyes were

transferred directly to 30% ethanol and dehydrated in an ascending ethanol series (10 min per 10% step) (Hayat 1981).

#### 2.5. LM and TEM of Pallial Eye

After fixation, eyes were infiltrated at room temperature with a 1:3 mixture by volume of hard-formula Spurr's resin (Spurr 1969) and 100% ethanol for 1/2 h, then with equal volumes of resin:absolute ethanol for 1/2 h, and finally with 100% Spurr's resin. The hard-formula Spurr's resin gave good results as minimal separation occurred between the resin and the lens and argentea of the eye. The solution containing the eyes was continuously agitated throughout infiltration, then polymerized (for 12 h at 70° C) in flat embedding molds to permit proper orientation.

Thick and ultrathin sections were obtained on an LKB Ultrotome III ultramicrotome. Contact cement, diluted with an equal volume of toluene (Henry 1977), was applied to the top and bottom sides of specimen blocks to enhance ribboning of sections. Semithin (1-2  $\mu\text{m}$ ) serial sections were cut with glass knives. Drops of distilled water were placed on the angle of the glass knife to provide a meniscus on which the sections could float. During sectioning, ribbons (10-15 sections long) were collected and transferred to a rectangular glass cover slip (22 X 70 mm) coated with distilled water. An eyelash mounted on an applicator stick was used to manipulate the ribbons. The ribbons were then

floated onto glass slides and aligned in series. Sections were dried over a spirit lamp to expand and secure the ribbons to the glass and were routinely stained with 0.5% toluidine blue in 1% borax (Richardson *et al.* 1960). Some material was stained with 1% methylene blue-2% basic fuchsin (Aparicio & Marsden 1969) to permit the localization of nerve tissue. The sectioned material was examined either with a Zeiss Photomicroscope II or with a Zeiss Axiomat Photomicroscope, each provided with a 60W tungsten light source. Kodak Wratten Filters (#22, orange + #48, green) were used to increase contrast. Light micrographs were obtained on Kodak Pan-X (32 ASA) film and Ilford Pan-F (50 ASA) film.

Ultrathin sections (gold to gray in color) were obtained using a diamond knife. Sections were picked up on uncoated 300 mesh and 400 mesh copper grids, stained with 0.22  $\mu\text{m}$  Millipore-filtered saturated aqueous uranyl acetate (Watson 1958) for 5 min, washed with filtered glass-distilled water and then counter-stained for 2 min with 0.22  $\mu\text{m}$  Millipore-filtered 0.5% lead citrate (Venable & Coggeshall 1965). The sections were viewed using a Zeiss EM9A or a Zeiss EM109 transmission electron microscope (accelerating voltages of 60kV and 50kV, respectively).

Transmission electron micrographs were obtained with Kodak Pan-X Professional Film FXP 120, Ilford Pan-F 120 Film and Kodak Electron Image Plate Film 4489.

## 2.6. SEM of Pallial Eye

Eyes were cryofractured and critical point dried for correlative examination by scanning electron microscopy.

This technique was chosen over freeze drying for tissue preparation in light of reports on the better quality of preservation of the ultrastructure of intracellular structures and surface structures by critical point drying (Nordestgaard & Rostgaard 1985). For critical point drying, tissue samples were carried through three changes of absolute ethanol for a total time of 1 h and then passed through a graded series of ethanol:Freon 113 from 15% to 90% Freon 113 (in 10% steps) for 15 min each, followed by three changes of Freon 113 for 20 min each. The eyes were then critical point dried from Freon 13 (Cohen et al. 1968) in a Bomar SPA-900/EX Critical Point Drying apparatus.

For cryofracturing, fixed, ethanol infiltrated (Humphreys et al. 1977) material was immersed in liquid nitrogen. The frozen tissue was then fractured in liquid nitrogen using a liquid N<sub>2</sub> pre-cooled razor blade, the fractured pieces were returned to absolute ethanol and processed for critical point drying.

All tissues were mounted on aluminum stubs with either silver paint or Scotch Copper Conductive Tape, surrounded with silver conducting paint to reduce charging, and sputter coated with gold for 2 1/2 to 3 min in an Edwards Vacuum Coating Unit S150A vacuum evaporator. To avoid the effects

of shrinkage during storage (c.f. Nordestgaard & Rostgaard 1985), most samples were viewed within 24 h either with a Cambridge Stereoscan Mark 2A scanning electron microscope operating at an accelerating voltage of 10kV, or with a Hitachi S-570 scanning electron microscope operating at an accelerating voltage of 20kV. Exposures were made on Polaroid Positive/Negative 665 Film. In addition, specimens shown in Figures 47, 83 and 84 were examined in a Cambridge S4-10 scanning electron microscope.

## 2.7. Collection and Maintenance of Scallop Larvae

Umbo veligers of Placopecten magellanicus were obtained from laboratory stock cultures at MSRL (in 1982 and 1984) and from the Department of Biology, Dalhousie University, Halifax, Nova Scotia, Canada (1984). The larvae were reared by standard aquaculture techniques (Loosanoff & Davis 1963). Those cultured at the MSRL were fed a diet of Isochrysis sp. (Tahitian strain). Details of techniques for spawning and rearing to early veliger larvae at the MSRL are outlined by Manning (1986). The larvae obtained from Dalhousie University were provided with a diet consisting of 1/3 each of: Chaetoceros gracilis, Chaetoceros calcitrans, Isochrysis sp. (Tahitian strain). Larvae were fixed for microscopical examination at 40 and 90 days of age.

## 2.8. TEM of Larval Photoreceptors

Unless otherwise indicated in the figure captions, the larval eye material for TEM was prepared in the manner described for the pallial eye. In addition, some larvae were prepared by the following techniques.

Larvae were postfixed 1 h in 1% osmium tetroxide containing 2.5% potassium ferricyanide ( $K_3Fe(CN)_6$ ) (Langford & Coggeshall 1980), rinsed (10 min) in buffer, or rinsed in 2 changes of distilled water (10 min each), and en bloc stained in aqueous uranyl acetate for 2 h prior to dehydration.

Larvae were infiltrated and embedded in hard-grade LR White (London Resin Co.) at 60°C.

All larvae were embedded in 'Hemi-Hyperboloid' tip BEEM capsules to ensure concentration of larvae in one area of the block. Blocks prepared in this way were then trimmed and embedded a second time in standard BEEM capsules (Size 00). Gray to gold sections were cut serially with a diamond knife and the ribbons mounted in known orientation on Butvar (J.B.EM Services Inc.) and carbon coated 1 mm single-slot copper grids. Staining procedures were the same as those outlined for the pallial eye.

## 2.9. Morphological Analysis

Diagrammatic representations of scallop eyes were

prepared by tracing enlargements of light micrographs to obtain the proper cell proportion and location. All drawings were supplemented with observations made with the SEM and/or TEM. Illustrations of the various photoreceptive cells were prepared by tracing TEM micrographs.

#### 2.10. Statistics

The number of eyes on the upper and lower mantle lobes, the sex, and the shell height and width were recorded for each scallop (Appendix A). The relationship of number of eyes to shell height was investigated using linear regression (General Linear Model procedure of the Statistical Analysis System (SAS Institute Inc.)). Differences in number of eyes between the upper and lower lobe, and between sexes were investigated by the appropriate t-tests procedure.

## CHAPTER THREE

RESULTS  
THE PALLIAL EYE

The giant scallop is shown in its natural posture in Figure 4. The eyes appear as a row of dark spots distributed nearly regularly on the mantle beneath the shell valves. The margin of each mantle lobe of Placopecten magellanicus consists of three folds. The eyes (Fig. 5), located on the middle of these folds, protrude among the long and short tentacles towards the light.

The major findings from statistical analysis performed on data collected from 105 scallops are summarized in Tables B1-B3 (Appendix B).

The total number of eyes per scallop increases with shell height (Fig. 6A) (Regression:  $r^2=0.43$ ). Furthermore, the number of eyes varies between the two mantle lobes ( $P<0.001$ ). The graph represented in Figure 6B illustrates that the upper mantle lobe bears more eyes for virtually all sizes of scallop than the lower lobe.

Results obtained from the t-test indicate that male and female scallops show no significant difference in the total number of eyes ( $P>0.1$ ).

Figure 7 is a photograph showing an eye nestled among the sensory tentacles. The optic tentacle consists of a

FIG. 4 Photograph of adult Placopecten magellanicus. Exposed mantle periphery shows eyes (e), long (lt) and short (st) tentacles and velum (ve).

FIG. 5 Photograph of eyes (e) projecting among tentacles at mantle edge. st, short tentacles; ve, velum.

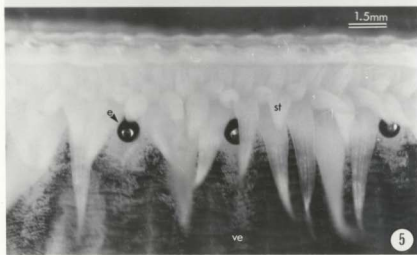
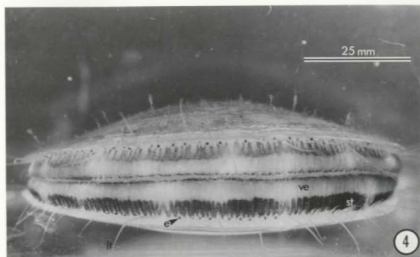
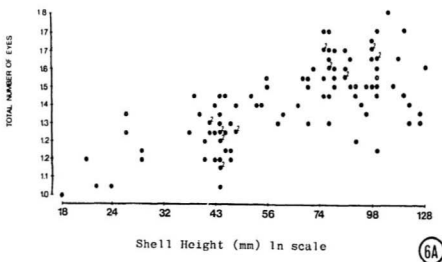
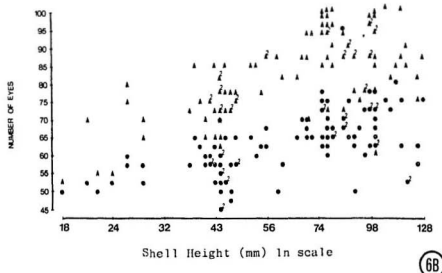


FIG. 6A Plot of total number of eyes per scallop  
against shell height (Y axis x 100).

FIG. 6B Plot of number of eyes on the upper ( $\Delta$ )  
and lower ( $\bullet$ ) mantle lobe per scallop  
against shell height.



(6A)



(6B)

short cylindrical stalk arising from the mantle surface. A black ring, termed the iris, and a transparent cornea are located at the distal end of the stalk. The silver iridescence seen through the cornea is produced by light reflected from the mirror, or argentea, lining the back of the eye. In the living animal the cornea protrudes well above the iris. However, the cornea consistently lies below the rim of the iris (Fig. 8) in eyes prepared for SEM indicating that shrinkage artifact occurs during the critical point drying process. This has been shown in many other specimens (Boyde 1978).

The general appearance of the eye in LM section and in freeze-fracture SEM is shown in Figure 9 and Figure 10, respectively. The columnar epithelium of the optic tentacle, which is modified into the pigmented iris and the cornea, is a direct continuation of the mantle epithelium. The lens, retina, reflecting argentea and pigmented tapetum lie within the optic tentacle.

The epithelium lining the proximal part of the optic tentacle (ie. that which extends from the mantle surface to the iris) is highly folded in the majority of microscopical preparations. This demonstrates that the contraction of the eye upon excision from the mantle is maintained after subsequent fixation.

Cells of the epithelium located at the base of the optic tentacle bear microvilli at their distal surface (Fig. 11). Cilia, as many as 70 per cell, arise from several of

FIG. 7 Whole mount of a pallial eye viewed with a stereomicroscope. The iridescence of the argentea is visible through the transparent cornea. X100

FIG. 8 SEM of pallial eye. co, cornea; i, iris. X210

FIG. 9 LM longitudinal section (2 $\mu$ m thickness) of pallial eye composed of cornea (co), iris (i), lens (l), retina (r), argentea (a) and tapetum (t). Argentea displays a fixation artifact. X110

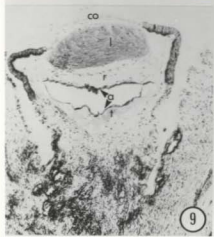
FIG. 10 SEM of a freeze-fractured pallial eye showing the organization of various components. a, argentea; co, cornea; i, iris; l, lens; r, retina; t, tapetum. X90



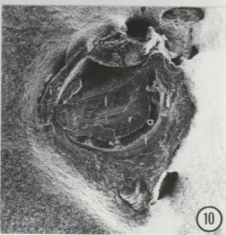
7



8



9



10

the cells (Figs. 11 & 12). The ciliary shaft is straight and unbranching (Fig. 12), and contains an axoneme composed of  $9 \times 2+2$  microtubule doublets (Fig. 13). The striated roots are long and bifurcate. A short basal foot projects from the basal body. Mitochondria are most numerous between the ciliary roots. The nucleus of the cell is located basally. The supranuclear portion of the cell contains large Golgi complexes, small secretory vesicles and free ribosomes. Residual bodies, multilamellar bodies and membrane-bound vesicles of various sizes and electron densities are abundant in the distal cytoplasm suggesting that an active process of degradation is occurring. Zonula occludens, zonula adhaerens and macula adhaerens, generally of the septate variety, lie between the lateral plasma membranes of adjacent cells.

## 3.1.

## The Iris

The iris extends down the eyestalk to a level adjacent to the argentea (Figs. 9 & 14). Figure 15 illustrates a longitudinal section through the columnar epithelial cells of the iris. The cells are tall and thin and gradually increase in height toward the apex of the optical tentacle. The shape of the iris cells appears polygonal in surface view (Fig. 16). The iris of some eyes in Placopecten magellanicus extends a shorter distance down the eyestalk on the shell side of the tentacle than on the velum side

- FIG. 11 TEM of an oblique section showing epithelial cells of eyestalk. The cells bear cilia (c) and microvilli (mv) at their apices. cr, ciliary root; G, golgi; N, nucleus. X5700
- FIG. 12 SEM of eyestalk epithelium showing cilia. X1100
- FIG. 13 TEM of a near cross section of cilia from eyestalk epithelial cells. Cilia have a 9x2+2 axoneme pattern. X21,000
- FIG. 14 LM longitudinal section (1.5 $\mu\text{m}$  thickness) of iris (i). The pigmented cells increase in height towards the cornea (co). X210
- FIG. 15 Higher magnification of the iris shown in Fig. 14 illustrating darkly stained pigment. X2700
- FIG. 16 SEM of iris epithelium showing polygonal outline of cells. X1200

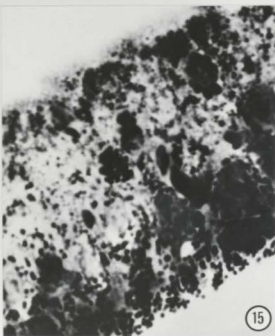
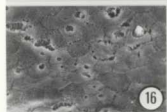
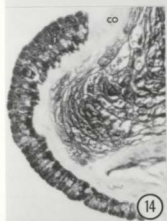
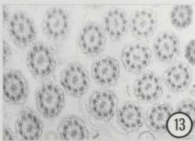
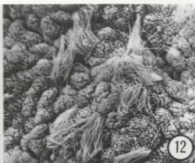
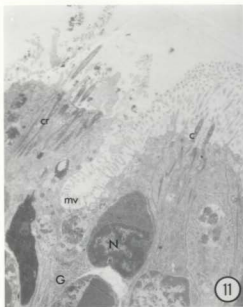


(Fig. 17). This observation is in agreement with reports for Pecten jacobaeus and Pecten opercularis (Patten 1887).

The color of the iris is derived from many pigment granules dispersed throughout the cells (Figs. 15 & 18). The pigment granules are typically round, membrane-bounded and densely packed. They extend from the distal-most area of the cell to the basement membrane. Many granules are not uniformly dense. Often an electron-lucent space surrounds the pigment granule. Numerous membrane-bounded inclusions containing material in transition from granular (Fig. 19) to flocculent material (Fig. 20) and electron-dense material (Fig. 21) are located among the pigment granules. Also, a single membrane may surround more than one granule (Fig. 18). These observations suggest that the pigment granules are constantly being formed, possibly by condensation and coalescence, within the iris cells.

Cells of the iris bear a border of microvilli, measuring approximately  $2.60\mu\text{m}$  in height and  $0.10\mu\text{m}$  in diameter, along their apical surface. The microvilli arise singly from the surface of the cell. Many microvilli branch into two near their base (Fig. 18). A mucous coat covers the optic tentacle supported by the tips of the microvilli (Figs. 18 & 19). In surface view (Fig. 22) the mucous coat appears as a thin variolate sheet.

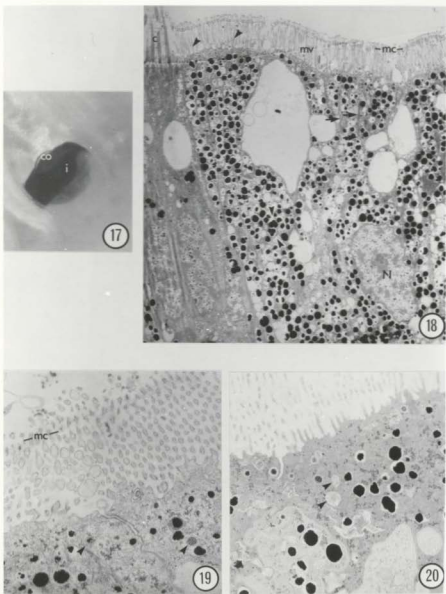
Golgi complexes (Fig. 21) are numerous between the pigment granules. Rough and smooth ER are plentiful but generally restricted to the perinuclear area. Other

FIG. 17 Whole mount of a pallial eye viewed with a stereomicroscope. The pigmentation extends further down one side (left) than the other (right). co, cornea; i, iris. X60

FIG. 18 TEM of longitudinal section showing pigmented iris cells bearing microvilli (mv), some of which branch (small arrowheads), and non-pigmented iris cells bearing cilia (c). Pigment granules are surrounded by an electron-lucent space and a membrane may bound more than one granule (large arrowheads). Arrows show microtubules within the pigmented cell. mc, mucous coat; N, nucleus. X4100

FIG. 19 Apex of pigmented iris cell showing membrane-bounded inclusions containing granular material (arrowheads). mc, mucous coat. X12,100

FIG. 20 Apex of pigmented iris cell showing membrane-bounded inclusions containing flocculent material (arrowheads). X11,300



cytoplasmic organelles include large vacuoles, coated vesicles and multilamellar bodies. Microtubules extend along the long axis of the cell (Fig. 18).

An SEM of a fractured iris is shown in Figure 23. The nuclei are positioned basally and vacuoles of varying sizes are distributed throughout the cells. This figure and a higher magnification view (Fig. 24) support TEM observations that pigment granules are numerous, densely packed and fill the entire cell.

Interspersed among the pigment cells are ciliated cells (Figs. 18 & 25). These cells possess noticeably less pigment than their neighbours and bear cilia. The cilia are located between the microvilli and have a 9x2+2 configuration of microtubule doublets. The ciliary roots are slender and striated. A shallow circumciliary space encloses the base of the ciliary shaft (Fig. 26). Intercellular contact between the ciliated iris cells and the pigmented cells is made by zonula occludens, zonula adhaerens and long septate junctions.

### 3.2.

### The Cornea

Light micrographs of the cornea are shown in Figures 9 and 27. The transparent cells are unpigmented and columnar in shape. The dense oval nucleus is generally located in the basal part of the cell.

Cells of the cornea bear a brush border of microvilli

- FIG. 21 Apex of pigmented iris cell showing membrane-bounded electron-dense pigment granules (arrowheads). Golgi complexes (G) are abundant. mlb, multilamellar body. X10,700
- FIG. 22 SEM of iris epithelium showing appearance of mucous coat. X2000
- FIG. 23 SEM of a freeze-fractured iris. Note the position of the nuclei (N) and the abundance of vacuoles. X1800
- FIG. 24 Higher magnification of iris shown in Fig. 23. Arrows indicate pigment granules. X5100
- FIG. 25 TEM of a longitudinal section of a ciliated iris cell. Note the absence of pigment granules. c, cilia; cr, ciliary root; mv, microvilli. X9800
- FIG. 26 TEM of a longitudinal section of iris cells showing cilia with basal bodies, striated roots (cr) and shallow circumciliary space (arrowhead). X15,300

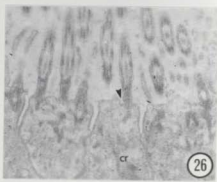
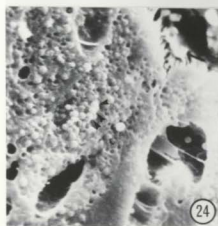
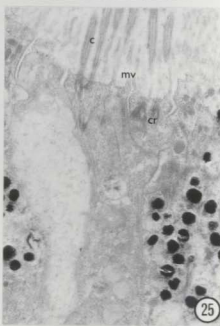
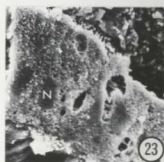
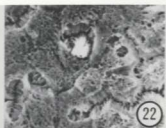
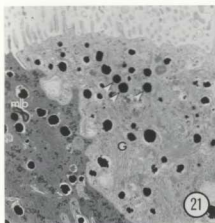


(Fig. 28), approximately  $2.8\mu\text{m}$  in height and  $0.10\mu\text{m}$  in diameter, upon which lies a coat of mucus. The cells situated along the margin of the cornea are short and interdigitate extensively with their neighbours (Fig. 29). The cells are bound to one another by zonula adhaerens and septate junctions. Vesicles of various sizes and densities are abundant in the distal portion of the cell. Smooth ER and vacuoles containing flocculent material (Fig. 30) or membranous material (Figs. 29 & 30) are widespread. Mitochondria are numerous.

For the most part, the cornea is devoid of ciliated cells (Fig. 31). However, small clusters of cilia may occur infrequently at the periphery of the cornea (Fig. 32). It was not possible to obtain TEM or LM sections of the ciliated corneal cells due to their scarcity.

### 3.3.

### The Lens

The lens lies immediately beneath the cornea (Fig. 9) and rests on a basal lamina. The entire structure has the shape of a Cartesian oval (Fig. 33). The lens is composed of many cells of varying shape and adjacent cells differ in electron density (Figs. 34 & 35). At the periphery of the lens, the cells are elongate and thin (Figs. 33 & 36). Rounded cells characterize the core. Large dense inclusions are abundant in all cells of the lens. In LM section, the inclusions appear circular (Fig. 34). Figures 35 and 36

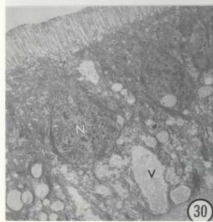
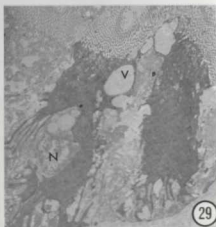
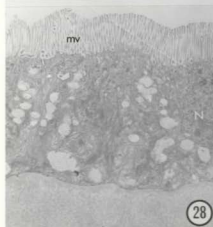
FIG. 27 LM longitudinal section (2 $\mu$ m thickness) of cornea epithelium. N, nucleus. X2700

FIG. 28 TEM longitudinal section of cornea cells. Note the abundance of vacuoles. mv, microvilli; N, nucleus. X3700

FIG. 29 TEM longitudinal section of cornea cells located at edge of cornea. Note extensive interdigitation of adjacent cells. N, nucleus; V, vacuole. X4000

FIG. 30 Vacuoles (V) of cornea cells contain flocculent or membranous material. N, nucleus. X3800

FIG. 31 SEM of pallial eye showing cornea (co) encircled by iris (i). X190



show inclusions of irregular shape. Inclusions are not bounded by a membrane and are distributed randomly throughout the cell.

The margins of each lens cell are demarcated by a moderately electron-dense band of homogeneous material of variable thickness. The nature of the material comprising this band is consistent with that composing the inclusions (Fig. 35). These elements are shown in freeze-fractured tissue in Figure 37. The fractured surface of the inclusions and cell periphery appear smooth compared to the textured nature of the cytoplasm (Fig. 38). It is interesting to note that the material of the peripheral band may be continuous with the matrix of the inclusions (Figs. 35 & 38).

Although each cell of the lens contains a nucleus (Figs. 34 & 39) other major cellular organelles were not observed.

### 3.4.

### The Retina

The eye of Placopecten magellanicus has a two-layered retina termed the distal and proximal retinae. The relationship between the retinae, the overlying lens and the argentea is shown in Figures 9, 10, 33 and 40.

#### 3.4.1. The Distal Retina

The distal retina is formed of a single layer of

FIG. 32 SEM of cornea showing ciliary bundle. X3200

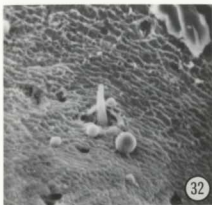
FIG. 33 LM longitudinal section ( $1.5\mu\text{m}$  thickness) of pallial eye showing profile of the lens (1) sectioned near the optic axis. a, argentea; co, cornea; i, iris; r, retina; t, tapetum. X140

FIG. 34 LM of lens cells. Inclusions (arrowheads) are numerous. N, nucleus. X1400

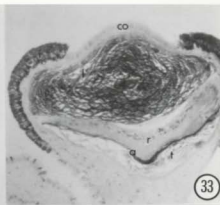
FIG. 35 TEM showing lens cells of different electron densities. Inclusion bodies (arrowheads) are irregular in shape. pb, peripheral band. X4100

FIG. 36 TEM of elongated peripheral lens cells. X2500

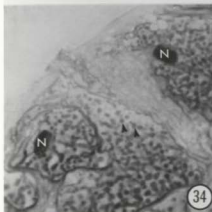
FIG. 37 SEM of a portion of freeze-fractured lens showing inclusion bodies (arrowheads) and the smooth-textured peripheral band surrounding each cell. X1800



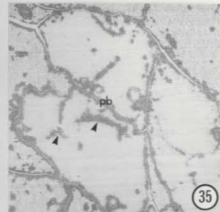
32



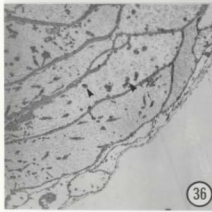
33



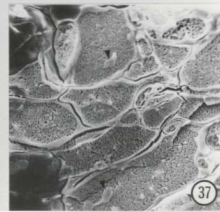
34



35



36



37

unipolar cells bearing photoreceptoral organelles of the ciliary type (terminology of Eakin 1963) (Fig. 42). These cells form a radial arrangement about the optic axis and occupy approximately one third of the diameter of the convex surface of the retina (Fig. 41).

The ciliated cells at the edges of the distal retina are smaller than the cells at the optic axis and the former bear fewer cilia. Axially located distal retinal receptor cells measure about  $9.3\mu\text{m}$  in width at the level of the nucleus, which lies at the center of the cell (Fig. 43), and  $16\mu\text{m}$  in height, excluding the ciliary projections.

Interstitial supporting cells located in the proximal retina interpose the distal retina by sending long thin processes between the distal retinal receptor cells (Fig. 43). The supporting cell processes are characterized by very dense cytoplasm containing mitochondria, Golgi cisternae and numerous electron-dense granules. Junctional connections join the apices of the receptor cells to the supporting cell processes.

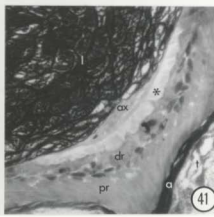
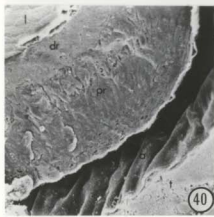
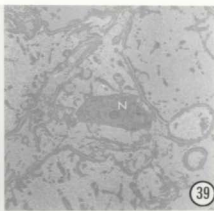
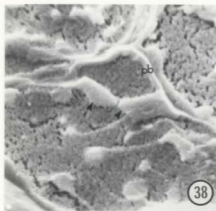
The distal surface of each receptor cell bears cilia and a sparse supply of microvilli which project into the extracellular space beneath the lens. The cilia are closely assembled (Fig. 44) and as many as 110 cilia have been counted in individual thin sections through distal retinal receptor cells. The cilia are associated with a basal body from which thin microfiber-like structures extend (Fig. 45). Typical roots were not observed. Basal feet project from

FIG. 38 SEM of freeze-fractured lens showing details of peripheral band (pb) and inclusion body (arrowhead). X5500

FIG. 39 TEM showing nucleus (N) of lens cell. X2500

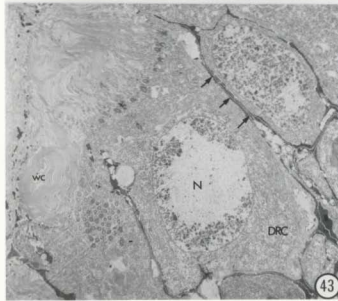
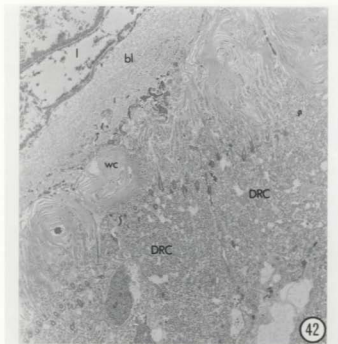
FIG. 40 SEM of a portion of longitudinally split freeze-fractured eye showing the relationship between the distal (dr) and proximal (pr) retinae to the lens (l) and argentea (a). t, tapetum. X500

FIG. 41 LM longitudinal section (1.5 $\mu$ m thickness) showing ciliary whorls (asterisk) of distal retina (dr). a, argentea; ax, axon; l, lens; pr, proximal retina; t, tapetum. X450



**FIG. 42** TEM oblique section of photoreceptive cells of distal retina. Cilia are numerous and coil into whorls (wc) beneath the basal lamina (bl). DRC, distal retinal receptor cell; l, lens. X5000

**FIG. 43** TEM longitudinal section of distal retinal receptor cell (DRC) showing a centrally positioned nucleus (N) and cilia either coiled into whorls (wc) or arranged in loose lamellar arrays. Electron-dense processes (arrows) of supporting cells extend between adjacent receptor cells. X5000



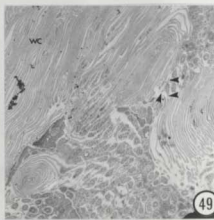
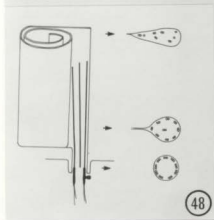
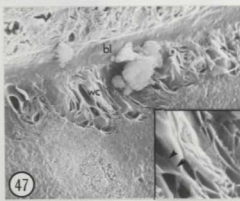
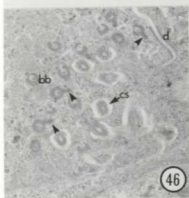
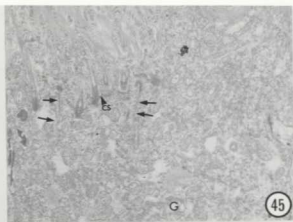
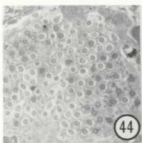
the basal body. The basal feet in one cell do not all point in the same direction (Figs. 44 & 46).

The ciliary shaft is modified along its length to form a flattened sheet. The SEM of a freeze-fractured distal retinal receptor cell in Figure 47 shows the sheet-like nature of the ciliary shaft. The flattened sheet-like shaft coils about itself parallel to the axoneme. The diagram in Figure 48 illustrates this arrangement. More rarely, the shaft is flattened into 2 or more sheets extending from the axoneme (Fig. 49) or it may coil as a single sheet about the axoneme.

The base of each cilium is surrounded by a circumciliary space (Figs. 45 & 46). More than one cilium may be recessed in the same space (Fig. 50). The cilia are long and in cross section are typically coiled into whorls extending almost to the lens (Figs. 42 & 43). Not all the cilia from one cell are incorporated into a whorl. A number of cilia extend in loose lamellar arrays towards the lens (Fig. 43). In some cases the latter arrangement represents longitudinal sections through the ciliary sheet. The cilia from one distal retinal receptor cell may form more than one whorl, but cilia from adjacent cells do not intermix.

The microtubules of the cilium show a 9x2+0 pattern close to the centriole and their cores are electron-lucent (Fig. 51). Sometimes axonemes containing 8 microtubule doublets arranged circumferentially around a central doublet are seen (Fig. 52). The axonemal configuration varies as

- FIG. 44 TEM tangential section through the distal tip of a distal retinal receptor cell showing arrangement of cilia. X6300
- FIG. 45 TEM oblique section through the distal tip of a distal retinal receptor cell. A circumciliary space (cs) surrounds each cilium and thin microfiber-like structures (arrows) extend proximally from the basal body. Mitochondria are numerous. G, golgi. X9400
- FIG. 46 TEM tangential section. The basal feet (arrowheads) do not all point in the same direction. Desmosomes (d) are evident between adjacent cells. bb, basal body; cs, circumciliary space. X13,300
- FIG. 47 SEM of ciliary whorls (wc) in the distal retina of a longitudinally freeze-fractured eye. bl, basal lamina. X3500. Inset shows ciliary shaft flattened into a sheet (arrowheads). X9500
- FIG. 48 Schematic diagram of a distal retinal receptor cell cilium illustrating axoneme pattern along the length of the ciliary shaft.
- FIG. 49 TEM oblique section of distal retinal receptor cell cilia. Occasionally ciliary shaft is flattened into two or more sheets (arrowheads) extending from the axoneme. X8700



the microtubules splay outwards from the cilium's base (Fig. 51) making the axoneme arrangement appear disordered in the distal aspect of the shaft. The disordered arrangement of microtubules is evident in Figure 50. The microtubules in the distal axoneme are frequently seen as singlets and contain an electron-dense core.

Adjacent distal retinal receptor cells do not interdigitate. Zonula occludens join the apical edges of adjacent receptor cells and zonula adhaerens bind the cells laterally.

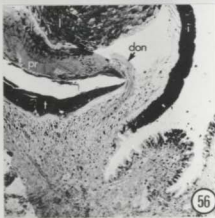
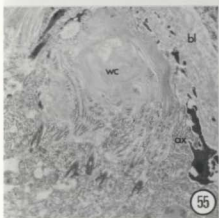
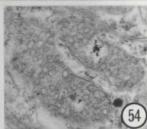
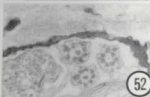
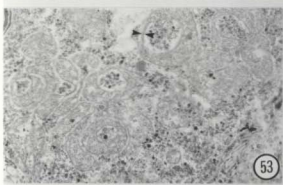
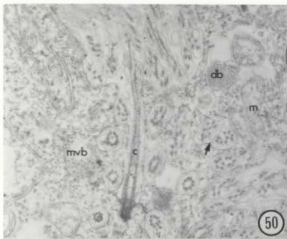
The nucleus of each distal retinal receptor cell is round (Fig. 43). Cytoplasmic organelles include microtubules, multilamellar bodies, multivesicular bodies and large Golgi complexes giving rise to numerous small vesicles of various densities. Membrane-bound dense bodies, perhaps of lysosomal origin, and inclusion bodies of membranous debris are dispersed in the cytoplasm. Mitochondria are plentiful throughout the cell but are particularly abundant at the apical cell surface. They are often observed assembled together in groups. The shape of the mitochondria is highly variable as evidenced in Figure 45. Figure 53 shows profiles of cytoplasm which protrude into the mitochondria. In such mitochondria, two bounding membranes are clearly visible between the cytoplasmic inclusion and the mitochondrial mass. Occasionally, however, intramitochondrial particles bounded by a single membrane are visible within the mitochondria (Fig. 54).

Endoplasmic reticulum, particularly the granular kind, is extensive within the receptor cells, and free ribosomes, along with dense droplets, are dispersed throughout the cytoplasm.

Each distal retinal receptor cell bears a cytoplasmic process which extends distally as a nerve axon. The axon arises from the side of the cell at the apical surface (Fig. 55). From serial sections it was determined that the axons of many distal retinal receptor cells join to run directly beneath the basal lamina of the lens (Fig. 41), course to the edge of the retina and form the distal optic nerve (Figs. 56 & 57) before passing proximally to the circumpallial nerve.

The distal and proximal optic nerves are distinguished by the size and number of their axons and by the location of each nerve in the optic tentacle. Typically the distal optic nerve lies at one edge of the optic tentacle in close proximity to the epithelium and is composed of a small number of large axons. In one section, where it was possible to count axon profiles within the distal optic nerve of a 5 year old scallop, 63 axons were observed. The proximal optic nerve is located at the center of the optic tentacle and is composed of a few thousand relatively small axons. The distal and proximal optic nerves are juxtaposed (Fig. 58), but independently enter the circumpallial nerve and show no interconnections between each other. Synapses were not observed between distal retinal receptor cell

- FIG. 50 TEM of oblique section through apical region of a distal retinal receptor cell. More than one cilium (c) may occupy a circumciliary space (arrow). Note the disordered arrangement of the axoneme pattern in some ciliary profiles. db, dense body; m, mitochondria; mvb, multivesicular body. X17,900
- FIG. 51 TEM showing longitudinal section of the base of a cilium (c) and a cross section of the ciliary shaft with a 9x2+0 axoneme pattern. X28,500
- FIG. 52 TEM of a cross section of cilia from a distal retinal receptor cell showing variations in the axoneme pattern. X29,300
- FIG. 53 TEM of distal retinal receptor cell mitochondria. Mitochondrial shape is variable and many envelope cytoplasm. Asterisk shows double membrane of mitochondria. X11,400
- FIG. 54 TEM of intramitochondrial particles. X27,900
- FIG. 55 TEM of the apical region of a distal retinal receptor cell showing a ciliary whorl (wc) and an axon (ax) arising from the side of the cell. bl, basal lamina. X8600
- FIG. 56 LM longitudinal section (1.5 $\mu$ m thickness) of pallial eye showing distal optic nerve (don) coursing past the edge of the retina. Stained with 1% methylene blue-2% basic fuchsin. dr, distal retina; i, iris; l, lens; pr, proximal retina; t, tapetum. X180



bodies nor between axons.

The axons of the distal optic nerve are large and closely packed (Fig. 59). Supportive glial cells, primarily recognized by their dense granular cytoplasm, envelope and invest the axon bundle. The cytoplasm of the axon is much clearer than that of the receptor cell body from which it arises. Axons are provided with neurotubules, mitochondria and many vesicles including small coated vesicles, dense-cored vesicles and variously sized electron-lucent vesicles. Neurofilaments are grouped together in conspicuous patches.

### 3.4.2. The Proximal Retina

The proximal retina is composed of many columnar-shaped bipolar sensory cells and non-sensory supportive cells of variate shape (Fig. 60). The receptor cells of the proximal retina lie in more than one layer. As many as 12 strata of proximal retinal receptor cells may be situated between the lens and the argentea.

Receptor cells of the proximal retina are of the rhabdomeric type (terminology of Eakin 1963). The sensory cell bears a rhabdomere at its apical end and tapers to an axon in the basal region of the cell body. The major features of a photoreceptor cell in the proximal retina are shown in the diagram in Figure 61. The rhabdomeres project into the moderately-dense extracellular space above the argentea (Fig. 62) thus forming a proximal retina of inverse photoreceptive cells (ie. light must pass through the axon

FIG. 57 SEM of a portion of freeze-fractured eye showing a transverse section of the distal optic nerve (don) lying superior to the retina (r). a, argentea. X350

FIG. 58 LM longitudinal section (1.5 $\mu$ m thickness) of the pallial eye showing separate proximal (pon) and distal (don) optic nerves. Stained with 1% methylene blue-2% basic fuchsin. i, iris; r, retina; t, tapetum. X180

FIG. 59 TEM of axons in the distal optic nerve. The axons contain mitochondria (m), small vesicles and neurofilaments (nf). glp, glial cell process; nt, neurotubules. X13,600

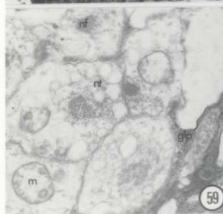
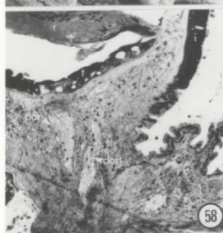
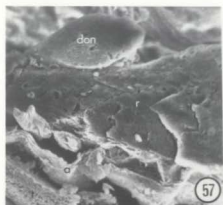


FIG. 60 TEM longitudinal section of proximal retina showing rhabdomeric photoreceptive cells. A, argentea; cr, ciliary root; l, lens; m, mitochondria; mv, microvilli; N, nucleus; PRC, proximal retinal receptor cell; scp, supporting cell process; SPC, supporting cell; V, vacuole. X4700



and the cell body before reaching the photoreceptive organelle).

Proximal retinal receptor cells in the central region of the eye are lined up with the optic axis. The cell bodies are broad and the conical processes are short. Towards the periphery of the retina, the receptor cells slant obliquely and gradually approach an orientation perpendicular to the optic axis. Such cells may be 5 $\mu$ m wide, as long as 30 $\mu$ m (Fig. 60) and the conical processes are approximately 1/3X the cell body in length.

The soma of the proximal retinal receptor cell contains many large mitochondria. A small nucleus is basally located. Cellular organelles including agranular ER, free ribosomes, Golgi and microfibers are widely distributed. The cell soma also contains variously-sized vesicles of different electron densities. Less common are multivesicular bodies, membrane-bound vacuoles and multilamellar bodies.

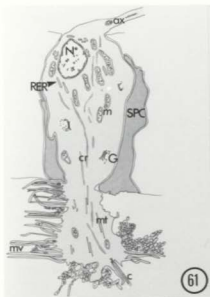
The conical process at the apical end of the receptor cell is round to square in transverse section. The cytoplasm is characterized by the presence of mitochondria, agranular ER, microtubules and numerous small vesicles.

Each rhabdomere is composed of a large number of microvilli arising as outgrowths of the plasma membrane on the sides and tip of the conical process (Figs. 60 & 63). The microvilli, approximately 3.5 $\mu$ m in length, are nearly round in transverse section, are approximately 0.10 $\mu$ m in diameter and do not appear to branch. The microvilli of

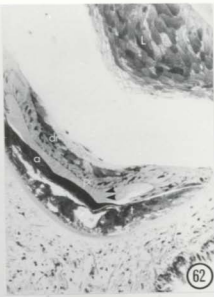
**FIG. 61** A schematic diagram of a proximal retinal receptor cell showing major cellular components. ax, axon; c, cilia; cr, ciliary root; G, golgi; m, mitochondria; mt, microtubules; mv, microvilli; N, nucleus; RER, rough endoplasmic reticulum; SPC, supporting cell.

**FIG. 62** LM longitudinal section (1.0 $\mu\text{m}$  thickness) of pallial eye showing the disposition of the proximal retina (pr) in relation to other eye components. Arrowheads show conical processes of proximal receptor cells. a, argentea; dr, distal retina; L, lens; t, tapetum. X150

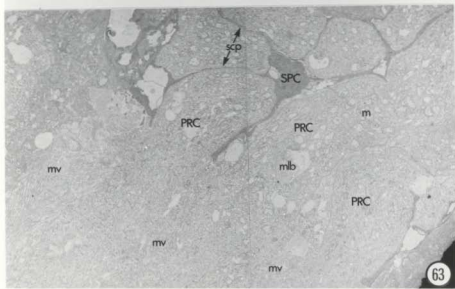
**FIG. 63** TEM oblique section through three proximal retinal receptor cells showing rhabdomeres formed from microvilli (mv) of the conical processes of adjacent cells. Electron-dense processes (scp) from a supporting cell (SPC) surround the soma of the proximal retinal receptor cell (PRC). The latter contains numerous mitochondria (m) and multilamellar bodies (mlb). X5000



61



62



63

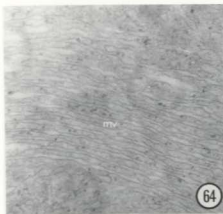
adjacent cells are complexly interwoven (Fig. 60). Although they are most often observed in irregular arrangements, the microvilli may be disposed in straight arrays (Fig. 64). The cytoplasm of the receptor cell process extends into the lumen of the microvilli as evidenced by the presence of variously-sized vesicles of different electron densities (Figs. 65 & 66) and the abundance of cytoplasmic granules in the core of each villus (Fig. 66).

Individual proximal retinal receptor cells bear up to 6 cilia extending approximately  $3.5\mu\text{m}$  into the extracellular space. The cilia (Fig. 67), each showing a  $9 \times 2+2$  pattern of microtubules, bear no relationship to the microvilli. The ciliary shaft is straight (Fig. 68) and arises from a shallow circumciliary pit. A prominent root system extends from the basal body (Fig. 69), traverses the length of the cell and terminates below the nucleus. The roots bifurcate along their length and show striations at  $720\text{\AA}$  intervals.

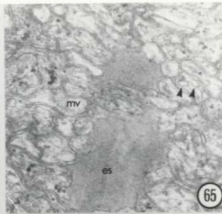
Processes arising from the supporting cells intrude between adjacent proximal retinal receptor cells. Short junctions of the zonula adhaerens type laterally interconnect the former to the base of the conical process of each receptor cell.

Intercellular vacuoles containing loosely consolidated material or membranous inclusions are apparent between the supporting cells and the receptor cells (Fig. 60). Supporting cells typically have a small soma (Fig. 70) containing a centrally located nucleus and several long,

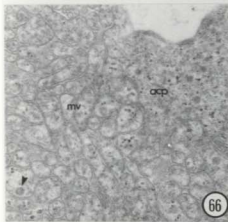
- FIG. 64** TEM showing microvilli (mv) of rhabdomere arranged in straight arrays. X38,600
- FIG. 65** Oblique section through rhabdomere showing cytoplasmic vesicles (arrowheads) in lumen of microvilli (mv). es, extracellular space. X38,200
- FIG. 66** Oblique section through rhabdomere showing cytoplasmic vesicles (arrowhead) and numerous small granules in the lumen of the microvilli (mv). acp, apical conical process. X27,900
- FIG. 67** Tangential section through proximal retinal receptor cell cilia (c) showing a 9+2 axoneme pattern. es, extracellular space; mv, microvilli. X21,300
- FIG. 68** Longitudinal section showing detail of proximal retinal receptor cell (PRC) cilium. bb, basal body; es, extracellular space. X14,400



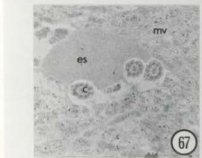
64



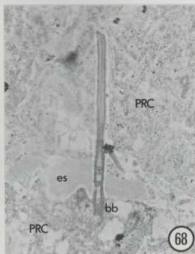
65



66



67



68

thin processes (Figs. 63 & 70) which enter both retinae. The cytoplasm of the supporting cells is characteristically dark and contains numerous electron-dense granules, mitochondria, Golgi, membranous bodies and large dense bodies possibly of lysosomal origin.

The base of each proximal retinal receptor cell tapers to an axon-like structure (Fig. 71) which contains mitochondria, granules, microfilaments and vesicles. The presumptive axons from receptors on each half of the proximal retina combine together at the edge of the retina (Fig. 72) to form two nerves, each leaving the retina on opposite sides of the eye. The SEM of part of a freeze-fractured eye in Figure 73 shows one of these nerves as it passes beneath the tapetum. A comparable structure is seen in the LM in Figure 74 and the TEM in Figure 75. These two nerve bundles join at the center of the optic tentacle beneath the tapetum to form the proximal optic nerve (Fig. 76) which passes to the circum pallial nerve of the mantle.

Each small nerve leaving the proximal retina contains several hundred axons, is oval in shape and is approximately 20 $\mu\text{m}$  in width along the widest axis. The axons typically contain mitochondria, neurotubules and neurofilaments (Fig. 77). Vesicles, such as coated vesicles, small dense-cored vesicles and large electron-lucent vesicles are prominent.

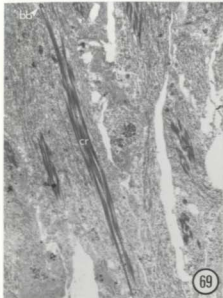
Electron-dense glial cells similar to the supporting cells of the retina sheath the nerve and send processes into it. Although glial cell bodies often occur on the surface

FIG. 69 TEM longitudinal section showing prominent root system (cr) in the conical process of a proximal receptor cell. bb, basal body. X4700

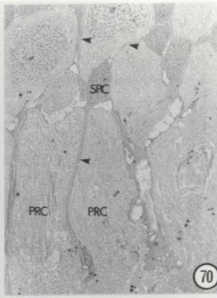
FIG. 70 Oblique section of a supporting cell (SPC). Note its small soma and several long thin cell processes (arrowheads). PRC, proximal retinal receptor cell. X3400

FIG. 71 TEM of axon of proximal retinal receptor cell. m, mitochondria; mf, microfilaments. X15,700

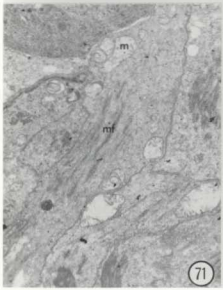
FIG. 72 Axonal processes of a number of proximal retinal receptor cells grouped together at the edge of the retina. ax, axon. X5500



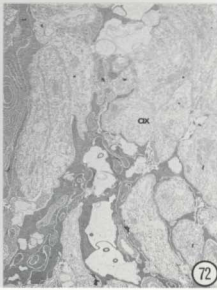
69



70



71



72

of the nerve (Fig. 75), they are not restricted to this area. As seen in Figure 78, the glial cell body may lie within the nerve proper.

Synapses have not been observed between adjacent proximal retinal receptor cells nor between receptor cells of the two retinae. However, at least two types of synaptic-like profiles can be distinguished between the axons of the proximal optic nerve. Synaptic connections may have both pre- and post-synaptic membrane densities (Fig. 79) or the membrane thickenings may be predominantly on the pre-synaptic side (Fig. 80).

### 3.5.

### The Argentea

The argentea is a concave reflector which lies at the back of the retina (Fig. 9) and it is responsible for the iridescent appearance of the scallop eye (Land 1981). The reflector is composed of several layers (Fig. 81) of regularly arranged thin rectangles of transparent crystals, each approximately  $1\mu\text{m} \times 1.5\mu\text{m} \times 0.3\mu\text{m}$ , embedded in clear cytoplasm (Fig. 82). The number of layers of crystals varies from 1 to as many as 40. There are always more layers present at the optic axis of the eye than at the margin of the argentea. Successive interfaces of the crystals are separated by strips of cytoplasm about  $0.3\mu\text{m}$  thick, and adjacent crystals in a single layer are placed less than  $0.2\mu\text{m}$  apart (Fig. 82).

FIG. 73 SEM of a portion of freeze-fractured eye showing a transverse section of one branch of the proximal optic nerve (bpn) passing below the tapetum (t). X1900

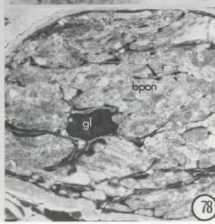
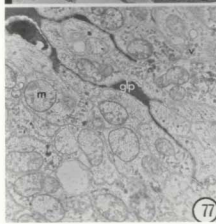
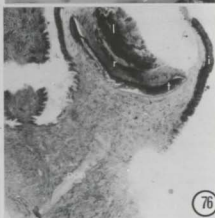
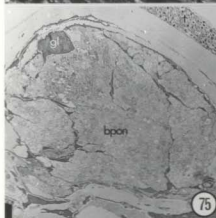
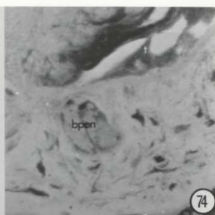
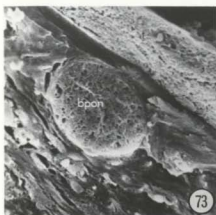
FIG. 74 LM transverse section (1.5 $\mu$ m thickness) showing branch of the proximal optic nerve (bpn) passing below the tapetum (t). Stained with 1% methylene blue-2% basic fuchsin. X190

FIG. 75 TEM transverse section showing a branch of the proximal optic nerve (bpn) passing below the tapetum (t). gl, glial cell. X2400

FIG. 76 LM longitudinal section (1.5 $\mu$ m thickness) of pallial eye showing the proximal optic nerve (pon). Stained with 1% methylene blue-2% basic fuchsin. i, iris; l, lens; r, retina; t, tapetum. X65

FIG. 77 TEM of a portion of a branch of the proximal optic nerve. The axons contain mitochondria (m), small vesicles (v) and neurofilaments. glp, glial cell process. X12,600

FIG. 78 TEM of a branch of the proximal optic nerve (bpn) showing a glial cell (gl) positioned within the nerve. X3700



Cells bounding the argentea are thin and rich in small granules. Mitochondria, Golgi, and large dense granules occur infrequently. The cytoplasmic processes investing the argentea contain no cytoplasmic organelles other than small granules.

In the living scallop, the argentea appears smooth and the reflected light varies from silver to yellow-green. Preparation for microscopy causes two consistent artifacts: splitting of the argentea along a cytoplasmic plane in the distal aspect of the reflector (Figs. 9, 10, 40, 56 & 58) and shrinkage of the argentea causing the layers to undulate and crystals to disarrange (Fig. 83).

### 3.6.

### The Tapetum

The tapetum abuts the lower surface of the argentea (Figs. 9, 10, 33, 40, 62 & 84) and is composed of many cells containing red pigment. Cells at the edge of the tapetum are long, thin (Fig. 85) and arranged in a single layer. In contrast, tapetal cells located around the optic axis are large, variously shaped and arranged in several layers.

The nucleus is convoluted in shape (Fig. 86) and is located centrally. Membrane-bounded pigment granules, ranging in size from  $0.10\mu\text{m}$  to  $0.4\mu\text{m}$ , are numerous and are dispersed throughout the cell. Tapetal cells also contain many small mitochondria, large vacuoles and Golgi complexes. Junctional complexes interconnecting adjacent cells were not

FIG. 79 TEM of a synaptic-like profile (sy) between axons in proximal optic nerve. Both pre- and post-synaptic membrane densities are visible. m, mitochondria. X20,000

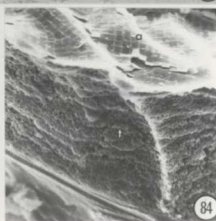
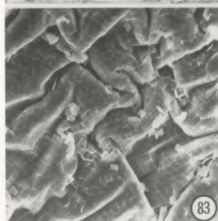
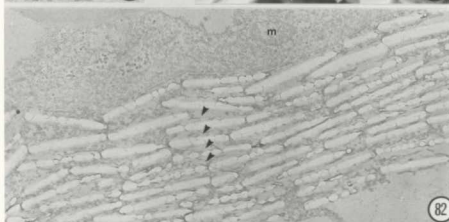
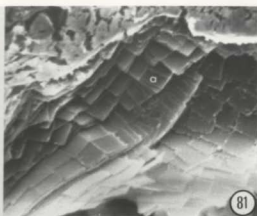
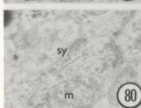
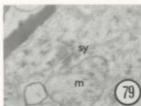
FIG. 80 TEM of a synaptic-like profile (sy) between axons in the proximal optic nerve. Membrane densities are present on the pre-synaptic side. m, mitochondria. X16,500

FIG. 81 SEM of freeze-fractured argentea (a) showing several layers of square crystals. X2100

FIG. 82 TEM oblique section of argentea showing several layers of crystals embedded between sheets of cytoplasm (arrowheads). m, mitochondria. X4500

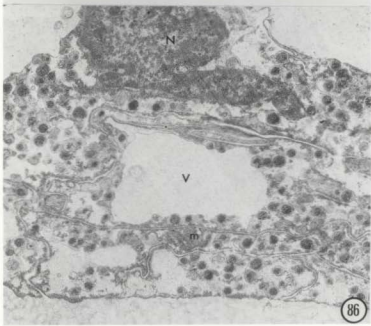
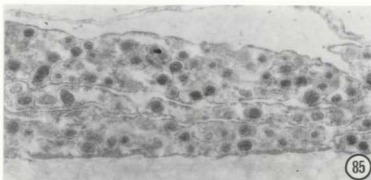
FIG. 83 SEM of distal surface of argentea. Shrinkage artifact causes layers to undulate and crystals to disarrange. X1800

FIG. 84 SEM of a portion of freeze-fractured eye showing tapetum (t) and argentea (a). X1900



**FIG. 85** TEM oblique section of pigment-containing cells positioned at the edge of the tapetum.  
X16,400

**FIG. 86** TEM oblique section of tapetal cells located near the optic axis of the eye. Large vacuoles (V) are conspicuous. m, mitochondria; N, nucleus. X9,800



observed.

DISCUSSION  
THE PALLIAL EYE

The morphology of the pallial eye of scallops has been widely studied by light microscopy in Pecten irradians (Hyde 1903; Dahlgren & Kepner 1928; Gutsell 1930), Pecten opercularis (Hickson 1880; Patten 1886, 1887; Rawitz 1888; Carrière 1889; Hesse 1900), Pecten jacobaeus (Hensen 1865; Hickson 1880; Sharp 1884; Patten 1887; Rawitz 1888; Hesse 1900; Dakin 1910a,b), Pecten maximus (Hickson 1880; Hesse 1900; Dakin 1910a), Pecten varius (Patten 1886; Rawitz 1883), Pecten pusio (Patten 1887; Rawitz 1888; Hesse 1900), Pecten hastatus (Sharp 1884), Pecten flexuosus (Rawitz 1888), Pecten magellani (Sharp 1884), Pecten tenuicostatus (Drew 1906) and Pecten tigrinus, Pecten aratus and Pecten inflexus (Hesse 1900) among others. The fine structure of the pallial eye of Placopecten magellanicus bears features common to accounts of scallop eye organization and confirms many of the observations of early light microscopists.

The eyes of Placopecten magellanicus, like those of other scallops, are borne on short tentacles situated amongst, but slightly displaced from, the sensory tentacles of the ophthalmic or middle mantle fold. All scallop eyes follow the same structural plan. Each consists of a cornea,

an iris, a biconvex lens, a double retina, a reflecting argentea and a pigmented tapetum. However, differences do exist. The transparent cornea, located at the summit of the stalk, is composed of interdigitating columnar cells. Patten (1887) reported that the midlateral regions of the cornea cells in Pecten jacobaeus and Pecten opercularis were highly folded resulting in adjacent cells being interlocked. In P. magellanicus the elaborate membrane interdigitations are not confined to the mid-region of the cell, but extend along the entire lateral edge.

Some early investigators reported that the transition from cornea cells to iris cells was gradual (Hickson 1880; Drew 1906) and many illustrated the position of the iris pigment granules in the cell's basal region (Hickson 1880; Sharp 1884; Rawitz 1888; Hesse 1900; Dahlgren & Kepner 1928). The transition from the clear cells of the cornea to the pigment-containing cells of the iris in Placopecten magellanicus is abrupt. Furthermore, the two cell types do not interdigitate at this boundary.

Patten (1887) described the iris cells of Pecten jacobaeus and Pecten pusio as being partially pigmented on the side of the eye that faces the shell and completely pigmented on the side that faces the light. In contrast to the accounts for other scallops, the iris of Placopecten magellanicus has pigment granules distributed throughout the cells.

Although all previous light microscopists agree that

the epithelial cells of the eye stalk bear a border of microvilli, Hensen (1865) was the only investigator to accurately describe the presence of cilia on the iris cells, which subsequent microscopists either disagreed with (Patten 1887) or were unable to confirm (Sharp 1884). The distribution of ciliated iris cells was left unnoticed.

The ciliated iris cells of Placopecten magellanicus are dispersed among the non-ciliated cells. Ciliated sensory cells have been shown to occur on the tentacles of P. magellanicus (Moir 1977). The optic tentacle and the long tentacles of scallops appear superficially homologous and it has been theorized that the eye stalk is a modified tentacle (Hickson 1880; Patten 1887; Drew 1906). It is, therefore, possible that the ciliated epithelial cells of the iris may serve a function analogous to their counterparts on the long tentacles, ie. mechanoreception. It is equally likely that the cilia of the iris cells are non-sensory and are perhaps responsible for the movement of mucus and removal of debris from the iris and corneal regions.

Evidence for the latter function is strengthened by three observations. The near absence of cilia on the cornea precludes removal of debris which might foul the transparent window of the optic vesicle and reduce the ability of the eye to gather information about its environment. The cilia bear a 9x2+2 content of microtubules characteristic of motile cilia. Moreover, no neural input has been found to

the ciliated iris cells, despite intensive search.

The average number of eyes in adult Placopecten magellanicus approaches 160, with significantly more eyes on the upper mantle edge than on the lower. Although this distribution pattern is a common feature of scallops, the total number of eyes appears to vary with species. For example, there are an estimated 80-120 eyes in Pecten maximus (Hickson 1880), 175 eyes in Spondylus goederopus (Dakin 1928), 163 eyes in Spondylus americana (Dakin 1928), 103 eyes in Chlamys opercularis (Harry 1980) and 58 eyes in Pecten ziczac (Wilkens 1981). A provocative and, as yet, unanswered question is posed: why is there such an abundance of eyes on the mantle edge?

One investigator has attempted to account for this enigma from different lines of evidence. Land (1965), in a study of the optical apparatus of Pecten maximus, demonstrated that although the field of vision of each eye was between  $90^{\circ}$ - $100^{\circ}$ , image definition was restricted to the central region of the retina. He suggested that the presence of a large number of eyes might help accommodate the optical handicap. Land (1984) went on to propose that, given the dim light conditions extant in the scallop's habitat, the presence of a large number of eyes might improve the signal to noise ratio of the perceived visual information.

Apart from the limitations presented by the dioptric and reflective apparatus, the visual field of an eye might

further be influenced by the disposition of the sensory structures at the mantle edge. It is of note that the scallop eyes are very often obstructed by the movements of the tentacles. A large number of eyes positioned to allow visual fields to overlap might counter the external determinants influencing the angle over which the animal is capable of receiving light.

An important feature that previous light and electron microscope studies have not demonstrated clearly is the presence of cilia and their associated root systems in the proximal receptor cells of the retina. Interpretations of these structures within the proximal retinal receptor cells have differed. Miller (1960) noted the presence of an axial system of striated filaments in the proximal retinal receptor cells of Pecten irradians and likened the structures to the striated roots of cilia. Interestingly, Miller failed to observe cilia. Although Barber et al. (1967) showed that axial structures were present in Pecten maximus, they were unable to confirm the presence of a root system. However, Barber et al. (1967) did establish the presence of 1 or 2 cilia arising from the conical projection of the proximal retinal receptor cells.

A remarkable feature of the proximal receptor cells in Placopecten magellanicus is the presence of several cilia, each possessing  $9 \times 2 + 2$  microtubule doublets, arising from the conical processes. The axoneme pattern established here is

in striking contradiction to that reported by Barber *et al.* (1967) who observed that each cilium of Pecten maximus contained a 9x2+0 axoneme content.

The presence of an extensive system of striated roots in Placopecten magellanicus is noteworthy. The roots, clearly associated with the basal bodies of cilia, extend axially through the length of the receptor cells. It is possible that the elaborate system of roots function as support mechanisms for anchoring the long receptor cells in position. A similar function for root systems has been suggested by Eakin & Kuda (1971), Burr & Burr (1975), Holley (1984) and Eakin & Brandenburger (1985). However, the intimate packing of the microvilli into rhabdoms would presumably stabilize the cells and obviate the need for internal supporting structures.

Ciliary structures have been demonstrated in the rhabdometric type photoreceptors of a variety of molluscs (Barber *et al.* 1967; Eakin & Brandenburger 1967; Eakin *et al.* 1967; Boyle 1969b; Hughes 1970; Rosen *et al.* 1978), arthropods (Such 1969; Home 1972, 1975; Juberthie & Muñoz-Cuevas 1973; Wachmann & Hennig 1974; Muñoz-Cuevas 1975, 1984; Eisen & Youssef 1980), annelids (Eakin 1963; Eakin & Westfall 1964; Röhlich *et al.* 1970; Hermans & Eakin 1974; Ermak & Eakin 1976; Eakin *et al.* 1977; Brandenburger & Eakin 1981; Eakin & Brandenburger 1985; Pietsch & Westheide 1985), echinoderms (Emerson 1977; Yamamoto & Yoshida 1978; Eakin & Brandenburger 1979; Brandenburger & Eakin 1980) and

sipunculans (Hermans & Eakin 1969). However, it is often debatable whether these structures are involved with photoreceptive function.

The consistent presence of cilia in the proximal receptor cells of Placopecten magellanicus is thought to be structurally unrelated to the photoreceptive function of the cell. All of the cilia are straight, relatively short and lack membranous expansions characteristic of ciliary type photosensitive organelles. Consequently their design is not favorable for the efficient arrangement of photopigment molecules to receive light. Furthermore, the cilia possess a normal axoneme pattern (ie. 9x2+2) and the ciliary shafts show no particular orientation with respect to the direction of impinging light. Collectively these features are not consistent with the structural characteristics representative of known ciliary type light sensitive organelles (Eakin 1963, 1972, 1979, 1982; Boyle 1969b).

It may be advanced that the microvilli of the proximal retinal receptor cells are most probably the primary, if not the only, photoreceptive organelles in the proximal retina of Placopecten magellanicus. Strong support for this proposal is provided by the abundance and organization of the microvilli. The microvilli are derivatives of the plasma membrane of the cell. They are extremely long and are arranged in extensive arrays with the microvilli positioned perpendicular to the path of light. This organization allows for favorable and efficient display of

photopigment on the microvillous membrane thus maximizing absorption of light energy. Further, albeit tenuous, support may be acquired from morphological comparisons with known photoreceptors. The arrangement of the microvilli in the proximal receptor cells of P. magellanicus shows structural affinity to arrays observed in the known light sensitive rhabdomeric cells of the snail Helix aspersa (Eakin 1965), the nudibranch Hemisenna crassicornis (Eakin et al. 1967) and the slugs Agriolimax reticulatus (Newell & Newell 1968) and Athoracophorus bitentaculatus (Eakin et al. 1980).

Conversely, if the cilia in the proximal retinal receptor cells of Placopecten magellanicus do play a role in light reception then these cells, which are primarily concerned with gradual changes in light intensity (Land 1966a, 1978, 1984), would have 9x2+2-characterized cilia producing well documented 'on' responses (Hartline 1938; Bell 1966; Land 1966a; McReynolds & Gorman 1970a). To date no ciliary type receptors are known to produce depolarizing 'on' responses and their functional presence in a retina already equipped with specialized ciliary hyperpolarizing 'off' receptors is unlikely.

It is possible that the cilia in the proximal receptor cells of Placopecten magellanicus are either vestiges remaining after morphogenesis of the proximal retina (Eakin 1965, 1968, 1972, 1979, 1982; Eakin & Westfall 1964; Eakin et al. 1977; Brandenburger & Eakin 1981; Eakin &

Brandenburger 1985) or remnants of ciliary structures acting as organizers of rhabdomeeric differentiation (Röhlich *et al.* 1970; Home 1975; Muñoz-Cuevas 1975; Vanfleteren & Coomans 1976; Coomans 1981; Vanfleteren 1982). These theories will be discussed in more detail in Chapter 6.

Photoreceptors composed of ciliary type receptor cells or a mixture of ciliary and rhabdomeeric type cells have been reported for a number of molluscs (Barber & Land 1967; Barber & Wright 1969a; Boyle 1969b; Hughes 1970; Levi & Levi 1971; Fankboner 1980, 1981; Kataoka & Yamamoto 1981; Howard & Martin 1984; Land 1984).

The ultrastructure of the cilia in the distal retinal receptors of Placopecten magellanicus varies in detail to that described by Miller (1958, 1960) for Pecten irradians and Barber *et al.* (1967) for Pecten maximus. According to these investigators the cilia are either globular in form (Miller 1960) or flattened into large plates (Barber *et al.* 1967), which may remain straight (Barber *et al.* 1967) or coil into whorls (Miller 1958, 1960; Barber *et al.* 1967). The three-dimensional appearance of the photoreceptive cilia in the scallop has not heretofore been established.

The comparative TEM and SEM observations on Placopecten magellanicus show the ciliary shaft to be modified along its length into a flattened sheet which coils about itself parallel to the axoneme. Some anomalies exist. Nonetheless, the ultrastructural model elucidated here

offers one explanation for the occurrence of the two types of ciliary shaft modifications (ie. straight lamellae, whorls) previously reported in the distal retina of the scallop.

The absence of synapses between adjacent cells of the distal retina, adjacent cells of the proximal retina and between receptor cells of the two retinae in Placopecten magellanicus supports previous suggestions that receptor cells of each retinal layer are primary sense cells (Hartline 1938; Toyoda & Shapley 1967; McReynolds & Gorman 1970a; Wilkens & Ache 1977). Furthermore, the fact that the cilia of adjacent distal retinal receptor cells do not intermix and the presence of two distinct and structurally separate optic nerves innervating the retinae of P. magellanicus lends added support to this belief.

Hensen (1865) was the only other investigator to report that the proximal and distal branches of the optic nerve passed separately to the circum pallial nerve. The presence of a common optic nerve in nearly all other scallops and its absence in Placopecten magellanicus is mystifying. Whether this may be accountable to species differences or to artifacts of technique remains to be addressed.

Many investigators have demonstrated that the scallop exhibits complex behaviors to light (Uexküll 1912; Wenrich 1916; Buddenbrock & Moller-Racke 1953; Land 1965, 1966a,

1968; Wilkens 1981) which are mediated by the pallial eyes.

On the basis of numerous observations, Land (1968, 1978, 1984) has found that the distal and proximal retinae of Pecten maximus each contain about 5000 receptors.

Although Placopecten magellanicus appears to have a like number of proximal retinal receptor cells, the number of receptors in the distal retina is impressively smaller. It is apparent from the present study that P. magellanicus is able to meet its visual requirements, specifically those tasks responsible for movement detection and spacial distribution, with nearly 80-fold fewer receptors than Pecten. This is quite intriguing considering that the diameters of the distal receptor cells are the same (ie. about 9 $\mu\text{m}$ ) in both Pecten (Land 1968, 1984) and P. magellanicus, and that the number of cilia in each distal receptor cell is also nearly identical in both scallops.

Interestingly, the vertical dimension of the ciliary whorls in Placopecten magellanicus is 3- to 4-fold greater than that observed in Pecten irradians (Miller 1958). Moreover the distal receptor cell axons in P. magellanicus are much larger (ie. about 3 $\mu\text{m}$ ) in diameter than those in Pecten maximus (ie. 0.5 $\mu\text{m}$ , Barber *et al.* 1967). Thus, the present observations suggest that P. magellanicus compensates for fewer receptors in the distal retina by increasing the surface area available for collecting light energy and by providing a large conduit for transmitting information about the visual environment.

The marked morphometric differences between the proximal and distal optic nerves has, to date, gone unnoticed. It is possible that the dissimilarities might have functional implications. The small number of large axons in the distal optic nerve produce phasic responses to light stimuli (Land 1966a, 1968, 1984) and perhaps allow information to be conducted to the central nervous system rapidly. Considering the role subserved by the distal retina, this would be of obvious behavioral value to the animal when immediate information about the visual environment is necessary. In contrast, the large number of small axons in the proximal optic nerve produce tonic responses (Land 1966a, 1968). The morphologic nature of these axons may effect a slower response in the transmission of light stimulus to the central nervous system, for although biologically relevant, continuous information about absolute light intensity is not of instantaneous value. Clearly more detailed ultrastructural examinations of the optic nerve(s) in scallops are warrented.

Barber & Land (1966) and Barber et al. (1967) described the fine structure of the argentea of the pallial eyes in Pecten maximus. According to these investigators, this optical component consisted of a single layer of cells containing 30-40 layers of thin square crystals measuring  $1.3\mu\text{m} \times 0.08\mu\text{m}$ . Similar mirror systems have been described in other invertebrates (eg. Land 1966b; Barber & Land 1967;

Barber & Wright 1969a; Homann 1971; Muñoz-Cuevas 1984) and are known to function as multilayered, thin-film interference reflectors.

In Placopecten magellanicus also, the argentea consists of a single layer of cells comprising up to 40 strata of flat crystals at the optic axis. These crystals are rectangular with surface dimensions, determined from scanning electron micrographs, of about  $1\mu\text{m} \times 1.5\mu\text{m}$ . This is comparable to Pecten. While the thickness of the crystals and the underlying strips of cytoplasm appear to be equal in P. magellanicus, it must be cautioned that these sizes were determined from examinations of transmission electron micrographs obtained from unsupported sections of the argentea showing the spaces occupied by the dissolved crystals. The measurement of  $0.3\mu\text{m}$  is likely much higher than the real value. The inaccuracy is due to distortion influences from technical manipulations. Nevertheless, in all likelihood, the high reflectivity of the mirror system in P. magellanicus is due to constructive interference.

107  
CHAPTER FIVE

RESULTS  
PALLIAL EYE DEVELOPMENT

It was not possible to estimate the exact age of a given eye. Therefore, the sequence of morphogenesis presented in this investigation of pallial eye development chronicles the successive stages by which the various eye components arise. The static image obtained in an electron micrograph can be misleading unless micrographs from several pieces of tissue, taken from eyes at a variety of maturational stages, are examined and a rational reconstruction of this sequence attempted.

A papilla-like prospective optic tentacle containing the retinal anlage, along with elements of the tapetum and argentea, was the first phase obtained in this study. Figure 87 represents a longitudinal section through the center of a papilla-like tentacle at this early stage of development. An immature proximal retina, the argentea, and the pigmented tapetum are illustrated at higher magnification in Figure 88. It is noteworthy that the epithelial cells of the primordial stalk lack pigment, and a lens and a distal receptor cell layer are absent. These observations compare well with TEM findings from the same stage of development.

## 5.1. Formation of The Tapetum and Argentea

The pigmented tapetum and reflecting argentea are clearly recognizable in all of the stages of eye morphogenesis obtained in this study.

In representative sections taken from the papilla-like primordial eye (Figs. 87 & 88), the young tapetum, although smaller in size, resembles closely the structural arrangement observed in the mature eye. Even in its earliest stages the developing tapetum is vivid red. In cross section it appears hemispherical and is composed, at the prospective optic axis, of as few as 5 layers of highly convoluted cells. The deep invaginations of the plasma membrane are tortuous. Therefore, clear distinction between tapetal cells is often precluded. Specialized junctions were not observed.

The most conspicuous elements of the tapetal cells are the numerous round to oval membrane-bounded pigment granules (Fig. 89) measuring  $0.1\mu\text{m}$  to  $0.5\mu\text{m}$  in diameter. A common feature to most granules is a thin uniform electron-lucent zone separating the delimiting membrane from the internal substructure (Fig. 90). This peripheral halo may be attributable to some extent to the extraction of material during osmium fixation in specimen preparation. Typically the pigment granules exhibit a pleomorphic internal substructure of finely granular material. Patterned matrices were not observed.

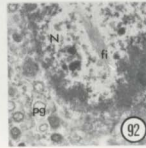
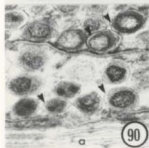
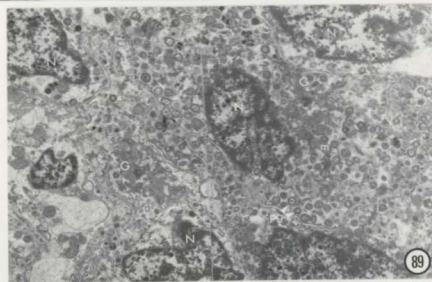
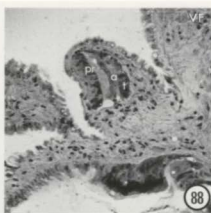
The pigment granule contents are usually of moderate electron density with frequent electron-lucent cores. Scattered more electron-lucent granules are often present, while in some cases a core of exceptionally electron-dense material can be distinguished from the rest of the granular contents. The varying degrees of pigmentation found in the granules of individual tapetal cells might reflect transitional stages in pigment granule formation.

Apart from the pigment granules, the young tapetal cells (Fig. 89) also contain a centrally positioned, deeply indented nucleus, sparse granular ER and moderately-sized vacuoles. Metabolic activity is indicated by the presence of polyribosomes, elaborate perinuclear Golgi complexes and numerous small mitochondria. Occasionally membraneous lamellae studded with ribosome-like particles (Fig. 91) appear in the cytoplasm and fibrillary inclusions (Fig. 92), although rare, are readily discernible in some nuclei.

Subsequent development of the tapetum is accompanied by a diminution of Golgi complexes and mitochondria together with an accumulation of pigment granules within the cells. The infoldings of the plasma membrane become more irregular as the tapetum develops and may serve to interconnect the cells. Furthermore, the number and size of the tapetal cells increases throughout development, although no evidence of mitosis was observed.

With the formation of the pigmented tapetum, or shortly thereafter, is the appearance of the argentea. Initially

- FIG. 87 LM longitudinal section through a papilla-like prospective optic tentacle (POT). Note its location relative to the velar fold (VF) and the shell fold (SF). X25
- FIG. 88 Higher magnification of Fig. 87 showing the presence of a proximal retina (pr), argentea (a) and tapetum (t) within the prospective optic tentacle. VF, velar fold. X70
- FIG. 89 TEM of tapetal cells. Note the presence of variously-sized membrane-bounded pigment granules (pg) in the cytoplasm along with Golgi complexes (G), mitochondria (m) and RER. N, nucleus. X10,500
- FIG. 90 High magnification TEM of pigment granules showing electron-lucent halo and delimiting membrane (arrowheads). a, argentea. X27,700
- FIG. 91 TEM of membranous lamellae (arrowheads) studded with ribosome-like particles. m, mitochondria; pg, pigment granule. X13,800
- FIG. 92 TEM showing fibrillary inclusion (fi) in a tapetal cell nucleus (N). pg, pigment granule. X13,800



the prospective argentea cells, which are positioned over the length of the distal margin of the tapetum, represent long and somewhat flattened tapetal cells with sparsely scattered pigment granules. The undifferentiated argentea cells also contain numerous mitochondria, well developed Golgi complexes, granular and agranular ER, and abundant free ribosomes. The nuclei are positioned basally.

The onset of argentea cell formation is characterized by a proliferation of attenuant infoldings in the plasma membrane. At several foci these infoldings form circular bodies (Fig. 93) containing complex systems of internal membranes. Early in the proliferative phase the internal membranes are disordered but as cell development advances the membranes, in profile, become juxtaposed and oblong compartments take shape (Fig. 94). The upper and lower surface of each chamber is bounded by 2 unit membranes separated by an electron-lucent zone. These membranes are closely apposed at each end of the chamber.

The chambers, measuring approximately  $1\mu\text{m}$  deep and  $0.1\mu\text{m}$  wide, form the matrices within which the reflecting crystals appear. As growth progresses, the matrices separate from the circular body. The latter becomes less distinct and eventually disappears. Gradually the oblong matrices, some of which already contain crystal rudiments, become arranged in layers (Fig. 95) and, also, subsequently align in rows (Fig. 96). Strips of cytoplasm are compressed between adjacent chambers. It should be noted that during

specimen preparation the crystalline material usually dissolves from the chambers leaving orthogonal spaces which distort in the electron beam (Figs. 94 & 96).

During the intermediate stages of argentea cell differentiation (Fig. 97) the production of membranes and crystals continues. Numerous mitochondria, elaborate Golgi complexes, granular ER and dispersed pigment granules are still noted although gradually displaced to the periphery of the cell by the spread of membranous matrices and crystals. Occasionally the contour of a crystal is visible inside a pigment granule (Fig. 98).

As shown in Figure 97, the membranous matrices lie in comparatively more ordered arrays than in earlier stages, with the long axis of each compartment nearly perpendicular to the light path. Crystals, which are tabular and square in outline, are abundant.

With subsequent development circular bodies become less prevalent until evidence of membrane proliferation disappears and crystal production ceases. The nucleus degenerates and the cell becomes devoid of organelles, except for occasional pigment granules compressed in the cytoplasm between the layers of crystals.

The morphology of the newly differentiated argentea is very similar to that of the mature reflector shown in Fig. 82. The newly formed argentea, although appearing more undulatory than smooth in sectioned material, is generally concave in shape with its central region having more layers

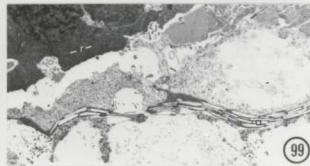
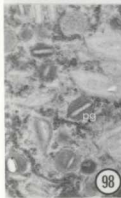
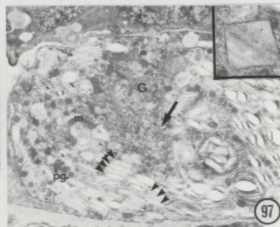
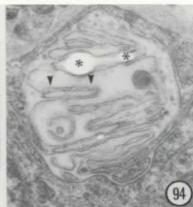
of crystals than the margins (Fig. 99). The dimensions of the argentea increase with the addition of cells during later development.

#### 5.2. Formation of The Proximal Retina

As the papilla-like protuberance emerges from the surface of the ophthalmic groove, the proximal retina differentiates from the retinal anlage to form a layer of cells aligned parallel to the prospective optic axis. The presumptive receptor cells of the developing proximal retina are initially arranged in a single uniform row and are connected to adjacent cells by prominent zonula adhaerens. The shape of the cells is not homogeneous over the entire layer as receptor cells positioned marginally are cuboidal while those located near the center of the layer are elongated. Many irregularly shaped undifferentiated cells are situated around the periphery of the developing retina (Fig. 100). These cells represent the retinal anlage.

As a prospective proximal retinal receptor cell differentiates from the anlage the cell becomes cuboidal in shape. It contains a large centrally located rectangular nucleus and dense cytoplasm (Fig. 101). Electron-dense autophagic-like inclusions are present in the subnuclear region of the cell (Fig. 102). Mitochondria, large Golgi complexes, abundant granular ER, pinocytotic coated vesicles and numerous free ribosomes are also evident. Ciliary

- FIG. 93 TEM of a circular body in the cytoplasm of a differentiating argentea cell. m, mitochondria. X17,300
- FIG. 94 TEM of a circular body showing a system of internal membranes and an oblong compartment (arrowheads) within which a reflecting crystal will form. Asterisks mark areas where crystalline material has dissolved during specimen processing. X37,000
- FIG. 95 TEM showing oblong compartments (arrowheads) stacked into layers within the cytoplasm of a differentiating argentea cell. m, mitochondria. X13,400
- FIG. 96 TEM showing oblong compartments (arrowheads) aligned in rows. Asterisks mark areas where crystalline material has dissolved during specimen processing. X15,500
- FIG. 97 TEM of an argentea cell at an intermediate stage of differentiation. The oblong compartments (arrowheads) form ordered arrays oriented nearly perpendicular to the direction of light (arrow). G, golgi; m, mitochondria; pg, pigment granule. X6400 Inset shows profile of chamber in normal section. X19,700
- FIG. 98 TEM of pigment granules (pg) containing compartments for crystals. X21,000
- FIG. 99 TEM of a differentiating argentea (a) in a papilla-like prospective optic tentacle. r, retina. X6400



structures in the form of basal bodies are prominent near the apex of the cell (Figs. 101 & 103). Similar ciliary rudiments are present in many of the undifferentiated cells of the retinal anlage.

Subsequent development includes elongation of the presumptive receptor cell and the formation of an apical conical process (Fig. 104). As the cell body lengthens the nucleus migrates basally and becomes irregular in shape (Fig. 105). Mitochondria and Golgi complexes are found in greater numbers and a variety of locations throughout the soma. Figure 106 is a cross section through the differentiating receptor cell at the level of the nucleus illustrating the circular nature of the cell body. Axons emanating from the base of each cell were not in evidence.

Concurrently, the apical end of the developing receptor cell prolongates and the immature process gives rise to irregular indentations of the plasma membrane (Fig. 104). Rhabdomere formation is progressive and not uniform. Agranular ER along with Golgi-derived dense-cored vesicles fuse to form vacuoles of irregular size and shape. Concurrently, albeit less predominantly, agranular ER consolidate into whorls of membranes located in areas adjacent to the plasma membrane. These multilamellar bodies together with the vacuoles containing fine flocculant material are gradually incorporated into the plasma membrane (Figs. 104, 107 & 108). In this way infoldings of the plasma membrane appear and the membranous projections

**FIG. 100** TEM of undifferentiated cells of the retinal anlage in a papilla-like prospective eye. N, nucleus. X5000

**FIG. 101** TEM showing rectangular nucleus (N) of prospective proximal retinal receptor cell. Note the presence of a basal body (bb) near the apex of the cell. m, mitochondria; za, zonula adhaerens. X9500

**FIG. 102** TEM transverse section through a prospective proximal retinal receptor cell showing autophagic inclusion bodies, arrays of RER and numerous free ribosomes in the subnuclear cytoplasm. m, mitochondria. X14,200

**FIG. 103** TEM oblique section through the apex of a prospective proximal retinal receptor cell showing a basal body (bb) near the cell surface. N, nucleus; za, zonula adhaerens. X20,200

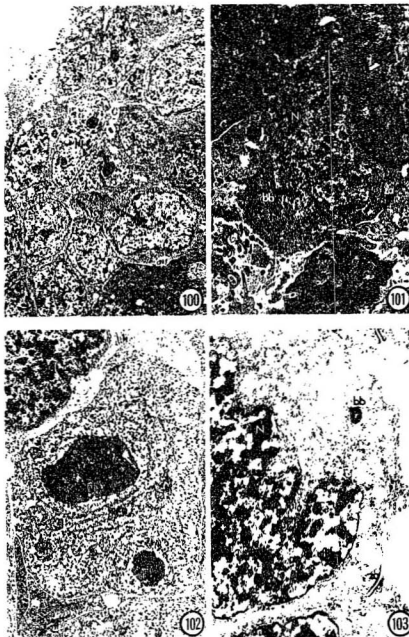
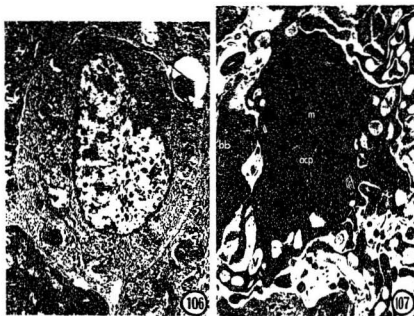
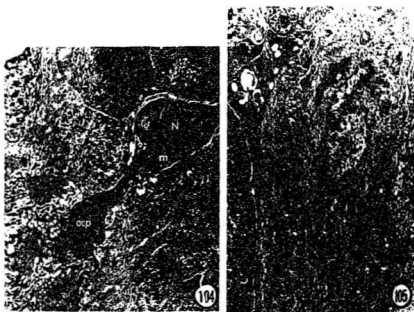


**FIG. 104** TEM longitudinal section showing a prospective proximal retinal receptor cell at a later stage of differentiation. Note the constriction and elongation of the cell body and the formation of an apical conical process (acp). Arrowhead shows a vacuole incorporated into the plasma membrane. c, cilia; m, mitochondria; N, nucleus. X5900

**FIG. 105** TEM longitudinal section through the distal end of a differentiating proximal retinal receptor cell showing irregular nucleus (N), numerous mitochondria (m) and Golgi complex (G). X9300

**FIG. 106** TEM transverse section through distal end of a differentiating proximal retinal receptor cell showing circular nature of cell body. m, mitochondria; N, nucleus; RER, rough endoplasmic reticulum. X11,400

**FIG. 107** TEM transverse section through a differentiating apical conical process (acp). Vacuoles (V) containing fine flocculant material are incorporated into the plasma membrane and finger-like projections (arrowhead) are formed. bb, basal body; m, mitochondria. X20,100



attenuate to stout finger-like structures representing microvilli (Figs. 104, 107-109) which eventually become organized into the prospective rhabdomere. The microvilli, approximately .08 $\mu$ m in diameter and 0.8 $\mu$ m in length, lack uniform orientation.

Cilia are present near the apex of the developing conical process at this stage. However, there is no evidence to demonstrate a connection between the ciliary elements and the formation of microvilli in the primitive rhabdomere. The cilia, less than 1 $\mu$ m in length, may occur singly (Fig. 110) or in groups of 4 or 5 (Fig. 111). They are straight and possess a 9x2+2 axoneme complement. A basal foot projects from the basal body. A system of striated roots, some of which bifurcate (Fig. 112), extends a short distance from the basal body into the conical process.

The low-power micrograph in Figure 113 illustrates the characteristic appearance of a proximal retinal receptor cell at a much later stage of development. Particularly apparent is the lengthening of the conical process and the complex array of the microvilli. As shown in Figure 114 the microvilli elongate and constrict. The inter-rhabdomeric space remains considerable and spatial organization is loose. As growth progresses, the microvilli of adjacent cells gradually become organized into the relatively more regular arrangement of interdigitations (Fig. 115).

The conical process is characterized by the presence of

FIG. 108 TEM transverse section through a differentiating apical conical process (ACP). Vacuoles (V) and multilamellar bodies (mlb) unite with the plasma membrane (arrowheads) to form short microvilli. X12,800

FIG. 109 TEM transverse section through a differentiating apical conical process (ACP). The microvilli (arrowheads) increase in number and length and eventually organize into a primitive rhabdome. X15,500

FIG. 110 TEM of cilium at the apex of the apical conical process (ACP). bb, basal body. X24,700

FIG. 111 TEM of a group of cilia on the apical conical process (ACP). cr, ciliary root; es, extracellular space. X21,000

FIG. 112 TEM of cilia showing system of bifurcating (arrowheads), striated roots. acp, apical conical process; es, extracellular space. X15,500

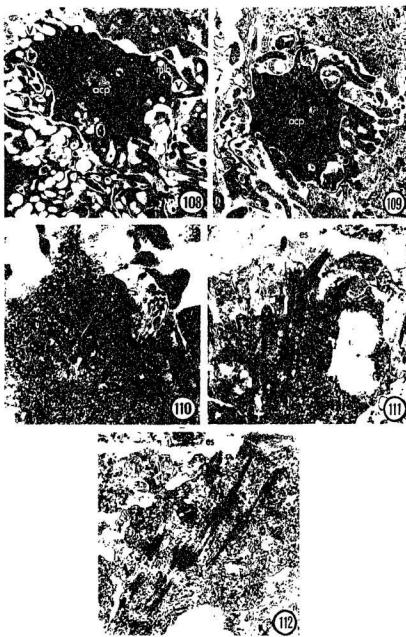


FIG. 113 Low magnification TEM longitudinal section of proximal retinal receptor cell in a late stage of differentiation. Note the lengths of the cell soma and apical conical process (ACP), the complex array of microvilli (MV) on the prospective rhabdomere, and the extensive ciliary root system (CR). es, extracellular space; N, nucleus; SPC, supporting cell; za, zonula adhaerens. X6600



es

113

multivesicular bodies, microtubules, numerous mitochondria and abundant small dense-cored vesicles possibly originating from the prominent Golgi complexes. Smooth ER is particularly abundant and dispersed throughout the cytoplasm.

The soma of the developing proximal retinal receptor cell elongates to a columnar shape, approximately 20 $\mu\text{m}$  in length and 2.5 $\mu\text{m}$  in width, and the cytoplasm is noticeably more electron-dense than in the mature receptor. A complex root system emanating from cilia in the conical process traverses the length of the cell body (Fig. 113). The ciliary root striation periodicity at this stage of development is similar to that measured in the mature receptor.

The basal region of each prospective receptor cell gives rise to a thin process that has been tentatively identified as an axon, containing mitochondria, clear vesicles, microtubules and free ribosomes. These 'axons' collect into small groups at the edge of the retina (Fig. 116) and pass downwards along the center of the eyestalk. It has not been unequivocally determined whether at this point in retinal development the groups of axons join to form the single proximal optic nerve.

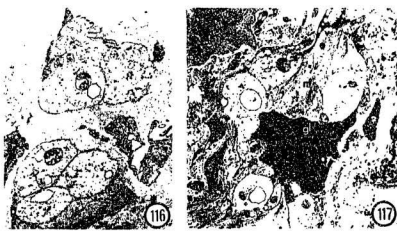
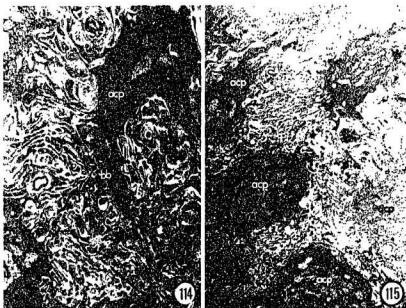
A definitive proximal optic nerve is present at the time of distal retina formation. The characteristic appearance of the young proximal optic nerve is shown in part in Figure 117. The axons contain mitochondria,

FIG. 114 TEM of the proximal end of an apical conical process (acp) showing the complex, disorganized array of microvilli (mv). Note the tangentially sectioned basal body (bb) and its basal foot. m, mitochondria. X9000

FIG. 115 TEM tangential section through the conical processes of a number of proximal retinal receptor cells at a late stage of differentiation. Note the presence of numerous microvilli in the apical conical processes (acp) and the interdigititation of microvilli from adjacent rhabdomeres. X5800

FIG. 116 TEM tangential section through axons of newly differentiated proximal retinal receptor cells. m, mitochondria. X13,000

FIG. 117 TEM oblique section through a portion of the newly differentiated proximal optic nerve. Note the presence of mitochondria (m), neurofilaments (nf) and small vesicles (v) in the axons. Glial cells (gl) are also present. X4500



aggregations of small clear vesicles, variously sized electron-dense vesicles, neurofilaments and neurotubules. Glial-like cells invest and surround the axons. Despite an extensive search, synapses were not observed.

The supporting cells appear relatively late in the developmental sequence. When first apparent the cells are located at the edges of the developing proximal retina and are morphologically distinct from cells of the retinal anlage.

With subsequent growth the supporting cells migrate into the immature proximal retina and become interposed among the cell bodies of adjacent developing receptor cells (Fig. 118). At first the pyramidal somas of the supporting cells are located proximally, but above the apical conical processes (Fig. 113). Processes emanating from the supporting cells pass distally toward the base of the receptor cells. As the proximal retina matures the electron-dense supporting cells become situated at the distal end of the receptor cells and the cell processes extend proximally towards the rhabdomeres. However, the supporting cell processes do not extend between the rhabdomeres. Junctional complexes of the zonula adhaerens type bind the supporting cell processes to the proximal end of the receptor cell body.

## 5.3. Formation of The Distal Retina

Formation of the distal retina commences soon after the proximal retina has attained a fair degree of differentiation.

There is no evidence to suggest that cell division occurs in the differentiating distal retinal receptor layer. Cells from the peripheral retinal anlage migrate to positions medial to the retina primordium and distal to the layers of maturing proximal retinal receptor cells (Fig. 119). Here, the cells which represent future distal retinal receptor cells become organized into a layer infused progressively by processes from well differentiated supporting cells, recognized by their electron-dense cytoplasm and irregular shape, which migrate from the anlage along with prospective receptor cells. In the earliest stages of distal retina formation supporting cells can be observed between the distal retinal receptor cells. Cell processes are present, but are thickset and few in number. As growth progresses these supporting cells move proximally and reorganize among the existing supporting cells below the layer of developing distal retina.

Initially, the primordial distal retinal receptor cells are undifferentiated and indistinguishable from each other. The irregularly shaped nucleus is large and centrally to basally located. The cells contain granular ER, multivesicular bodies, large dense inclusion bodies and

relatively few mitochondria. A few Golgi complexes along with small coated vesicles and membrane-bounded vesicles of varying densities are also dispersed in the cytoplasm. Junctional complexes were not observed.

The onset of distal retinal receptor cell differentiation is marked by an elongation of the prospective receptor cells and by the appearance of two elements: cilia and axons.

Cilia formation is reconstructed in Figures 120 to 127. Ciliary rudiments appear in the distal cytoplasm well below the surface of the plasma membrane (Fig. 120). These elements initially take the form of a centriole or basal body. Gradually the long axis of the basal body becomes oriented nearly parallel to that of the receptor cell and a thin, flattened vesicle appears immediately above the distal end (Fig. 121). Concurrently, tenuous fiber-like structures emanate from the proximal margin of the basal body. These thin fibers can be traced a short distance into the cytoplasm.

The basal body migrates closer to the apical plasma membrane as the vesicle enlarges (Figs. 122 & 123). However, no contact is made with the plasma membrane. As can be seen in Figure 124, microtubules from the basal body plus the membrane enveloping them extend into the ever enlarging vesicle and a ciliary bud (terminology of Stubblefield & Brinkley 1966) is formed (Fig. 125). The wall of the vesicle is incorporated gradually into a ciliary

FIG. 118 LM of oblique section through a papillae-like prospective optic tentacle showing clear cytoplasm of proximal retinal receptor cells (PRC) and dark cytoplasm of supporting cells (SPC). Supporting cell processes do not extend proximally between the rhabdomeres (rh). X60

FIG. 119 TEM of oblique section through a young retina showing the presence of proximal retinal receptor cells (PRC), supporting cells (SPC) and prospective distal retinal receptor cells (PDRC). rh, rhabdom. X3700

FIGS. 120-127 TEM longitudinal sections through the apical region of prospective distal retinal receptor cells showing stages of cilia formation.

FIG. 120 Centriolar elements appear in the cytoplasm below the cell surface. zo, zonula occludens. X13,000

FIG. 121 Fiber-like structures (arrows) appear from the base of the basal body and a thin, flat vesicle (arrowheads) becomes juxtaposed over the distal end. X19,000

FIG. 122 The vesicle (arrowhead) enlarges over the basal body. X20,500

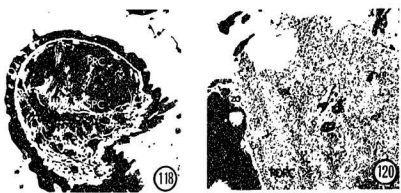
FIG. 123 The distinct vesicle (arrowhead) continues to expand. X19,000

FIG. 124 Microtubules from the basal body along with the membrane enveloping them extend into the vesicle (arrowhead). Arrows indicate terminal fibers. X16,000

FIG. 125 A mushroom-shaped ciliary bud (cb) is formed. X20,000

FIG. 126 A ciliary shaft becomes recognizable with subsequent growth. bb, basal body. X16,500

FIG. 127 The ciliary elements gradually migrate to the cell surface at which stage the membrane of the vesicle is fused with the apical plasma membrane and a rudimentary cilium (c) emerges. bb, basal body. X17,000



sheath. As the microtubules and cell membrane extend into the vesicle the ciliary bud is transformed into a recognizable ciliary shaft (Fig. 126). The ciliary elements approach the surface of the cell until the membrane of the vesicle becomes fused with the apical plasma membrane.

The ciliary shaft begins to broaden and flatten once it has emerged a short distance from the cell surface. This arrangement is seen in Figure 127. The shaft contains a 9x2+0 axoneme complement at this stage of development.

Figure 128 shows the characteristic appearance of a developing distal retinal receptor cell near to the beginning of lens formation. Typically the prospective receptor cells are columnar in shape and contain a basally located nucleus. Mitochondria and small vesicles are numerous, particularly in the distal regions of the cell, and large Golgi complexes are prominent in the supranuclear cytoplasm. Electron-dense lysosome-like inclusion bodies along with free ribosomes and glycogen-like particles are dispersed throughout the cell. Granular ER is profuse.

It is noteworthy that although many short cilia project from the apical plasma membrane at this stage of maturation (Fig. 128), the whorls of lamellae characteristic of the mature organelle are absent prior to the appearance of the lens.

At the time of lens differentiation the ciliary shaft continues to elongate and flatten. As this occurs the microtubules of the axoneme splay apart (Fig. 129), the

ciliary sheath becomes laminate and the whorls of lamellae characteristic of the mature distal retinal receptor cell form (Figs. 129 & 130).

The process of ciliogenesis is continuous. As can be seen in Figure 131 cilia at different stages of growth occur in individual maturing distal retinal receptor cells.

The onset of cilia formation in the differentiating distal retinal receptor cells is coincident with the appearance of a nerve process emanating from the apical surface of each cell. Figure 132 illustrates the characteristic appearance of one such process. Each contains mitochondria, moderately electron-dense bodies, membrane-bounded granules, small vesicles and microtubules. The nerve processes of many prospective distal retinal receptor cells join together above the developing retina to form a nerve bundle (Fig. 133), the future distal optic nerve. It is apparent from serially sectioned eyes that the developing nerve bundle passes down the side of the retina (Fig. 134) and extends a short distance below the pigmented tapetum. At this early stage of maturation the bundle of nerve fibers could be traced no further.

Synapses were not observed in the bundle of developing nerve fibers up to the time when the lens starts to form. Also, junctional complexes joining adjacent developing axons were not seen. However, electron-dense glial-like cell processes do invest and penetrate the developing nerve bundle (Fig. 135).

- FIG. 128 TEM longitudinal section of a prospective distal retinal receptor cell (PDRC) at an early stage of differentiation. Note the presence of short cilia (c) at the apical surface. m, mitochondria; N, nucleus. X4000
- FIG. 129 TEM showing whorls of cilia (wc) at the surface of a distal retinal receptor cell at the stage of lens formation. Note that the microtubules of the axoneme splay apart. bb, basal body. X14,500
- FIG. 130 TEM oblique section through the apical region of a differentiating distal retinal receptor cell at the time of lens formation. The ciliary shaft (arrowheads) flattens and whorls of cilia (wc) form. X17,000
- FIG. 131 TEM oblique section through the apical region of a differentiating distal retinal receptor cell with cilia (c) at different stages of formation. Arrow shows centriole; arrowhead shows basal body (bb) with adjoining distal vesicle. wc, whorl of cilia. X9700

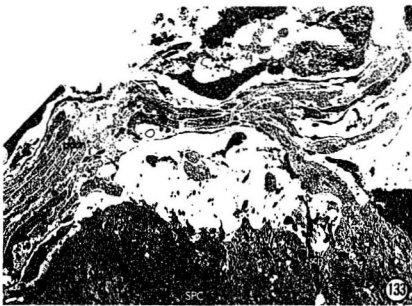
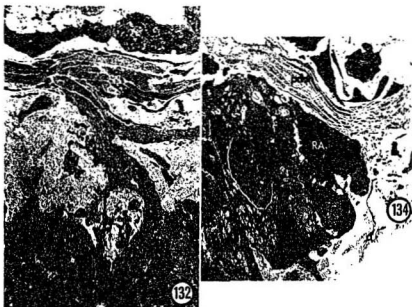


**FIG. 132** TEM longitudinal section through the apical region of a differentiating distal retinal receptor cell (PDRC) showing the characteristic appearance of a newly formed axon (asterisk). pdon, prospective distal optic nerve; scp, supporting cell process. X6000

**FIG. 133** Lower magnification view of Fig. 132 showing axons (asterisk) from a number of prospective distal retinal receptor cells (PDRC) joining above the differentiating retina and passing down the side of the eye as the prospective distal optic nerve (pdon). Note the presence of a short cilium (c). scp, supporting cell process; SPC, supporting cell. X4500

**FIG. 134** TEM oblique section showing the prospective distal optic nerve (pdon) coursing past the side of the retina and the argentea (a). PRC, proximal retinal receptor cell; RA, retinal anlage. X2500

140



SPC

135

At about the time of lens morphogenesis the prospective distal optic nerve subsequently lengthens and passes down the side of the eyestalk towards the circum pallial nerve in the mantle. The former lies very close to the surface epithelium as it courses to the base of the eyestalk (Fig. 136).

When the developing axons enter the mantle each broadens to a club-shaped protuberance (Fig. 137) containing mitochondria, microtubules, variously-sized membrane-bound granules of different densities and clear vesicles. Tight junctions join contiguous developing axonal fibers. The terminal swellings of adjacent axons are closely opposed and although increased membrane densities and small vesicles are observed at these sites, definitive synapses have not been found.

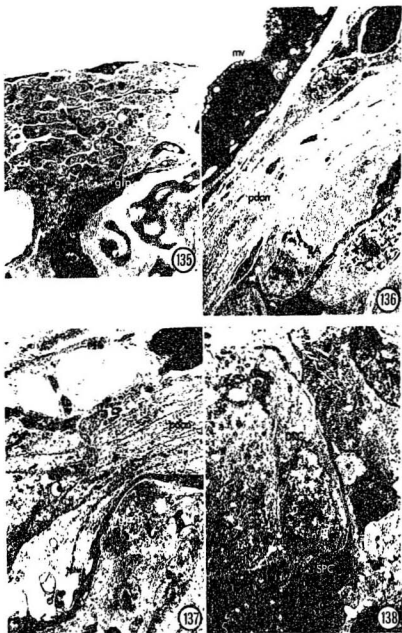
There appears to be a uniformity in pattern among adjacent receptor cells of the distal retina by the time of lens formation. Figure 138 shows the relationship between a distal retinal receptor cell and a supporting cell at this late stage of the development sequence. The large nucleus of the columnar receptor cell lies proximally and is surrounded by abundant granular ER. Electron-dense inclusion bodies and mitochondria are comparably more numerous than in younger cells, and prominent Golgi along with small vesicles, multilamellar bodies and free ribosomes are scattered in the distal cytoplasm. Well-formed whorls of cilia are present and junctional complexes of the zonula

FIG. 135 TEM transverse section showing glial cell processes (glp) investing the young nerve bundle. X12,000

FIG. 136 TEM longitudinal section showing the prospective distal optic nerve (pdon) in close proximity to the eyestalk epithelium. mv, microvilli; RA, retinal anlage. X4500

FIG. 137 TEM longitudinal section showing the club-shaped protuberancy (dashed outline) formed when an axon from a prospective distal retinal receptor cell enters the mantle at the base of the eyestalk. pdon, prospective distal optic nerve. X9200

FIG. 138 TEM longitudinal section showing a supporting cell lying below a differentiated distal retinal receptor cell (DRC). scp, supporting cell process. X4300



adhaerens type bind the apices of the receptor cells to their neighbours and to the supporting cell processes.

Invariably the soma of the supporting cell lies proximal to the distal retina and a large nucleus occupies nearly all of the cell body. The processes leading from each supporting cell are attenuated and penetrate the distal and proximal retinae. Typically, the cytoplasm of the supporting cell is electron-dense and contains mitochondria, small vacuoles, multilamellar bodies and tonofibrils.

The completion of distal retina formation is marked by a broadening of the elongate receptor cells to a cuboidal shape and the movement of their basal nuclei to a central position. Furthermore, there is a progressive addition of cilia and ciliary whorls to each receptor cell and a continuous introduction of prospective receptor cells to the periphery of the distal retina.

#### 5.4. Formation of The Iris

The observations reported here refer to the formation of the pigmented cells that make up the main part of the iris. The non-pigmented ciliated iris cells have not been investigated.

Differentiation of the iris commences prior to the appearance of a lens. The characteristic features of the undifferentiated iris epithelium are illustrated in Figure 139.

Prospective iris cells are first evident in the epithelium of the optic tentacle bordering the retina. At the onset of iris formation prospective iris cells lose their cuboidal form and become more columnar in shape. Their cytoplasm contains a large centrally placed nucleus, cisternae of agranular ER, abundant free ribosomes, glycogen and small membrane-bounded Golgi-derived vesicles. Golgi complexes and numerous mitochondria occupy the supranuclear cytoplasm.

The appearance in the supranuclear cytoplasm of aggregations of variously-sized vesicles marks the beginning of pigment granule formation, many stages of which are revealed in Figures 140 and 141.

Precursory pigment granules are formed from the distended cisternae of agranular ER. Initially the membrane-bounded bodies contain either flocculant aggregations of thin fibers or assemblages of small granules that resemble ribosomes by virtue of their size and staining properties.

As the iris cells mature, Golgi complexes become prominent in the supranuclear cytoplasm while mitochondria become less prevalent. Notably, Golgi-derived vesicles become very abundant between the differentiating pigment granules. With subsequent growth the bounding membranes of the prospective pigment granules enlarge, possibly by accretion, and their contents coalesce to a moderately electron-dense coarsely granular pigment. The shape of the

granular aggregation is very irregular at this intermediate stage of development (Figs. 140 & 141). Furthermore, intragranular synthesis of pigment appears to be extremely variable. As shown in Figure 140 pigment deposition may be more advanced in one area of the prospective pigment granule than in adjacent regions.

Deposition of pigment continues until very electron-dense granules showing the characteristic morphology of a mature pigment granule are formed. The mature pigment granules are usually oval or spherical. Their size is variable.

The intracellular distribution of pigment granules is localized to the supranuclear cytoplasm in immature iris cells. However, with cell maturation the pigment granules, once formed, migrate proximally (Fig. 142) and gradually occupy all regions of the iris cell (Fig. 143).

#### 5.5.

#### Formation of The Lens

The lens of the pallial eye is formed from cells which migrate to a site directly over the retina (Fig. 144). No mitotic figures have been observed at this germinative center throughout lens development.

In the earliest stages of lens formation obtained in this investigation, cells in at least three phases of differentiation can be distinguished.

The distal-most region of the puerile lens is composed

- FIG. 139 TEM longitudinal section showing undifferentiated epithelium of the iris. mv, microvilli; N, nucleus; V, vacuole. X6000
- FIG. 140 TEM oblique section through apical region of a prospective iris cell at an early stage of differentiation showing several stages of pigment granule formation. 1. distended cisternae of SER, 2. membrane-bounded body containing granular material, 3. membrane-bounded body containing irregularly coalesced electron-dense material, 4. mature pigment granule. G, golgi; mv, microvilli. X16,500
- FIG. 141 TEM oblique section through apical region of a prospective iris cell at an intermediate stage of differentiation showing several stages of pigment granule formation. See caption Fig. 140 for description of numbers. G, golgi; m, mitochondria; N, nucleus. X10,800
- FIG. 142 TEM oblique section of prospective iris cells showing distribution of pigment granules (pg). mv, microvilli; N, nucleus; V, vacuole. X13,000
- FIG. 143 TEM oblique section of differentiated iris epithelium. Note the distribution of the pigment granules and the presence of non-pigmented, ciliated iris cell. c, cilia; mv, microvilli; N, nucleus; V, vacuole. X4300

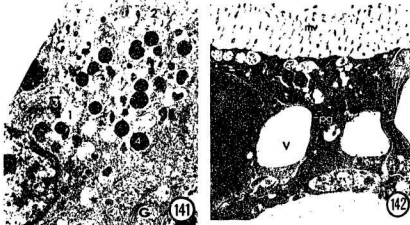


FIG. 144 Composite; TEM longitudinal section of differentiating pallial eye showing elements of the retina, a prospective distal optic nerve (pdon) and a lens in an early stage of formation. An iris and cornea are absent.  
bl, basal lamina; DRC, distal retinal receptor cell; lc, lens cell; mv, microvilli; RA, retinal anlage; SPC, supporting cell. X2900



predominantly of an anlage of lens precursor cells (Fig. 145). These cells, although irregular in shape, are generally elongate and flat. The cell elongation is loosely oriented to extend across the immature lens mass. The nuclei are ellipsoidal to round and are located terminally. In addition to extensive arrays of granular ER, the cytoplasm, which is characteristically electron-dense, also contains abundant free ribosomes, sparse mitochondria and few Golgi complexes. Intercellular spaces separate lateral cell membranes and specialized junctions are absent.

The most striking feature of the lens precursor cell is the appearance of a ciliary structure at the surface of the cell body (Figs. 145 & 146). Closer examination reveals a typical cilium with its basal body (Fig. 147).

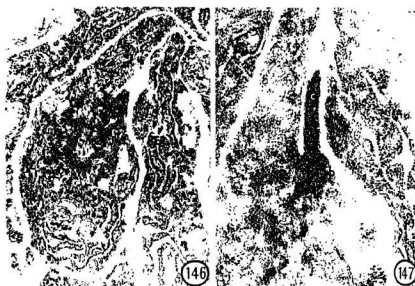
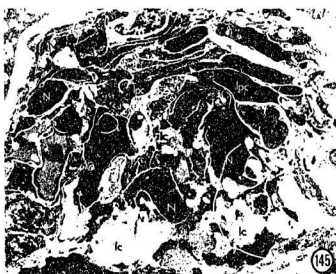
Tonofilaments are located subadjacent to the basal body (Figs. 146 & 148), although ciliary roots and a basal foot are lacking. The axoneme pattern was not evident in the sections examined. Interestingly, the ciliary structures do not persist although their exact fate during subsequent differentiation is uncertain.

Following aggregation the lens precursor cells lose their elongate shape and assume a globular conformation typical of the intermediate-type of lens cell. Most, but not all, of the cells in the intermediate stage of differentiation are located in the middle portion of the immature lens (Fig. 145). The highly indented nuclei of these cells exhibit a variety of profiles depending on the

FIG. 145 Higher magnification of developing lens in Fig. 144 showing lens precursor cells (lpc), intermediate lens cells (ilc) and lens cells (lc). Note the presence of cilia (arrowheads) in the lens precursor cells. N, nucleus. X4000

FIG. 146 TEM oblique section of lens precursor cell showing a basal body (bb) at the plasma membrane and cytoplasmic tonofilaments (tf). M, mitochondria; RER, rough endoplasmic reticulum; X22,500

FIG. 147 TEM oblique section showing short cilium (c) of a lens precursor cell. bb, basal body. X37,000



plane of section. The cytoplasm is excessively rich in granular ER, free ribosomes and small granules, but is poor in mitochondria. Golgi were not observed. Occasionally conspicuous assemblages of fibrous material appear in the cytoplasm of the intermediate stage cells (Fig. 149). Cells containing this material are usually restricted to the periphery of the primordial lens.

As differentiation continues the granular ER dilate and a moderately electron-dense substance appears within the distended cisternae (Fig. 150). Figure 151 shows the particulate nature of this consolidated material upon liberation. Subsequently, the material disperses as discrete granules (Fig. 152), spreads throughout the cell and progressively supplants the cytoplasm (Fig. 153).

Late in the intermediate stage multilamellar bodies and multivesicular bodies appear (Fig. 154). The plasma membrane, although vague, is still visible (Figs. 153 & 154).

The proximal-most region of the developing lens consists of cells in the third phase of differentiation. These recognizable lens cells (Fig. 155) are large, oval and closely applied to each other resulting in greatly diminished intercellular spaces. The plasma membrane is absent. Furthermore, with the exception of an occasional nucleus, no cellular organelles could be found despite prolonged search.

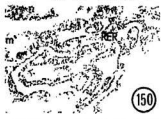
The granular contents are widely dissipated throughout

- FIG. 148 TEM oblique section showing cilium (c) of lens precursor cell and adjacent cytoplasmic tonofilaments (tf). bb, basal body. X56,000
- FIG. 149 TEM longitudinal section showing assemblage of fibrous material in an intermediate-type lens cell. X18,000
- FIG. 150 TEM showing moderately electron-dense material within the distended cisternae of RER. m, mitochondria. X24,000
- FIG. 151 TEM showing particulate nature of consolidated material upon liberation from cisternae. X23,000
- FIG. 152 TEM showing dispersed granular material. X25,000
- FIG. 153 TEM of intermediate lens cell in a late stage of differentiation showing granular material pervading the cell. Arrowheads indicate cell membrane. X25,000

156



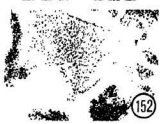
149



150



151



152



153

FIG. 154 TEM oblique section of intermediate lens cell in a late stage of differentiation showing multilamellar bodies (mlb) and multivesicular bodies (mvb) in the cytoplasm. Arrowheads indicate cell membrane. X28,000

FIG. 155 TEM longitudinal section showing differentiated lens cells (lc) with electron-dense consolidations (arrowheads) most prominent at the cell periphery. N, nucleus. X9500

158



154



155

the lens cells. However, occasional discrete electron-dense consolidations occur with the most extensive deposits always associated with the periphery of the cell (Figs. 145 & 155).

The newly formed lens rests on a fine, filamentous basal lamina which appears relatively late in lens formation.

The shape of the developing lens is plano-convex (Fig. 144) unlike the hemispherical-shaped lens in the fully formed eye. Throughout eye development the lens continually increases in size by further application of lens precursor cells to its surface.

#### 5.6. Formation of The Cornea

The cornea is the last component of the pallial eye to differentiate and it develops long after the processes of iris and lens morphogenesis are complete.

Despite many attempts it was not possible to fix tissue during the sequence of cornea differentiation. However, cornea precursor cells were observed during the course of this investigation.

The cornea precursor cells (Fig. 156) are multifarious in size and shape prior to the presence of the lens. Although adjacent cells may differ in electron-density, each rests on a basal lamina and contains a large centrally positioned nucleus, Golgi apparatus, abundant mitochondria, numerous free ribosomes and agranular ER. Many moderately-

sized vesicles containing granular or flocculant material occupy the supranuclear cytoplasm. Intermediate junctions and long septate desmosomes bind adjacent cells together.

Apart from transforming to a cuboidal shape (Fig. 157) and accumulating large cytoplasmic vacuoles at the time of lens formation, no other changes were noted in the cornea of the young eyes examined.

FIG. 156 TEM oblique section showing cornea precursor cells prior to the formation of a lens. bl, basal lamina; G, golgi; m, mitochondria; mv, microvilli; N, nucleus; v, vesicles; V, vacuole; zo, zonula occludens. X12,400

FIG. 157 TEM oblique section of corneal epithelium at the stage of lens formation. lc, lens cell; mv, microvilli; N, nucleus; V, vacuole; za, zonula adhaerens. X4700



163  
CHAPTER SIX

DISCUSSION

PALLIAL EYE DEVELOPMENT

In this study the development of the pallial eye in a scallop, Placopecten magellanicus is described. Although some observations reported in previous studies are confirmed, many of the developmental events do not occur as formerly believed. This investigation clarifies dissimilarities concerning the order of appearance of pallial eye components.

The scallop pallial eye originates at the base of the ophthalmic fold. The earliest reported event in the formation of the eye is the invagination of surface epithelium and subsequent formation of a closed optic vesicle within the ophthalmic groove (Patten 1887; Dakin 1910b; Butcher 1930). The stimulus responsible for prompting pallial eye development through the downgrowth of mantle epithelium and subsequent acquisition of anlage cells is not known and could not be ascertained from the present investigation. Unlike other scallop species the formation of the ectodermally-derived optic vesicle has not been demonstrated in Pecten testae (Küpfer 1916) nor in placopecten magellanicus. However, in P. magellanicus the presence of a papilla-like prospective optic tentacle

containing the retinal anlage and components of the tapetum and argentea is in accord with that observed in all other scallops studied to date (Patten 1887; Dakin 1910b; K  pfer 1916; Butcher 1930).

The precise ordering of the sequence of appearance of the various eye components has been the subject of much confusion. Patten (1887) in a study of Pecten opercularis reported the presence of the argentea and retinal anlagen first followed by the appearance of the lens, the formation of the outer ganglionic cells (=distal retinal receptor cells) and the extention of optic nerve fibers from the circum pallial nerves towards the developing retina. Patten (1887) further observed the appearance of the iris and cornea followed by the formation of the tapetum and lastly, the development of the inner ganglionic cells (=proximal retinal receptor cells).

K  pfer's (1916) account of eye development in Pecten agreed with that of Patten (1887) in two respects; the retinal anlage was present at the stage of argentea formation and distal retinal receptor cells differentiated well before proximal retinal receptor cells. However, K  pfer (1916) noted the appearance of both the tapetum and argentea prior to the development of the retinae. Furthermore, he reported that differentiation of the distal retina was followed by the formation of the lens, iris, cornea and proximal retina, respectively.

Although Butcher (1930) was non-committal on the order

of appearance of the two retinae, he concluded their presence was coincident with that of the pigmented tapetum. In addition, Butcher noted that the argentea was derived from the tapetum followed by the differentiation of the lens, cornea, iris and optic nerves. Butcher was the first to correctly report the outgrowth of the optic nerves from the retinae towards the circumpallial nerve.

While the present investigation does not establish the sequence of appearance of the eye components unequivocally, the available evidence does indicate that the developmental pattern in Placopecten magellanicus is not consistent with that reported for other scallops.

It is with prudence that one draws conclusions regarding dynamic events from static images viewed in micrographs, even when the latter are obtained in progressive series. However, in the present investigation the following conclusions are warrented.

Preparations of the earliest stages of pallial eye development obtained for Placopecten magellanicus contained elements of the tapetum, argentea and proximal retina. Although there is little doubt that the reflecting argentea is formed by special cells from the pigmented tapetum, it should be emphasised that the simultaneous or successive appearance of the tapetal and retinal anlagen has not been effectively answered.

Nevertheless the present study has, for the first time, clearly demonstrated that morphogenesis of the pallial eye

goes from the sequential differentiation of the tapetum, argentea and proximal retina (inclusive of the development of the proximal retinal receptor cells with the ordered appearance of the apical conical processes, rhabdomeric microvilli and axons prior to the presence of supporting cells) to the formation of the distal retina (inclusive of the simultaneous migration of prospective distal retinal receptor cells and supporting cells from the retinal anlage and the differentiation of the distal retinal receptor cells beginning with the acquisition of cilia and the outgrowth of axons), followed by the appearance of the proximal optic nerve and the formation of the iris. The development of the lens is coincident with the appearance of whorls of cilia on the distal retinal receptor cells and the connection of the distal optic nerve to the circum pallial nerve. The cornea is the last optic structure to form.

The mode of synthesis of the reflecting crystals in the developing argentea cells of invertebrates has not been previously described. In Placopecten magellanicus young argentea cells acquire unique circular bodies comprising complex arrays of membranes which gradually transform into ordered, oblong compartments between which strips of cytoplasm are compressed. These orthogonal chambers are a template for crystal growth. Whether the surrounding cytoplasm secretes into the chambers materials which create a chemical microenvironment that favors the formation of

crystals, or whether the crystals form independently of the influence of the surrounding cellular milieu is not known.

As argentea cell differentiation continues, the newly formed stratified crystal arrays separate from the circular bodies and progressively displace the cytoplasm. Ultimately the argentea cells fill with multiple layers of reflecting crystals and become devoid of organelles. Comparably, Barber & Land (1966) and Barber *et al.* (1967) demonstrated the presence of mitochondria, vesicles and lamellae in the argentea cells of Pecten maximus.

Interestingly, Melamed & Trujillo-Cenóz (1966) reported the presence of a complicated system of internal membranes in the cytoplasm compressed between the reflecting crystals in the tapetum of the secondary eyes of the wolf spiders Lycosa thorelli and Lycosa erythrogaster. Whether this may be taken to imply the existance in spiders of a comparable phenomenon for the synthesis of crystals is a matter of conjecture.

The mechanisms by which the developing argentea cells actually control the regular spacing and positioning of the repeating crystalline elements as well as the precise dimensions of the crystals and cytoplasmic interspaces are intriguing problems that have yet to be confronted.

During pallial eye development in Placopecten magellanicus the retina thickens. This is due to a combined increase in the size and number of retinal cells. Although

it is now established that mitosis does not occur in the retina, it is observed in the peripheral anlage from which the new receptor cells are derived. It is noteworthy that the formation of receptor cells in the pallial eye is not synchronous over the entire retina, but progresses from the prospective optic axis to the edges. This mode of retinal growth results in the oldest photoreceptive cells located centrally and younger cells marginally.

Rhabdomeric photoreceptive cells undergo dramatic changes during development of the proximal retina. These changes involve lengthening of the cell bodies and conical processes and the formation of microvilli along the plasma membrane of the latter.

The differentiation of microvilli on the apical conical processes of Placopecten magellanicus proximal retinal receptor cells initiates with the cisternae of agranular ER. The cisternae either dilate into vacuoles by accrual of material through fusion with Golgi-derived dense-cored vesicles or, less frequently, transform into multilamellar bodies and subsequently migrate to the cell surface to be incorporated into the rhabdomeric membrane forming short, irregular microvilli.

This interpretation of the sequence of events occurring during production of microvilli in Placopecten magellanicus is similar to that advanced for membrane synthesis obtained from studies on the renewal of rhabdomeric membrane during

dark adaptation. The implication of cisternae of ER as the source of new photoreceptoral membrane has been demonstrated in many invertebrates including arthropods (Eguchi & Waterman 1976; Itaya 1976; Blest 1978; Blest & Day 1978; Stowe 1980, 1981; Blest & Price 1981; Toh & Waterman 1982), molluscs (Kataoka & Yamamoto 1981; Eakin & Brandenburger 1982; Kataoka & Yamamoto 1983), echinoderms (Brandenburger & Eakin 1980) and a polychaete (Brandenburger & Eakin 1985) implying that a comparative morphological process likely exists between microvilli production in P. magellanicus differentiating receptor cells and rhabdomere assembly during daily membrane turnover in other invertebrates.

Itaya (1976) and Stowe (1980), respectively, observed that ER-derived vacuoles and tubules become elongated in the same direction as the prospective microvilli. Comparably, Toh & Waterman (1982) report that the swollen saccules of ER located at the villus base are most frequently oriented parallel to the future microvilli. Although ER-derived vacuoles are seen in Placopecten magellanicus, there appears to be no predictable pattern of alignment with respect to the orientation of future microvilli. This supports the inference by Stowe (1980) that, notwithstanding the commonality of ER cisternae in microvilli membrane synthesis, the actual mode of assembly of microvilli from ER elements is variable. Moreover, it is noteworthy that fusion of the vacuoles to the bases of the rhabdomeric microvilli appears to be the predominant method of

incorporation of membrane material in P. magellanicus and other invertebrates (Itaya 1976; Stowe 1980; Toh & Waterman 1982; Burr 1984; Brandenburger & Eakin 1985).

Interestingly, multilamellar bodies which are typical of the membrane degradative system during membrane turnover (Eguchi & Waterman 1976; Itaya 1976; Blest & Day 1978; Stowe 1981; Toh & Waterman 1982) are present in Placopecten magellanicus differentiating proximal retinal receptor cells during formation of microvilli. Eakin and Brandenburger (1982) regard the whorls of membranes in the dark adapted photosensory cells of the snail Helix aspersa a result of membrane overproduction. It is quite conceivable that the multilamellar bodies observed in P. magellanicus could be an indicator of such a process, particularly considering the abundance of precursor material presumed in the cell soma prior to rhabdomere differentiation.

Alternatively the presence of multilamellar bodies in the conical processes of Placopecten magellanicus might be an ultrastructural indication of two events occurring simultaneously: rhabdomere differentiation complicated by the process of membrane turnover during daily cycling. Whether, in fact, a response to daily modulated rhabdomeric membrane turnover proves to exist in P. magellanicus, how such a response is triggered and exactly when it is turned on are fundamental problems which remain to be determined.

Finally, the argument that multilamellar bodies might be an artifact resulting from inadequate fixation is not

untenable.

Photoc vesicles responsible for storage and transport of photopigment precursors to rhabdomic microvilli in gastropod molluscs (Eakin & Brandenburger 1967, 1970, 1975, 1976, 1980, 1982; Brandenburger & Eakin 1970; Eakin 1972; Brandenburger 1977) were not observed in Placopecten magellanicus. Therefore, the photopigment must be delivered to the rhabdomic membrane by another, yet unidentified, route. It is conceivable that the role of the Golgi-derived dense-cored vesicles is two-fold in P. magellanicus. Apart from being a potential source of vacuole membrane, the vesicles might contain photopigment precursors. Upon fusion of the vesicles with the cisternae of ER, the resulting vacuolar structures and associated photopigment would then be transported to the rhabdomic surface and incorporated into new microvilli membrane.

Although there is no firm evidence that photopigment is synthesised by the Golgi in Placopecten magellanicus, the role of the Golgi in photopigment production has been supported by other investigators. Indeed, Eakin & Brandenburger (1970), in a study of the photosensory cells in Helix aspersa, showed that the photopigment was derived from the Golgi. More recently Brandenburger (1977) alluded to the origin of photopigment in the Golgi apparatus and Eakin & Brandenburger (1982) indicated that synthesis of rhodopsin and retinochrome occurred in the ER and Golgi centers.

Another interesting observation that emerged from this investigation is the presence of cilia, either singly or in small groups, on the apical conical processes of the proximal receptor cells. Centrioles are encountered in anlage cells located at the edges of the developing retina and at the apices of the young differentiating proximal receptor cells. However, ciliary precursor figures were not observed in the developing apical conical processes. This contrasts with the situation in differentiating distal receptor cells where many stages of cilia formation are clearly represented.

The inability to distinguish stages of cilia development in the proximal receptor cells is most likely attributable to the inherent scarcity of cilia on the apical conical processes. It is also possible that their absence may reflect the rapidity with which the dynamic process of ciliogenesis occurs.

The presence of cilia and the extensive system of striated roots in differentiating rhabdomeric photoreceptive cells of Placopecten magellanicus is perplexing.

Vanfleteren and Coomans (1976) explain the presence of cilia and prominent root structures encountered in many rhabdomeric photoreceptive cells as morphogenic remnants of evolution and further contend that the ciliary structures are involved in rhabdom formation. These investigators (Vanfleteren & Coomans 1976; Coomans 1981; Vanfleteren 1982) maintain that all photoreceptors are ciliary and have

advanced the theory that proliferation of the receptoral membranes in both ciliary and rhabdomeric photoreceptor cells is induced by ciliary structures. After initiating the elaboration of the photoreceptive organelle, the ciliary structures may persist (ciliary type photoreceptors) or may become abortive (rhabdomeric type photoreceptors). Hense, rudimentary ciliary structures (centriole, basal body, ciliary root) may be present in rhabdomeric photoreceptive cells (Vanfleteren 1982) and, furthermore, serve an organizing role in microvillar differentiation of the rhabdomere (Vanfleteren & Coomans 1976).

It has been argued that induction of rhabdomeric microvilli by ciliary structures has not been established (Eakin 1982). However, Home (1975) alludes to the influence of a ciliary bud in rhabdomere differentiation in the pupa of Coccinella septempunctata. Furthermore, Muñoz-Cuevas (1975, 1984) has proposed a model for ciliary induction of rhabdomeric differentiation from ultrastructural data collected during studies of embryonic development in the Harvestman, Ischyropsalis luteipes. Vanfleteren (1982) interprets this model as evidence for the induction theory.

Although Eakin (1982) does concede the possibility of ciliary structures serving as inductive stimuli in microvilli formation, he prefers to regard the short cilia in rhabdomeric photoreceptive cells of cerebral ocelli as adventitious structures (Eakin 1979, 1982, 1985), ascribing their presence to the developmental origin of the retina

from ciliated ectoderm (Eakin & Brandenburger 1967; Eakin 1968, 1979, 1982; Eakin et al. 1977), and he considers the appearance of ciliary vestiges in integumentary ocelli as cenogenetic (ie. newly evolved) structures (Eakin et al. 1977; Eakin 1979, 1982). Furthermore, Eakin attributes the presence of well developed ciliary root structures in some rhabdomeric photoreceptive cells to a mechanical role, suggesting they serve as support rods (Eakin & Brandenburger 1985).

The fact that short cilia and an extensive root system are present in the differentiating proximal retinal receptor cells of Placoplecten magellanicus at the stage of rhabdomere formation suggests they indeed serve some definitive role. Clearly, the highly developed root system might serve as a support mechanism to aid the proximal receptor cells in maintaining spacial and structural integrity owing to the length of the cell bodies.

The contention that photoreceptor differentiation is always dependant on ciliary induction has no direct supporting evidence from the current investigation. However, the close contact of ciliary structures with developing microvilli in a variety of rhabdomeric photoreceptors (Home 1972, 1975; Muñoz-Cuevas 1975) and their appearance during early developmental stages followed by their disappearance later on (Wachmann & Hennig 1974; Eisen & Youssef 1980; Vanfleteren 1982) offers strong circumstantial evidence for the induction theory.

In view of the fact the the rhabdomeric proximal photoreceptors of the scallop are responsible for fundamental phototoxic behaviours by serving to monitor environmental light intensity (Land 1965, 1966a, 1968, 1978) it is hardly surprising that they develop before the ciliary distal photoreceptors.

Moreover, the existence of a pallial eye containing a tapetum, argentea and retina composed entirely of proximal 'on' receptor cells may be of some biological importance to scallop spat that have lost their larval ocelli and are starting to form mantle eyes. Light entering the immature photoreceptors would be diffuse due to the absence of a dioptric apparatus, and directional sensitivity would be severely inhibited by the lack of an iris although the pigmented tapetum may offer limited directional appreciation by filtering light entering from the back of the eye. In addition, much of the light entering the immature photoreceptor would be reflected back through the proximal retina by the argentea. This is of particular importance to vision in dim illumination.

Thus, from a functional viewpoint, the immature photoreceptor might be continuously capable of perceiving the presence and the effective intensity of light in the surrounding environment. The ability to interpret the distribution of brightness has important implications towards orientation behaviours in the young scallop, notwithstanding the roles served by the olfactory and

tactile senses.

The mode of formation of photoreceptive cilia in the differentiating distal receptor cells of the retina of Placopecten magellanicus is similar in some respects to events described by Stubblefield & Brinkley (1966) during ciliogenesis in Chinese hamster fibroblasts and by Sorokin (1968) in epithelial cells from the lungs of faetal rats.

Essentially, the distal end of a cilia-forming centriole in the supranuclear region of the cell, formed either from centriole division or de novo from fibrogranular aggregates (Sorokin 1968; Dirksen 1971; Friedmann & Bird 1971; Thornhill 1972; Gordon & Lane 1984; Gould et al. 1986; Menco & Farbman 1987), comes into close proximity to a Golgi-derived (Sorokin 1962, 1968; Stubblefield & Brinkley 1966) cytoplasmic vesicle. The shape of this primary ciliary vesicle (terminology of Sorokin 1962) may be rounded (Sorokin 1962, 1968; Stubblefield & Brinkley 1966; Such 1969) or flattened (Dirksen 1971; Home 1975) as in Placopecten magellanicus.

Concurrently thin longitudinally arranged marginal fibers are generated from the proximal end of the centriole. These fibers persist in the mature cilium. Such fibers have not been reported in any accounts of cilia formation to date. Although rootlet structures have been reported in a variety of cell types and are suggested to be involved in ciliary support and anchorage (Friedmann & Bird 1971; Carr &

Toner 1982; Holley 1984), it is unlikely that the fibers in Placopecten magellanicus play a similar role. However, it is not improbable that the fibers might serve to assist in stabilizing the centriole in its alignment perpendicular to the apical plasma membrane during ciliogenesis. The consistent orientation of the centriole as it travels to the cell surface supports this idea.

Alternatively, it is possible that the fine fibers represent vestigial or rudimentary ciliary rootlets. The thin fibers in Placopecten magellanicus are not striated. This contrasts with descriptions of typical rootlet structure in which the fine rootlet fibers display a pattern of transverse striations (Friedmann & Bird 1971; Home 1972, 1975; Wachmann & Hennig 1974). If the fibers in the differentiating receptor cells of P. magellanicus are atavistic, they would be of no functional significance.

Subsequently, microtubules develop from the distal end of the centriole and lengthen, together with the adjoining vesicle membrane, into the resultant ciliary sheath. In this way a ciliary bud is formed. Structures of this type have been well documented either in the cytoplasm of the cell (Sorokin 1962, 1968; Stubblefield & Brinkley 1966; Such 1969; Dirksen 1971; Home 1975) or recessed in the plasma membrane at the surface of the cell (Nilsson 1964; Eakin & Brandenburger 1967; Friedmann & Bird 1971; Thornhill 1972; Juberthie & Muñoz-Cuevas 1973).

The elongation of the ciliary shaft within the vesicle

is accompanied by migration of the pre-ciliary structure towards the apical plasma membrane. It is not exactly known how this is achieved (Gordon & Lane 1984). However, Curtis *et al.* (1987), in a study of ciliogenesis in the ferret, Mustela putorius furo demonstrated ciliary necklace particles within the apical plasma membrane of ciliated epithelial cells and suggested that they might function to initiate the process of ciliogenesis and signal the movement of procentrioles in the apical cytoplasm. Although the existence of intramembranous ciliary necklace particles in Placopecten magellanicus was not ascertained, Burr (1984) states that the particles are universally present in all cilia.

The membrane of the ciliary sheath unites with the plasma membrane when the pre-ciliary structure comes to rest at the surface of the cell (Sorokin 1962, 1968) and the short ciliary shaft emerges. Distal filaments, reported to link the outer doublet microtubules to the ciliary membrane throughout ciliary growth (Dentler 1980) and purported to be responsible for outer doublet microtubule assembly (Dentler 1980; Portman *et al.* 1987), are not present in the emergent cilia of the distal retinal receptor cells of Placopecten magellanicus. It may be speculated that the axonemal microtubules in P. magellanicus, which extend to the tips of the ciliary shafts, are formed *in situ* as reported in epithelial cells from the lungs of faetal rats (Sorokin 1968). Another possibility is that the microtubules might

be assembled from materials incorporated through the fusion of small vesicles found within the ciliary shaft (Sorokin 1962, 1968). Unfortunately, neither of these mechanisms of microtubule construction can be corroborated for P. magellanicus from the available data.

It has been suggested that the distal filaments may serve also to maintain the organization and stability of the microtubule doublets during growth of the cilia (Portman *et al.* 1987) and to prevent billowing of the ciliary membrane (Dentler 1980). Indirect support for these roles comes from observations that the absence of distal filaments in the cilia of the distal retinal receptor cells of Placopecten magellanicus is accompanied by a disordered arrangement of axonemal microtubules within the developing shaft during ciliary growth and in the fully-formed photoreceptoral organelle. Moreover, the ciliary membrane in scallop distal retinal receptor cells either bulge into sacs (Barber *et al.* 1967; Land 1968; Eakin 1972, 1979) or are expanded and compressed into sheet-like lamellae (Powell 1984).

The present study has demonstrated that ciliogenesis is initiated before the distal retinal receptor cells are innervated. However, development of the ciliary whorls of lamellae, which contain the visual pigment (Eakin 1963, 1965, 1968, 1972; Barber *et al.* 1967), does not occur until the axons growing out from the receptor cells have made contact with the circum pallial nerve and consequently with

the central nervous system. This suggests that a high degree of structural differentiation is necessary for sensory function.

Furthermore, innervation of the distal retinal receptor cells occurs after cells of the iris begin to differentiate and is coincident with lens formation. The optical system of scallops is based on a lens/argentea system (Land 1965, 1968). In order for the distal retina to receive an image light must first be reflected from the argentea (Land 1965, 1966b, 1968, 1981, 1984). This structure is already in place at the back of the eye of Placopecten magellanicus prior to distal retinal receptor cell differentiation. For the image to be clear and for visual acuity to be maximized, a lens must be present to correct for spherical aberration (Land 1965) as light passes towards the argentea. Indeed, a lens is present by the time the distal retinal receptor cells of P. magellanicus acquire neural connection. Moreover, coincident with the presence of the iris, the lens/argentea combination and neural connection is the existence of a well developed receptor surface, consisting of whorls of ciliary membranes.

The implications here are twofold. At the stage of distal retina formation the young pallial eye of Placopecten magellanicus not only possesses the ability to collect photons via the lens/argentea system in combination with the ciliary receptoral surfaces of the distal retinal receptor cells, but also is capable of transmitting information about

the surrounding environment to the central nervous system by way of the distal optic nerve.

It can be speculated that individual distal retinal receptor cells might serve as 'off' receptors once neural connection with the CNS is achieved, although this remains to be confirmed by electrophysiological data. Consequently the initial function of a distal retina containing a few receptor cells would be to detect an overall decrease in light intensity and evoke a shadow response. As more distal receptor cells differentiate in the young retina, decreases in light intensity would be perceived by successive cells from particular sections of the visual field and hence gradual improvements in movement detection effected. 'Form' vision is likely precluded.

It is immediately evident that at early stages of retinal development light is able to pass through the distal retina from many angles and as an unfocused beam. Consequently image contrast will be diluted and the quality of the received image will be poor. However, with the presence of a fully differentiated iris to restrict the angle over which the retina can receive light, directional sensitivity would improve.

The ability of a pallial eye to detect an image and the degree of sensitivity and resolution of the distal retina is further dependant on the following:

1. the development of a cornea to permit unimpeded photon influx, and

2. the addition of more distal retinal receptor cells to increase the receptoral area of the distal retina thus allowing for improved spatial resolution.

Generally, results from the present investigation are in accord with previous reports of lens development. However, the electron microscopic observations on Placopecten magellanicus provide a description of the process of lens formation in the scallop pallial eye in greater detail.

In his monograph K  pfer (1916) reported that in Pecten prospective lens cells originated in the mesoderm and migrated into the eye papilla to comprise the lens anlage. Butcher's (1930) histological observation that lens cells of Pecten gibbus borealis were derived from the connective tissue rather than from the ectoderm as in cephalopod molluscs (Arnold 1967; Bon et al. 1967; Brahma 1978) confirmed K  pfer's description.

The lens anlage of Placopecten magellanicus is similarly derived from cells originating in the mesoderm. These cells migrate into the anterior chamber of the optic vesicle and aggregate between the surface epithelium of the optic tentacle and the developing retinae as the lens anlage. Contrary to the reports of K  pfer (1916) the anlage cells do not undergo mitosis and contradictory to Butcher's (1930) observations the lens anlage cells are not pigmented.

Initially the oldest lens cells are located proximally

and the youngest cells distalmost. As growth of the lens progresses new cells are applied to the surface of the developing mass promoting a central to peripheral gradient of maturation and perhaps influencing the plano-convex shape of the immature lens. These observations are consistent with those of K ipfer (1916) who reported that the cortex of the lens remains embryonic.

Typical cilia exceeding 1.5 m in length have been described in early ectodermally-derived lens cells of vertebrates (Zwaan 1975). The present investigation shows clearly that the lens precursor cells of Placopecten magellanicus possess cilia. This feature is unique and has not been reported in the developing cellular lenses of other invertebrates studied to date.

What functional role, if any, a cilium may serve in a lens precursor cell is unknown. In view of the fact that rudimentary cilia occur in a variety of cells of mesodermal origin including fibroblasts, pericytes and histiocytes (personal observations) as well as in chondrocytes and osteocytes (Eakin 1979, 1982), it is perhaps hardly surprising that they are present in lens anlage cells.

The transformation of lens precursor cells into intermediate lens cells and ultimately into fully differentiated lens cells is characterized by the production of non-membrane bounded granular material presumably representing lens protein. The Golgi apparatus has been implicated as the source of lens material both in the

cellular-derived lenses of the cephalopod molluscs Loligo pealii and Octopus vulgaris (Arnold 1967) and in the secreted lens of the pulmonate snail Helix aspersa (Eakin & Brandenburger 1967). However, Brahma (1978) postulated that polyribosomes accounted for lens protein production in Loligo vulgaris, Sepia officinalis and O. vulgaris. The synthesis of lens proteins in Placopecten magellanicus appears also to involve the ribosomes. The newly precipitated lens protein material passes into the cisternae of the endoplasmic reticulum where it is concentrated and isolated from the cytoplasm. Protein synthesis proceeds until the membranes of the ER cisternae are lost and the granular material is liberated eventually replacing the cytoplasm of the lens cell. The present investigation provided no evidence that the Golgi centers served a role in lens protein synthesis. Indeed, due to the paucity of these organelles in developing lens cells, it is unlikely that the Golgi are associated with the production of the lens material in P. magellanicus.

Coincident with the accumulation of granular material in the developing lens cell is a reduction in the number of cytoplasmic organelles and their subsequent disappearance. The diminution of organelles during lens cell formation is a widespread phenomenon and has been reported to occur in the rat lens (Leeson 1971), in cephalopod lenses (Arnold 1967; Brahma 1978) and in chick lenses (Modak & Perdue 1970).

A final note of interest on lens formation in

Placopecten magellanicus is the absence of junctional complexes in differentiating lens cells. In their place are intermittent complex interdigitations which invest adjacent lens cells. These interlocking processes reportedly serve to stabilize the lens structure (Leeson 1971).

## RESULTS

## LARVAL PHOTORECEPTORS

Each veliger larva of Placopecten magellanicus, just prior to settlement, possesses a pair of photosensory organs (ocelli) each of which is located in the body wall of a gill cavity near the base of the velar lobes (refer to Fig. 158). The ocelli are conspicuous as black spheres positioned dorsal and posterior to the center of the almost transparent shell valves (Fig. 159).

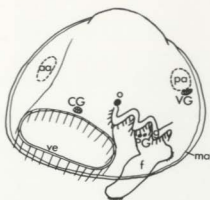
The larval ocelli are open epidermal invaginated pigment-cups. At least two different types of cells make up the photoreceptive organ. These are pigmented cells that bear a deep concavity in the apical surface and non-pigmented cells with at least 3 cilia per cell. The relationship of these two cell types is shown diagrammatically in Figure 160.

The pigment-cup is formed by a single cell containing a dense granular cytoplasm. The pigmented cell is characterized by the possession of many variously sized melanin-like, membrane-bounded, spherical granules of pigment (Fig. 161). Often an electron-lucent space, probably artifactual, surrounds the granule. The granules are not uniformly dense (Fig. 162), and whilst the majority

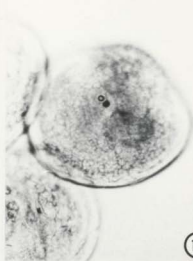
FIG. 158 Schematic diagram of pediveliger larva of Placopecten magellanicus illustrating the relationship of the ocellus (o), cerebral ganglion (CG) and visceral ganglion (VG). The positions of the foot (f) and the adductor muscles are also shown. aa, anterior adductor muscle; g, gill; ma, mantle; pa, posterior adductor muscle; PG, pedal ganglion; ve, velum.

FIG. 159 A photograph of a glutaraldehyde fixed veliger larva of Placopecten magellanicus indicating position of ocellus (o). X880

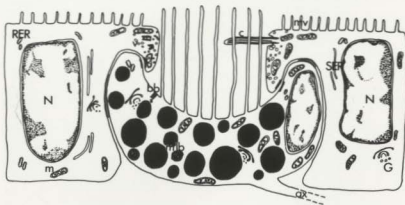
FIG. 160 Schematic diagram of a section through the photoreceptor of Placopecten magellanicus. Long microvilli (mv) arise from the pigmented cell and extend beyond the opening of the ocellar cavity. The non-pigmented cells bear cilia (c). ax, axon; bb, basal body; G, golgi; m, mitochondria; mlb, multilamellar body; N, nucleus; RER, rough endoplasmic reticulum; SER, smooth endoplasmic reticulum; v, vesicles.



158



159



160

are strongly osmophilic, some contain less electron-dense granular material (Figs. 161 & 162). The granules are distributed throughout the cell irrespective of their electron density. Golgi bodies and mitochondria occupy regions between the pigment granules.

The shape of the pigmented cell ranges from circular to U-shaped in section. The cell bears a deep concavity in its apical surface which opens to the gill cavity. This depression extends almost to the base of the cell. The U-shaped cavity has a breadth of approximately 4 $\mu\text{m}$  and a height of approximately 2.5 $\mu\text{m}$ .

Microvilli pack the lumen of the cavity (Fig. 163). As many as 110 microvilli have been observed in frontal sections through the lumen of the cavity. They are approximately 4 $\mu\text{m}$  in length and 0.1 $\mu\text{m}$  in diameter, originate directly from the pigmented cell surface inside the cavity (Fig. 164), are uniform in size and shape, aligned in moderately straight arrays (Fig. 165), and all appear to be oriented in the same direction (ie. pointing towards the opening of the pigment-cup). They appear to be circular in cross section (Figs. 163 & 166). The interiors of the microvilli often appear granular and vary in electron density from clear to electron-dense. The microvilli extend through the neck of the pigment-cup beyond the epidermal surface (Fig. 165).

A profile of a basal body is evident in the cytoplasm below the distal surface of the cavity (Fig. 167). Ciliary

FIGS. 161-165 Larvae were postfixed in OsO<sub>4</sub> containing K<sub>3</sub>Fe(CN)<sub>6</sub>, en bloc stained and embedded in LR White resin.

FIG. 161 TEM of an oblique section through the pigmented cell of an ocellus showing the U-shaped ocellar cavity (oc) and the presumptive axon (\*). c, cilia; gc, gill cavity; NPC, non-pigmented cell. X6000

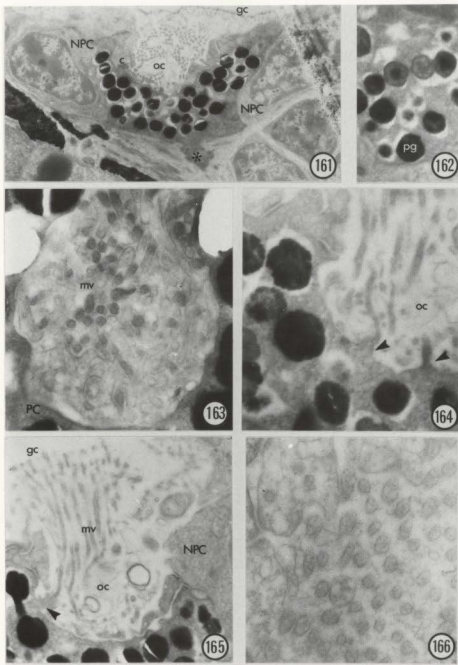
FIG. 162 TEM of pigment granules (pg). X11,000

FIG. 163 TEM of normal section showing microvilli (mv) of pigmented cell (PC) in the lumen of the ocellar cavity. X30,500

FIG. 164 TEM of cross section showing long microvilli originating at the distal surface of the pigmented cell (arrowheads) and extending into the ocellar cavity (oc). X25,000

FIG. 165 TEM of cross section showing array of pigmented cell microvilli (mv) extending through the aperture of the ocellar cavity (oc), beyond the epidermal surface and into the gill cavity (gc). Arrowhead indicates microvillus originating from surface of pigmented cell. NPC, non-pigmented cell. X14,500

FIG. 166 TEM of cross section of pigmented cell microvilli. Embedded in LR White resin. X44,500



rootlets and other ciliary structures were not observed in the pigmented cell.

The nucleus of the pigmented cell is ovoid (Fig. 168) and lies next to the cell membrane at the distal end of the pigment-cup. Many mitochondria and free ribosomes are distributed around the nucleus. Multilamellar bodies (Fig. 169) are occasionally present in the proximal portion of the cell and short, granular ER occur in the peripheral regions.

A narrow cell process or possible axon (Fig. 161) extends from the base of the pigmented cell possibly converging with a clear process with the aspect of a nerve fiber (Fig. 170). Synapses have not been observed. The precise origin of the clear process, which contains microtubules, mitochondria and small vesicles, is not known although it was followed in serial sections to the level of the cerebro-pleural-visceral commissure. The latter arises from the cerebral ganglion (Fig. 171).

The pigmented cell is surrounded by at least four cells which are devoid of pigment. The non-pigmented cells (Fig. 172) are continuous with the surface epithelium of the gill cavity and bear short, straight microvilli, measuring less than  $0.6\mu\text{m}$  in length, on the distal cell surface (Figs. 169 & 172). A thin coat of mucus is supported by the apical aspect of the microvilli (Fig. 169). These microvilli do not contribute to the contents of the ocellar cavity. An extension of the lateral surface of each non-pigmented cell projects over the rim of the pigment-cup and extends into

FIGS. 167-172 Larvae were postfixed in  $OgO_4$  containing  $K_3Fe(CN)_6$ , en bloc stained and embedded in LR White resin.

FIG. 167 TEM of oblique section showing apical region of pigmented cell and ocellar cavity (oc). Note the presence of a basal body (arrowhead) at the cell surface. X14,500 Inset shows higher magnification view of basal body (bb). X24,000

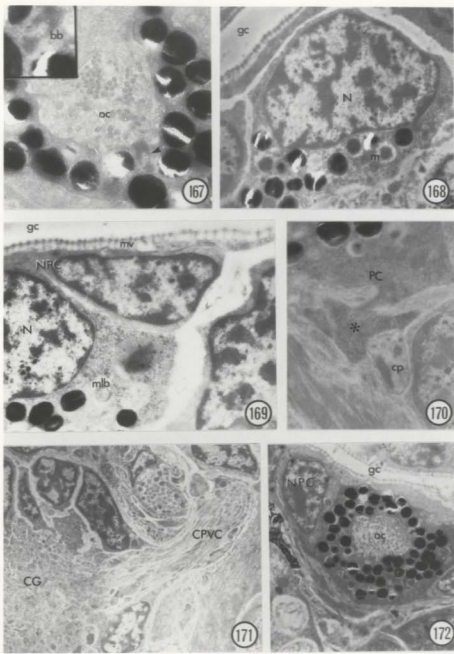
FIG. 168 TEM of nucleus (N) of pigmented cell. gc, gill cavity; m, mitochondria. X9000

FIG. 169 TEM of oblique section showing a multilamellar body (mlb) in the perinuclear cytoplasm of the pigmented cell and short microvilli (mv) extending from the distal surface of a non-pigmented cell (NPC). gc, gill cavity; N, nucleus. X12,500

FIG. 170 TEM of cross section showing presumptive axon (\*) of pigmented cell (PC) converging with a clear process (cp) of a nerve fiber. X14,500

FIG. 171 TEM of cerebral ganglion (CG) and cerebral-pleural-visceral commissure (CPVC) of Placoplecten magellanicus. X4600

FIG. 172 TEM of a larval photoreceptor showing a non-pigmented cell (NPC) adjacent to the pigmented cell. The non-pigmented cell bears short microvilli on its surface. gc, gill cavity; oc, ocellar cavity. X5300



the cavity (Figs. 161 & 173). Contacts between the luminal margin of the pigment-cup and the non-pigmented cells involve zonula adhaerens and septate junctions.

At least three cilia, each showing a 9x2+2 axoneme pattern, arise from the extension of each non-pigmented cell (Fig. 174). In almost all instances the cilia are observed to extend across the aperture of the pigmented cell and bend into the lumen of the cup (Fig. 175) where they project between the microvilli (Fig. 176). Less commonly, the cilia project from the margin of the pigment-cup into the gill cavity. Ciliary rootlets and a basal foot were not observed. A circumciliary space encloses the basal body (Figs. 176 & 177).

The nucleus of the non-pigmented cells is large and occupies the center of the cell (Fig. 172). Mitochondria are distributed throughout the non-pigmented cell but are generally concentrated in the region of the distal plasma membrane, along with aggregations of small membrane-bounded vesicles of various electron densities (Figs. 173 & 176). The cytoplasm of the non-pigmented cells also contain perinuclear Golgi complexes, granular and agranular ER, and free ribosomes. Axons were not observed arising from the non-pigmented cells.

Innervation of the photosensory organ originates at the cerebral ganglion (Figs. 171 & 178). The cerebral ganglion is a spherical structure located in the antero-ventral aspect of the larva (refer to Fig. 158) immediately below

FIG. 173 TEM of oblique section showing lateral surfaces of non-pigmented cells (NPC) projecting into the ocellar cavity (oc). v, vesicles. X16,000\*

FIG. 174 TEM of cross section showing basal bodies (arrowheads) of three cilia in non-pigmented cell (NPC). gc, gill cavity; m, mitochondria; pg, pigment granule. X24,000 Inset shows 9x2+2 axoneme pattern of cilium. X25,000

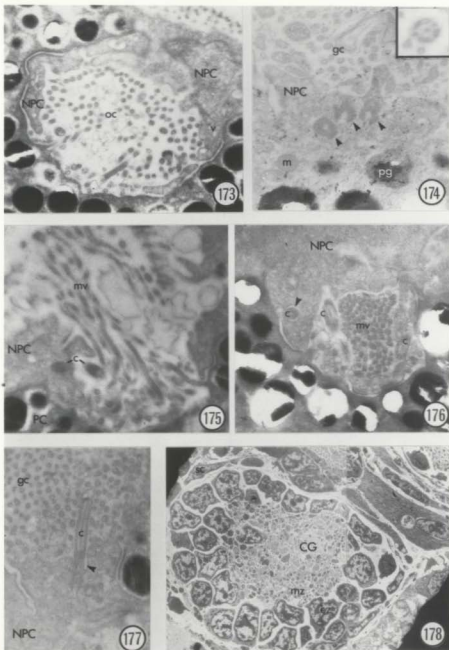
FIG. 175 TEM of cross section showing a cilium (c) of a non-pigmented cell (NPC) extending into the ocellar cavity next to array of pigmented cell microvilli (mv). PC, pigmented cell. X16,500\*

FIG. 176 TEM of oblique section showing cilia (c) of non-pigmented cells (NPC) projecting between microvilli (mv) of pigmented cell in the ocellar cavity. Arrowhead indicates circumciliary space surrounding cilium. X14,500\*

FIG. 177 Cilium (c) of non-pigmented cell (NPC). Note the absence of a basal foot and root. Arrowhead indicates circumciliary space. gc, gill cavity. X16,500

FIG. 178 Cerebral ganglion (CG) of Placoplecten magellanicus showing cells of cortical zone (cz), medullar zone (mz) and sheath (sc). X2200\*

\* Larvae were fixed in OsO<sub>4</sub> containing K<sub>3</sub>Fe(CN)<sub>6</sub>, en bloc stained and embedded in LR White resin.



the apical sensory organ of the velum. The ganglion is enclosed in a sheath of thin, flat connective tissue cells. A cortical-like zone comprising one or more layers of large nerve cells lies beneath the outer sheath. The cells of the cortical-like zone are typically oval to square and possess nuclei that occupy most of the cell. A medullar zone composed of small nerve cells and glial cells lies under the cortex-like layer.

## DISCUSSION

## LARVAL PHOTORECEPTORS

The basic morphology of photoreceptors in larval bivalves is best known from light microscope descriptions and the fine structure has not been fully appreciated. The only published ultrastructural study of cerebral ocelli in a bivalve larva is that of Waller (1981). His report is part of a scanning electron microscope study on the morphology and development of the veliger larvae of the oyster, Ostrea edulis. Unfortunately, the account by this author of ocelli fine structure is incomplete; the description of eye morphology ends at the veliger stage and does not detail the morphology or development of the photoreceptors during the pediveliger stage of the life history. Nonetheless, Waller's account provides valuable information on the early development of larval photoreceptors and comparisons between his study and the present investigation are possible.

The ocelli of larval bivalves first appear in the early prodissoconch II stage of development. They are located at the base of the gills on either side of the primordial foot, each appearing as a tuft of microvilli anterior to the openings of the duct from the statocyst (Waller 1981). As the larva grows, the microvilli become submerged in the

ectoderm (Cole 1938; Raven 1966; Waller 1981; Moor 1983) so that the microvilli project minimally from beneath the epithelial surface. This accords with observations from the present study. In pediveligers of Placopecten magellanicus, the elongate microvilli of the pigmented cell extend beyond the aperture of the ocellar cavity demonstrating a feature common to previous observations. During the pediveliger stage the ectodermal invagination becomes pigmented.

Some authors report the presence of a lens at the aperture of the pigment-cup. In Ostrea edulis this lens takes the form of a gelatinous mass (Hickman & Gruffydd 1971; Waller 1981). Pelseneer (1908) and Field (in Rosen *et al.* 1978) described a lens-like body in veligers of Mytilus edulis, but Rosen *et al.* (1978) proved this interpretation incorrect demonstrating an array of microvilli instead of a lens. The ocellar cavity of the photoreceptor of Placopecten magellanicus does not contain a lens.

In contrast to that of most larval invertebrates studied to date, the photoreceptors of Placopecten magellanicus larvae are very simple in form. The pigment-cup of the scallop larva is not composed of a number of cells as in oysters (Cole 1938; Hickman & Gruffydd 1971), gastropods (Eakin & Brandenburger 1967), nudibranchs (Hughes 1970; Chia & Koss 1983), polyplacophorans (Rosen *et al.* 1979) and polychaetes (Hermans 1969), but rather, a single invaginated pigmented cell forms the ocellar cavity into

which the photoreceptive organelles extend. The ocellar cavity lies open to the gill cavity and its receptor organelles are exposed directly to the environment. This situation is similar to that described for the simple photoreceptors of a number of marine invertebrates (Patten 1887; Raven 1966; Hyman 1967; Tonosaki 1967; Barber & Wright 1969a; Hickman & Gruffydd 1971; Holborow 1971; Rosen *et al.* 1978, 1979; Ruppert 1978; Waller 1981).

The ocelli of Placopecten magellanicus larvae have both ciliated and microvillous cells associated with them. It is unclear from the present account as to which of these cell types is photosensory. It should be noted that the necessary criterion from spectrophotometric observations to determine the presence and alignment of photopigment on the receptor membranes is lacking. However, the morphological observations from the present study demonstrate that at least two choices exist:

1. the non-pigmented ciliated cells are the receptor cells.
2. the pigmented cell constitutes the receptor cell.

Up to now detailed examinations on the morphology of ocelli have been reported for the larvae of few molluscan species (light microscope study: Ostrea edulis, Cole 1938; Hickman & Gruffydd 1971; Mytilus edulis, Bayne 1971; Chlamys hastata, Hodgson & Burke 1988; electron microscope study: Helix aspersa, Eakin & Brandenburger 1967; Trinchesia aurantia, Hughes 1970; Katharina tunicata, Rosen *et al.* 1979; O. edulis, Waller 1981; Rostanga pulchra, Chia & Koss

1983; Lepidochiton cinerea, Fisher in Moor 1983). From the majority of these investigations it can be inferred that the common organization of the ocellus of molluscs consists of a number of pigmented supportive cells forming an eyecup that encloses the receptoral region of one or more photosensory cells.

It has been demonstrated in Placopecten magellanicus that cilia extend into the cavity of the pigment-cup. Therefore, if the first proposal is to be accepted the photoreceptor would consist of at least four sensory cells with their ciliated receptors sheathed by a single pigmented cell. This arrangement closely conforms to that of other larvae within the phylum but perhaps more interestingly, it shows a striking morphological similarity to the larval ocelli of the marine flatworm Pseudoceros canadensis (Müller's larva), a primitive ancestor of the molluscs in the evolutionary lineage (Eakin & Brandenburger 1981). Moreover, the non-pigmented ciliated cells of the scallop ocellus contain an abundance of small vesicles and mitochondria indicating a high level of cellular activity commonly associated with photoreceptive cells (Eakin 1972).

It is noteworthy that if the non-pigmented cells are photosensory, then Placopecten magellanicus larvae will possess ciliary type cerebral eyes and would therefore prove an exception to Eakin's theory of diphyletic origin of photoreceptors (Eakin 1963, 1965, 1968, 1972, 1982).

Evidence against the possibility that the non-pigmented

cells of Placopecten magellanicus are sensory may be summarized as follows. The ciliary shaft does not show any of the membrane elaborations characteristic of ciliary type receptor cells (Eakin 1972; Salvini-Plawen & Mayr 1977). Also, the membrane system in ciliary photoreceptors is formed from cilia that typically show a reduction in the number of microtubules in the axoneme (Barber & Wright 1969b; Hermans & Eakin 1969; Eakin 1972). In P. magellanicus ocelli this situation is not seen. Instead, the ciliary axoneme bears a central pair of microtubules (ie.  $9x2+2$ ). Furthermore, the cilia in the scallop ocellus extend across the aperture of the pigment-cup and either bend into it (in the vast majority of cases) or remain external to the ocellar cavity. The ability of the cilia to assume different orientations makes the hypothesis that they serve as photosensory structures untenable. However, it does indicate the possibility that the cilia are motile. Rosen et al. (1978) suggested that the cilia found in the cerebral ocelli of adult Mytilus edulis were not photosensory and they proposed instead that the cilia served a cleansing function. It is possible that the cilia of the non-pigmented cells of P. magellanicus ocelli serve a like function to keep debris from entangling in the microvilli and clogging the lumen of the pigment-cup thus reducing the amount of light reaching the receptors.

A final important point is that axons have not been found in the non-pigmented cells of 40-day old pediveliger

larvae examined in this study indicating that the cells, if sensory, are probably not functional at this stage of development. The notion that the photoreceptors in the pediveliger larvae of Placopecten magellanicus are not operational is somewhat weakened by behavioral observations which indicate that as early as 23 days of age

P. magellanicus veliger larvae show evidence of positive phototaxis (Culliney 1974).

Rhabdomeric photoreceptor cells are a fundamental characteristic of cerebral photoreceptors of the Protostomata (Eakin 1963, 1965, 1972, 1979, 1982). Evidence from the present investigation makes the second proposal (ie. the pigmented cell is photosensory) most probable. The single pigmented cell in the ocellus of Placopecten magellanicus is provided, at its distal end, with a large surface area in the form of a loosely packed array of microvilli to carry photopigment. The microvilli are elongate and oriented parallel to the path of incident light. This makes the rhabdomere well suited for collecting the maximum amount of available light energy.

At the proximal end of the cell is a process that is thought to be an axon connecting the pigmented cell to the cerebral-pleural-visceral commissure. The axon would provide a pathway for the transference of information from the ocellus to the commissure and thus to the cerebral ganglion where the information is presumably integrated with sensory information from other sources.

Assuming the pigmented cell is photosensory, it shows certain fine-structural peculiarities from previously described molluscan ocelli. The photoreceptor of Placopecten magellanicus represents a unique case within the Mollusca studied to date because the entire structure consists of a single cell. It also demonstrates a rare instance where the rhabdomere arises directly from a pigmented cell. Although, as a rule, photosensory cells lack pigment (Eakin 1972) exceptions are known to exist (gastropods: Tonosaki 1967; cnidarians: Bouillon & Nielsen 1974; polyclads: Ruppert 1978; Eakin & Brandenburger 1981; polyplacophorans: Rosen et al. 1979; cephalopods: Messenger 1981). An additional anomaly is intimated by the reduced number of organelles such as mitochondria and aggregations of small vesicles in the receptoral end of the cell which implies a low level of cellular activity atypical of photoreceptive cells (Eakin 1972).

Further, this study has demonstrated the presence of a basal body-like structure (centrioles ?) positioned close to the distal plasma membrane of the presumptive pigmented receptor of Placopecten magellanicus. The presence of degenerate ciliary components in photosensory cells has been previously undescribed in the cerebral ocelli of molluscs. Cilia conforming closely to classic organization have been reported in rhabdomeric ocelli of a number of gastropods (Eakin et al. 1967; Tonosaki 1967; Hughes 1970; Mayes &

Hermans 1973), polyplacophorans (Boyle 1969a,b; Rosen et al. 1979; Moor 1983) and a bivalve (Rosen et al. 1978). The significance, if any, of vestigial cilia in receptor cells has remained obscure. Eakin (1968) and others (Eakin & Brandenburger 1967; Eakin et al. 1977; Brandenburger & Eakin 1981) dismiss the presence of vestigial or adventitious cilia in some rhabdomeric type photoreceptors as incidental, suggesting their presence is due to the developmental origin of the ocelli from a ciliated ectoderm. Indeed, the ocelli of bivalve veligers are ectodermal in origin (Raven 1966; Waller 1981; Moor 1983). Consequently, it is possible that the centriole-like structures in the pigmented cell of P. magellanicus are remnants of an epidermal cilium which has persisted after the invagination of the cell. However, ultrastructural studies on the development of ocelli in scallop veligers are needed to determine if the ciliary rudiments are incidental.

Thornhill (1972) presented the hypothesis that a cilium may exert an organizing influence over the development of microvilli. Vanfleteren & Coomans (1976) applied this concept to the differentiation of photoreceptor organelles and theorized that cilia may induce photoreceptor membrane formation. To date, researchers have been unable to demonstrate a connection between centrioles (or other ciliary vestiges) and rhabdom formation (Home 1972, 1975; Wachmann & Hennig 1974; Eisen & Youssef 1980).

At present, the identity of the pigmented cell in the

ocellus of Placopecten magellanicus as photosensory must remain tentative. However, until further investigations prove otherwise, it appears that this study demonstrates agreement with Eakin's evolutionary hypothesis concerning cerebral ocelli in the protostomes (Eakin 1963, 1965, 1968, 1972, 1982).

It is with caution that one attributes functions based solely on morphological examinations to simple ocelli. However, functional interpretations analogous to those proposed for the ocelli of other larval invertebrates (Cole 1938; Dilly 1964, 1969; Eakin & Kuda 1971; Burr & Burr 1975; Rosen et al. 1978, 1979; Eakin & Brandenburger 1981; Chia & Koss 1983; Xylander 1984; Kajiwara & Yoshida 1985) are worthy of review.

The small size of the ocellus of Placopecten magellanicus, the loose arrangement of the presumed rhabdomeric microvilli, and the absence of a pinhole aperture or a lens indicates an optical design which provides poor resolution and precludes image formation (Land 1981).

The simple nature of the structural configuration of the ocelli in scallop larvae suggests the animals use their photoreceptors primarily to detect the direction of light. The presence of a pigment-cup enclosing the receptoral organelles allows some directional sensitivity by restricting or excluding light from reaching the photosensitive membranes in all but one direction. The

ability of the larvae to respond differentially to the direction of illumination may be enhanced by the presence of two symmetrical photoreceptors which independently monitor the environment. The cerebral ganglion may then integrate the output signals from each ocellus and generate the phototactic responses shown by bivalve larvae.

There are few laboratory experiments on photic behavior in bivalves. Bayne (1964) showed that Mytilus edulis is strongly positive to light during the early veliger stage of development. Larvae of Placopecten magellanicus also demonstrate positive phototaxis during this stage of their life history (Culliney 1974).

The ability of veligers to detect the direction of light may play an important role in the larval biology of Placopecten magellanicus by enhancing the ability of the larva to find food. By possessing a sensitivity to the direction of light the larva might possibly be able to maintain itself in the photic zone where algal feeding is best.

Assuming the ocelli of Placopecten magellanicus larvae are rhabdomeric type photoreceptors, they would most likely respond to the onset of illumination (Land 1968; Vanfleteren & Coomans 1976; LaCourse & Northrop 1983) and may function in monitoring environmental light intensity. The ocelli of P. magellanicus are arranged in a manner which permits simultaneous comparisons of light; this does not obviate the possibility that the photoreceptors may function to detect

changes in the amount and intensity of incident light and thus serve to aid the larva in maintaining its position in relation to the source of light. However, during the veliger stage, P. magellanicus larvae lead a planktonic existence drifting with the currents. Although they are strong swimmers it is doubtful that the larvae can maintain a specific orientation in the strong water movements.

Negative phototaxis becomes more intense during the pediveliger stage (Bayne 1964, 1965; Culliney 1974) resulting in the movement of larvae towards the substrate. Chia & Koss (1983) have suggested that the ocelli in the larvae of some species may provide information in the search for settlement sites. It seems possible that the ocelli of the pediveliger of Placoplecten magellanicus may contribute sensory information needed to help orient the larva during crawling; a behavior intimately associated with settlement (Cranfield 1973). However, it is unlikely that photoreception is the only sense required in this process. Other sensory structures such as the statocysts and receptors in the foot probably play a more direct role in settlement site selection.

Chia & Koss (1983) also reported that the ocelli in the larvae of the nudibranch Rostanga pulchra may be sensitive to a particular wavelength of light. Such a simple function for the ocelli of Placoplecten magellanicus cannot be rejected, but further behavioral and electrophysiological observations are necessary to test its efficacy.

Another function of the ocelli may be ascribed to polarization sensitivity. According to Eakin & Brandenburger (1981) the ocelli of Müller's larva (Pseudoceros canadensis) may act as an analyzer to detect polarized light because the cilia and the microvilli of the sensory cells lie at right angles to each other. A comparable situation has been observed, on occasion, in Placopecten magellanicus. However, the ability for the scallop larva to detect polarized light necessitates the presence of at least two sense cells. The arguments presented previously in this discussion offer evidence to dispute this idea. Also, a dichroic mechanism depends on the receptor membranes being arranged in a closely packed regular alignment (Waterman 1975). In P. magellanicus the microvilli are loosely arranged. Further, no experimental data have so far been given to corroborate this role in bivalves.

211  
CHAPTER NINE

GENERAL CONCLUSIONS

This investigation is the first description, by correlative techniques of light microscopy, transmission electron microscopy and scanning electron microscopy, of aspects of the functional morphology and development of the photoreceptive organs of the scallop. The current study complements existing data on the structure of the pallial photoreceptors of bivalve molluscs and adds to the accumulating knowledge of the fine structure of visual organs in invertebrates. It contributes to a measured understanding of the phylogenetic relationships among invertebrates, the morphological sequence of differentiation in eyes at the mantle edge of Bivalvia and the role of vision at specific stages of ontogeny, with special attention to form, function and the environment.

From a morphological standpoint, the visual organs of the scallop show considerable complexity and although the structural appearance has been well characterized by light microscopy, ultrastructural data are limited. This study shows that the structure of the pallial eye of the Atlantic Deep Sea Scallop Placopecten magellanicus is similar to that of other scallops. However, differences are evident; the most noteworthy being the absence of a common optic nerve,

the presence of fewer photoreceptor cells in the distal retina than in the proximal retina and the size difference between axons of the distal and proximal optic nerves. Additionally, the presence of cilia and their ancillary structures in the proximal retinal receptor cells is established, the absence of synapses within the retinae is confirmed, and the three-dimensional structure of the distal retinal receptor cell cilia is ascertained. Further comparative study would prove worthwhile in order to discover whether these structural features are widespread or restricted to P. magellanicus. Such information would be useful in explanations of behavioral and electrophysiological phenomena.

The provocative question concerning the necessity for so many pallial eyes still remains. Comparative analysis of the optical systems of a variety of scallops, indeed of other molluscs, would be beneficial.

Comprehensive investigations on the development of the pallial eye in other bivalves are called for. The earliest events in the developmental sequence were not addressed by this study and remain a subject of debate. Nevertheless, this investigation has established that the order of appearance of the optical components differs from that described for other scallops. Moreover, it has documented many developmental events not previously observed in the scallop photoreceptor: the mode of synthesis of the reflecting crystals of the argentea, morphogenesis of the

proximal and distal retinal receptor cells from retinal anlage cells including the differentiation of rhabdomeric microvilli in the proximal retina and ciliogenesis in the distal retina, neurogenesis of the two retinae, and the morphological changes in the transformation of mesodermal cells to lens cells. Clearly the mechanisms by which formation of the various elements are controlled require further work. This would be beneficial in refining the understanding of organogenic processes.

Immunocytochemical and autoradiographic techniques would be useful in the unequivocal determination of the origin of the anlage cells of many of the optical components. These or comparable labelling techniques might also be applied to help clarify such dynamic processes as photopigment production and transport, receptor organelle formation and membrane turnover during light and dark adaptation.

The presence of ciliary structures in the rhabdomeric type receptor cells is of interest. In particular, their occurrence in the presumed rhabdomeric photoreceptive cell of the cerebral ocelli of the pediveliger begs the question, 'is their presence merely adventitious relating to the ectodermal origin of the organ, or are they the organizers of rhabdomeric differentiation?' A survey of the fine structure of larval invertebrate cerebral ocelli may aid in resolving this matter.

The pallial eyes are strictly post-larval

specializations, developing after settlement and metamorphosis. The cerebral ocelli have been observed in post-metamorphosed bivalves. The fate of the larval photoreceptors during metamorphosis and in early juvenile development is not clear and needs further investigation. As the juveniles grow the ocelli presumably become proportionally reduced relative to body size, and the functional role subserved by these visual organs is gradually lost, or replaced by the developing pallial eyes. Clearly the relationships between the various types of photoreceptive organs present during ontogeny and their implications on behavior warrant future studies.

The eye of the scallop is, unquestionably, an intricate and perplexing sensory organ and as Hensen (1865) aptly stated, "...but how much more toil will be necessary before the entire structure of this cubic millimeter will be understood?" (translation from Gutsell 1930).

## CHAPTER TEN

## BIBLIOGRAPHY

Anonymous 1886. Review: Patten on the eyes of Molluscs and Arthropods. Q. J. Micros. Sci. 285-292.

Aparicio, S.R. & P. Marsden 1969. A rapid methylene-blue basic fuchsin stain for semi-thin sections of peripheral nerve and other tissues. J. Microscopy. 89:139-141.

Arnold, J.M. 1967. Fine structure of the development of the cephalopod lens. J. Ultrastruct. Res. 17:527-543.

Autrum, H. 1979. Introduction. In: Handbook Of Sensory Physiology VII/6A (H. Autrum, ed). Springer-Verlag, Berlin. 1-22.

Barber, V.C. & M.F. Land 1966. The physical properties of a biological reflector: the argentea of the eye of Pecten. Proc. Physiol. Soc. 185:1-2.

Barber, V.C. & M.F. Land 1967. Eye of the cockle, Cardium edule: Anatomical and physiological investigations.

Barber, V.C. & D.E. Wright 1969a. The fine structure of the eye and optic tentacle of the mollusc Cardium edule. J. Ultrastruct. Res. 26:515-528.

Barber, V.C. & D.E. Wright 1969b. The fine structure of the sense organs of the cephalopod mollusc Nautilus. Z. Zellforsch. 102:293-312.

Barber, V.C., E.M. Evans & M.F. Land 1967. The fine structure of the eye of the mollusc Pecten maximus. Z. Zellforsch. 76:295-312.

Bayne, B.L. 1964. The responses of the larvae of Mytilus edulis (L.) to light and gravity. Oikos. 15:162-174.

Bayne, B.L. 1965. Growth and the delay of metamorphosis of the larvae of Mytilus edulis (L.). Ophelia. 2(1): 1-47.

Bayne, B.L. 1971. Some morphological changes that occur at the metamorphosis of the larvae of Mytilus edulis. 4th European Marine Biology Symposium, Bangor, Wales. 1969. 259-280.

Bell, A.L. 1966. The fine structure of the eye of the

scallop, Pecten irradians. Biol. Bull. 131(2):385.

Blest, A.D. 1978. The rapid synthesis and destruction of photoreceptor membrane by a dinopid spider: a daily cycle. Proc. R. Soc. Lond. 200:463-483.

Blest, A.D. & W.A. Day 1978. The rhabdomere organization of some nocturnal pisaurid spiders in light and darkness. Phil. Trans. R. Soc. Lond. B. 283:1-23.

Blest, A.D. & D.G. Price 1981. A new mechanism for transitory, local endocytosis in photoreceptors of a spider, Dinopis. Cell Tissue Res. 217:267-282.

Bon, W.F., A. Dohrn & H. Batink 1967. The lens proteins of a marine invertebrate Octopus vulgaris. Biochim. Biophys. Acta. 140:312-318.

Bouillon, J. & M. Nielsen 1974. Études de quelques organes sensoriels de cnidaires. Arch. Biol. (Bruxelles). 85: 307-328.

Boyde, A. 1978. Pros and cons of critical point drying and freeze drying for SEM. In: Scanning Electron Microscopy (R.P. Becker & O. Johari, eds). AMF O'Hare, Illinois. 2:303-314.

Boyle, P.R. 1969a. Rhabdomeric ocellus in a chiton.

Nature (Lond.). 222(5196):895-896.

Boyle, P.R. 1969b. Fine structure of the eyes of  
Onithochiton neglectus (Mollusca: Polyplacophora). Z.  
Zellforsch. 102:313-332.

Brahma, S.K. 1978. Ontogeny of lens crystallins in marine  
cephalopods. J. Embryol. exp. Morph. 46:111-118.

Brandenburger, J.L. 1977. Cytochemical localization of  
acid phosphatase in regenerated and dark-adapted eyes  
of a snail, Helix aspersa. Cell Tissue Res. 184:  
301-313.

Brandenburger, J.L. & R.M. Eakin 1970. Pathway of  
incorporation of vitamin A<sup>3</sup>H<sub>2</sub> into photoreceptors of a  
snail Helix aspersa. Vision Res. 10:639-653.

Brandenburger, J.L. & R.M. Eakin 1980. Cytochemical  
localization of acid phosphatase in ocelli of the  
seastar Patiria miniata during recycling of photorecep-  
toral membranes. J. Exp. Zool. 214:127-140.

Brandenburger, J.L. & R.M. Eakin 1981. Fine structure of  
ocelli in larvae of an archiannelid, Polygordius cf.  
appendiculatus. Zoomorphology. 99:23-36.

Brandenburger, J.L. & R.M. Eakin 1985. Cytochemical localization of acid phosphatase in light- and dark-adapted eyes of a polychaete worm, Nereis limnicola. Cell Tissue Res. 242:623-628.

Buddenbrock, W.v. & I. Moller-Racke 1953. Über den Lichtsinn von Pecten. Publ. Statz. Zool., Napoli. 24: 217-245.

Bullock, T.H. & G.A. Horridge 1965. Structure And Function In The Nervous Systems Of Invertebrates. Vol. II. W.H. Freeman. San Francisco, London.

Burr, A.H. 1984. Evolution of eyes and photoreceptor organelles in lower phyla. In: Photoreception And Vision In Invertebrates (M.A. Ali, ed). Plenum Press, New York. 131-178.

Burr, A.H. & C. Burr 1975. The amphid of the nemtode Oncholaimus vesicularius: Ultrastructural evidence for a dual function as chemoreceptor and photoreceptor. J. Ultrastruct. Res. 51:1-15.

Butcher, E.O. 1930. The formation, regeneration and transplantation of eyes in Pecten (gibbus borealis). Biol. Bull. 59:154-164.

Carr, K.E. & P.G. Toner 1982. Cell Structure. Churchill Livingstone. Edinburgh, London. 3rd ed. 388p.

Carrière, J. 1885. Die Sehorgane der Tiere. München und Leipzig. 99-107.

Carrière, J. 1889. Über Molluskenaugen. Archiv. f. mikr. Anat. 33:378-402.

Chia, F.S. & R. Koss 1983. Fine structure of the larval eyes of Rostanga pulchra (Mollusca, Opisthobranchia, Nudibranchia). Zoomorphology. 102:1-10.

Cohen, A.L., D.P. Marlow & G.E. Garner 1968. A rapid critical point method using fluorocarbons ('Freons') as intermediate and transitional fluids. J. Microscopy. 7:331-342.

Cole, H.A. 1938. The fate of larval organs in the metamorphosis of Ostrea edulis. J. mar. biol. Assoc. U.K. 22:469-484.

Coomans, A. 1981. Phylogenetic implications of the photoreceptor structure. Accad. Naz. Lincei, Rome. 49:23-68.

Cornwall, M.C. & A.L.F. Gorman 1979. Contribution of

calcium and potassium permeability changes to the off response of scallop hyperpolarizing photoreceptors. J. Physiol. 291:207-232.

Cranfield, H.J. 1973. Observations on the behaviour of the pediveliger of Ostrea edulis during attachment and cementing. Marine Biology. 22:203-209.

Culliney, J.L. 1974. Larval development of the Giant Scallop Placopecten magellanicus (Gmelin). Biol. Bull. 147:321-332.

Curtis, H. 1966. The bright-eyed scallop. Sea Frontiers. 12(4):194-202.

Curtis, L.N., J.L. Carson, A.M. Collier, T.M. Gambling, S.S. Hu, M.W. Leigh & T.F. Boat 1987. Features of developing ferret tracheal epithelium: Ultrastructural observations of in vivo and in vitro differentiation of ciliated cells. Exp. Lung Res. 13:223-240.

Dahlgren, U. & W.A. Kepner 1928. Principles Of Animal Histology. The MacMillan Co., N.Y. 246-249.

Dakin, W.J. 1910a. The visceral ganglion of Pecten, with some notes on the physiology of the nervous system, and an inquiry into the innervation of the Osphradium in

the Lamellibranchiata. Mitt. Zool. Statz. Neapel.  
20:1-41.

Dakin, W.J. 1910b. The eye of Pecten. Q. J. Micros. Sci.  
55:49-112.

Dakin, W.J. 1928. The eyes of Pecten, Spondylus, Amussium  
and allied lamellibranchs, with a short discussion on  
their evolution. Proc. Roy. Soc. Lond. B. 103:355-  
365.

Dawes, C.J. 1971. Biological Techniques In Electron  
Microscopy. Barnes & Noble. New York.

Dentler, W.L. 1980. Structures linking the tips of ciliary  
and flagellar microtubules to the membrane. J. Cell  
Sci. 42:207-220.

Dilly, P.N. 1964. Studies on the receptors in the cerebral  
vesicle of the ascidian tadpole II. The ocellus.  
Q. J. Micros. Sci. 105:13-20.

Dilly, P.N. 1969. Studies on the receptors in Ciona  
intestinalis III. A second type of photoreceptor in  
the tadpole larva of Ciona intestinalis. Z.  
Zellforsch. 96:63-65.

Dirksen, E.R. 1971. Centriole morphogenesis in developing ciliated epithelium of the mouse oviduct. *J. Cell Biol.* 51:286-302.

Drew, G.A. 1906. The habits, anatomy, and embryology of the Giant Scallop (Pecten tenuicostatus, Mighels). *Univ. of Maine Studies*, No. 6. 1-71.

Eakin, R.M. 1963. Lines of evolution of photoreceptors. In: General Physiology Of Cell Specialization (D. Mazia & A. Tyler, eds). McGraw-Hill, N.Y. 393-425.

Eakin, R.M. 1965. Evolution of photoreceptors. *Cold Spr. Harb. Symp. quant. Biol.* 30:363-370.

Eakin, R.M. 1968. Evolution of photoreceptors. In: Evolutionary Biology Vol. II (T. Dobzhansky, M.K. Hecht & W.C. Steere, eds). Appleton-Century-Crofts, N.Y. 194-242.

Eakin, R.M. 1972. Structure of invertebrate photoreceptors. In: Handbook Of Sensory Physiology VII/I (H.J.A. Dartnall, ed). Springer-Verlag, Berlin. 625-684.

Eakin, R.M. 1979. Evolutionary significance of photoreceptors: In retrospect. *Am. Zool.* 19:647-653.

Eakin, R.M. 1982. Continuity and diversity in photoreceptors. In: Visual Cells In Evolution (J.A. Westfall, ed). Raven Press, New York. 91-105.

Eakin, R.M. & J.L. Brandenburger 1967. Differentiation in the eye of a pulmonate snail Helix aspersa. J. Ultrastruct. Res. 18:391-421.

Eakin, R.M. & J.L. Brandenburger 1970. Osmic staining of amphibian and gastropod photoreceptors. J. Ultrastruct. Res. 30:619-641.

Eakin, R.M. & J.L. Brandenburger 1975. Retinal differences between light-tolerant and light-avoiding slugs (Mollusca: Pulmonata). J. Ultrastruct. Res. 53:382-394.

Eakin, R.M. & J.L. Brandenburger 1976. Sensory microvilli and photic vesicles in the eye of the snail Helix aspersa. In: The Structure Of The Eye, III (E. Yamada & S. Mishima, eds.). Jap. J. Ophthal., Toyoko. 203-213.

Eakin, R.M. & J.L. Brandenburger 1979. Effects of light on ocelli of seastars. Zoomorphology. 92:191-200.

Eakin, R.M. & J.L. Brandenburger 1980. Studies on calcium

in the eye of the snail Helix aspersa. 38th Ann. Proc. EMSA. 566-567.

Eakin, R.M. & J.L. Brandenburger 1981. Fine structure of the eyes of Pseudoceros canadensis (Turbellaria, Polycladida). Zoomorphology. 98:1-16.

Eakin, R.M. & J.L. Brandenburger 1982. Pinocytosis in eyes of a snail, Helix aspersa. J. Ultrastruct. Res. 80:214-229.

Eakin, R.M. & J.L. Brandenburger 1985. Effects of light and dark on photoreceptors in the polychaete annelid Nereis limnicola. Cell Tissue Res. 242:613-622.

Eakin, R.M. & A. Kuda 1971. Ultrastructure of sensory receptors in ascidian tadpoles. Z. Zellforsch. 112: 287-312.

Eakin, R.M. & J.A. Westfall 1964. Further observations on the fine structure of some invertebrate eyes. Z. Zellforsch. 62:310-332.

Eakin, R.M., J.A. Westfall & M.J. Dennis 1967. Fine structure of the eye of a nudibranch mollusc, Hermissenda crassicornis. J. Cell Sci. 2:349-358.

Eakin, R.M., G.G. Martin & C.T. Reed 1977. Evolutionary significance of fine structure of archiannelid eyes. *Zoomorphology.* 88:1-18.

Eakin, R.M., J.L. Brandenburger & G.M. Baker 1980. Fine structure of the eye of the New Zealand slug, Athoracophorus bitentaculatus. *Zoomorphology.* 94: 225-239.

Eguchi, E. & T.H. Waterman 1976. Freeze-etch and histochemical evidence for cycling in crayfish photoreceptor membranes. *Cell Tiss. Res.* 169:419-434.

Eisen, J.S. & N.N. Youssef 1980. Fine structural aspects of the developing compound eye of the Honey Bee, Apis mellifera L. *J. Ultrastruct. Res.* 71:79-94.

Emerson, C.J. 1977. Larval development of the sea star, Leptasterias polaris, with particular reference to the optic cushion and ocelli. In: *Scanning Electron Microscopy*, Vol. II, Chicago. 631-638.

Erdmann, W. 1935. Untersuchungen über die Lebensgeschichte der Auster, 5. Über die Entwicklung und die Anatomie der 'Ansatzreifen' Larve von Ostrea edulis mit Bemerkungen über die Lebensgeschichte der Auster. *Wiss. Mera. Komm. z. wiss. Untersuch. der Deut. Mere in*

Ermak, T.H. & R.M. Eakin 1976. Fine structure of the cerebral and pygidial ocelli in Chone ecaudata (Polychaeta: Sabellidae). J. Ultrastruct. Res. 54: 243-260.

Fankboner, P.V. 1980. Siphonal eyes of Giant Clams (Bivalvia, Tridacnidae) and their relationship to adjacent zooxanthellae. Am. Zool. 20(4):889.

Fankboner, P.V. 1981. Siphonal eyes of Giant Clams and their relationship to adjacent zooxanthellae. Veliger 23(3):245-249.

Friedmann, I. & E.S. Bird 1971. Ciliary structure, ciliogenesis, microvilli. Laryngoscope. 81:1852-1868.

Garner, R. 1837. On the nervous system of molluscous animals. Trans. Linn. Soc. Lond. XVII:485-501.

Gordon, R.E. & B.P. Lane 1984. Immunolocalization of myosin and tropomyosin in cells undergoing ciliogenesis during regeneration of rat tracheal epithelium. Tissue & Cell. 16(3):337-343.

Gorman, A.L.F. & M.C. Cornwall 1976. Ionic mechanism of

color dependent membrane responses of opposite polarity  
in single photoreceptors of Pecten irradians. Biophys.  
J. 16:147a.

Gorman, A.L.F. & J.S. McReynolds 1969. Hyperpolarizing and  
depolarizing receptor potentials in the scallop eye.  
Science. 165:309-310.

Gorman, A.L.F. & J.S. McReynolds 1974. Control of membrane  
 $K^+$  permeability in a hyperpolarizing photoreceptor:  
similar effects of light and metabolic inhibitors.  
Science. 185:620-621.

Gorman, A.L.F. & J.S. McReynolds 1978. Ionic effects on  
the membrane potential of hyperpolarizing photo-  
receptors in scallop retina. J. Physiol. 275:345-355.

Gould, P.R., L. Ling, D.W. Henderson, R.A. Barter & J.M.  
Papadimitriou 1986. Cilia and ciliogenesis in  
endometrial adenocarcinomas. Arch. Pathol. Lab. Med.  
110:326-330.

Gruffydd, Ll.D. & A.R. Beaumont 1972. A method for rearing  
Pecten maximus larvae in the laboratory. Mar. Biol.  
15:350-355.

Gutsell, J.S. 1930. Natural history of the Bay Scallop.

U.S. Bureau of Fisheries Bull. 46:569-632.

Harry, O.G. 1980. Damage to the eyes of the bivalve  
Chlamys opercularis caused by the ciliate Licnophora  
auerbachii. J. Invert. Path. 36:283-291.

Hartline, H.K. 1938. The discharge of impulses in the  
optic nerve of Pecten in response to illumination of  
the eye. J. cell. comp. Physiol. 11(3):465-478.

Hayat, M.A. 1981. Fixation For Electron Microscopy.  
Academic Press. New York. 501p.

Henry, E.C. 1977. A method for obtaining ribbons of serial  
sections of plastic embedded specimens. Stain Technol.  
52:59-60.

Hensen, V. 1865. Über das Auge einiger Cephalopoden.  
Zeitsch. f. wiss. Zool. 15:155-243.

Hermans, C.O. 1969. Fine structure of the segmental ocelli  
of Armandia brevis (Polychaeta:Opheliidae). Z.  
Zellforsch. 96:361-371.

Hermans, C.O. & R.M. Eakin 1969. Fine structure of the  
cerebral ocelli of a sipunculid, Phascolosoma  
agassizii. Z. Zellforsch. 100:325-339.

Hermans, C.O. & R.M. Eakin 1974. Fine structure of the eyes of an alciopid polychaete, Vanadis tagensis (Annelida). Z. Morph. Tiere. 79:245-267.

Hesse, R. 1900. Untersuchungen über die Organe der Lichtempfindung bie niederen Thieren. VI. Die Augen einiger Mollusken. Zeitsch. f. wiss. Zool. 118:379-477.

Hesse, R. 1902. Untersuchungen über die Organe der Lichtempfindung bie niederen Thieren. VIII. Weitere Tatsachen. Zeitsch. f. wiss. Zool. 72:565-657.

Hesse, R. 1908. Das Sehen der nieder Tiere. Verlag von Gustav Fischer. 47p.

Hesse, R. 1916. Die sehorgane am Mantelrande der Kammuscheln. Naturw. Vierter Jahrgang. 239-240.

Hickman, R.W. & Ll.D. Gruffydd 1971. The histology of the larva of Ostrea edulis during metamorphosis. 4th Europ. Mar. Biol. Symp., Bangor, Wales. 1969. 281-294.

Hickson, S.J. 1880. The eye of Pecten. Q. J. Micros. Sci. 20:443-455.

Hickson, S.J. 1882. The eye of Spondylus. Q. J. Micros.

Hodgson, C.A. & R.D. Burke 1988. Development and larval morphology of the spiny scallop, Chlamys hastata. Biol. Bull. 174:303-318.

Holborow, P.L. 1971. The fine structure of the trochophore of Harmothoe imbricata. 4th Europ. Mar. Biol. Symp., Bangor, Wales. 1969. 237-246.

Holley, M.C. 1984. The ciliary basal apparatus is adapted to the structure and mechanics of the epithelium. Tissue & Cell. 16(2):287-310.

Homann, H. 1971. Die augen der Araneae. Anatomie, ontogenie und bedeutung für die systematic (Chelicerata, Arachnida). Z. Morph. Tiere. 69: 201-272.

Home, E.M. 1972. Centrioles and associated structures in the retinula cells of insect eyes. Tissue & Cell. 4(2):227-234.

Home, E.M. 1975. Ultrastructural studies of development and light-dark adaptation of the eye of Coccinella septempunctata L., with particular reference to ciliary structures. Tissue & Cell. 7(4):703-722.

Howard, D.R. & G.G. Martin 1984. Fine structure of the eyes of the interstitial gastropod Fartulum orcutti (Gastropoda, Prosobranchia). *Zoomorphology*. 104: 197-203.

Hughes, H.P.I. 1970. The larval eye of the aeolid nudibranch, Trinchesia aurantia (Alder and Hancock). *Z. Zellforsch.* 109:55-63.

Humphreys, W.J., B.O. Spurlock & J.S. Johnson 1977. Critical-point drying of cryofractured specimens. In: *Principles And Techniques Of Electron Microscopy* Vol 6 (M.A. Hayat, ed). 136-158.

Hyde, I. 1903. The nerve distribution in the eye of Pecten irradians. *Mark Anniversary Volume*. New York. 471-482.

Hymen, L.H. 1967. *The Invertebrates* Vol 6. *Mollusca*. 1, McGraw-Hill. N.Y.

Itaya, S.K. 1976. Rhabdom changes in the shrimp, Palaemonetes. *Cell Tissue Res.* 166:265-273.

Juberthie, C. & A. Muñoz-Cuevas 1973. Présence de centriole dans la cellule visuelle de l'embryon d'Ischyropsalis luteipes (Arachnides, Opilions). *C.R.*

Kajiwara, S. & M. Yoshida 1985. Changes in behavior and ocellar structure during the larval life of solitary ascidians. Biol. Bull. 169:565-577.

Kataoka, S. & T.Y. Yamamoto 1981. Diurnal changes in the fine structure of photoreceptors in an abalone, Nordotis discus. Cell Tissue Res. 218:181-189.

Kataoka, S. & T.Y. Yamamoto 1983. Fine structure and formation of the photoreceptors in Octopus ocellatus. Biol. Cell 49:45-54.

Keferstein, W. 1863. Untersuchungen über niedere Seetiere. IX. Über den Bau der Augen von Pecten. Zeitsch. f. wiss. Zool. 12:133-136.

Krohn, A. 1840. Über augenähnliche Organe bei Pecten und Spondylus. Müllers Arch. f. Anat. und Phys. 381-386.

Küpfer, M. 1916. Sehorgane am Mantelrande der Pecten arten. Verlag von Gustav Fischer. 1-312.

LaCourse, J.R. & R.B. Northrup 1983. Eye of the mussel, Mytilus edulis Linnaeus: Electrophysiological

investigations. Veliger. 25(3):225-228.

Land, M.F. 1964. The eye of the scallop, a concave reflector. J. Physiol. 175:9-10.

Land, M.F. 1965. Image formation by a concave reflector in the eye of the scallop. Pecten maximus. J. Physiol., Lond. 179:138-153.

Land, M.F. 1966a. Activity in the optic nerve of Pecten maximus in response to changes in light intensity, and to pattern and movement in the optical environment. J. Exp. Biol. 45:83-99.

Land, M.F. 1966b. A multilayer interference reflector in the eye of the scallop, Pecten maximus. J. Exp. Biol. 45:433-447.

Land, M.F. 1968. Functional aspects of the optical and retinal organization of the mollusc eye. Symp. zool. Soc. Lond. 23:75-96.

Land, M.F. 1972. The physics and biology of animal reflectors. Prog. Biophys. Mol. Biol. 24:75-106.

Land, M.F. 1978. Animal eyes with mirror optics. Sci. Am. 239(6):126-134.

- Land, M.F. 1981. Optics and vision in invertebrates. In: *Handbook Of Sensory Physiology VII/6B* (H. Autrum, ed). Springer-Verlag, Berlin. 471-592.
- Land, M.F. 1984. Molluscs. In: *Photoreception And Vision In Invertebrates* (M.A. Ali, ed). Plenum Press, New York. 699-726.
- Langford, L.A. & R. Coggeshall 1980. The use of potassium ferricyanide in neural fixation. *Anat. Rec.* 197:297-304.
- Laverack, M.S. 1968. On the receptors of marine invertebrates. *Oceanogr. Mar. Biol. Ann. Rev.* 6:249-324.
- Leeson, T.S. 1971. Lens of the rat eye: an electron microscope and freeze-etch study. *Exp. Eye Res.* 11:78-82.
- Levi, P. & C. Levi 1971. Ultrastructure des yeux palleaux d'Arca noe (L.). *J. Microscopie.* 11:425-432.
- Loosanoff, V.L. & W.C. Davis 1963. Rearing of bivalve molluscs. In: *Advances In Marine Biology* (F.S. Russell, ed). Academic Press, New York. 1-136.
- Manning, D.A. 1986. Aquaculture studies of the giant

scallop Placopecten magellanicus (Gmelin): conditioning of broodstock and energy requirements of the larvae and juveniles. M.Sc. Thesis, Memorial University, St. John's. 201p.

Maser, M.D., T.E. Powell & C.W. Philpott 1967.

Relationships among pH, osmolarity and concentration of fixative solutions. *Stain Technol.* 42:175-182.

Mayes, M. & C.O. Hermans 1973. Fine structure of the eye of the prosobranch mollusc, Littorina scutulata. *Veliger.* 16:166-169.

McReynolds, J.S. & A.L.F. Gorman 1970a. Photoreceptor potentials of opposite polarity in the eye of the scallop, Pecten irradians. *J. Gen. Physiol.* 56:376-391.

McReynolds, R.S. & A.L.F. Gorman 1970b. Membrane conductances and spectral sensitivities of Pecten photoreceptors. *J. Gen. Physiol.* 56:392-406.

McReynolds, J.S. & A.L.F. Gorman 1974. Ionic basis of hyperpolarizing receptor potential in scallop eye; Increase in permeability to potassium ions. *Science.* 183:658-659.

Melamed, J. & O. Trujillo-Cenóz 1966. The fine structure of the visual system of Lycosa (Araneae: Lycosidae). I. Retina and optic nerve. *Z. Zellorsch.* 74:12-31.

Menco, B. & A.I. Farbman 1987. Genesis of cilia and microvilli of rat nasal epithelia during prenatal development. III. Respiratory epithelium surface, including a comparison with the surface of the olfactory epithelium. *J. Anat.* 152:145-160.

Messenger, J.B. 1981. Comparative physiology of vision in molluscs. In: *Handbook Of Sensory Physiology VII/6C* (H. Autrum, ed.). Springer-Verlag, Berlin. 93-200.

Miller, W.H. 1958. Derivatives of cilia in the distal sense cells of the retina of Pecten. *J. Biophysic. Biochem. Cytol.* 4(2):227-231.

Miller, W.H. 1960. Visual Photoreceptor Structures. In: *The Cell: Biochemistry, Physiology, Morphology IV/1* (J. Brachet & A.E. Mirsky, eds.). Academic Press, New York. 325-364.

Modak, S.P. & S.W. Perdue 1970. Terminal lens cell differentiation. *Exp. Cell Res.* 59:43-56.

Moir, A.J.G. 1977. Ultrastructural studies on the ciliated receptors of the long tentacless of the Giant Scallop, Placopecten magellanicus (Gmelin). Cell Tiss. Res. 184:367-380.

Moor, B. 1983. Organogenesis. In: The Mollusca, Vol 3 (N.H. Verdonk, J. Biggelaar & A.S. Tampa, eds.). Academic Press, N.Y., London. 123-177.

Muñoz-Cuevas, A. 1975. Modèle ciliaire de développement du photorécepteur chez l'Opilion Ischyropsalis luteipes (Arachnida). C. R. Acad. Sc. Paris. 280:725-727.

Muñoz-Cuevas, A. 1984. Photoreceptor structures and vision in arachnids and myriapods. In: Photoreception And Vision In Invertebrates (M.A. Ali, ed.). Plenum Press, New York. 335-399.

Newell, P.F. & G.E. Newell 1968. The eye of the slug, Agriolimax Jreticulatus (Müll.). Symp. zool. Soc. Lond. 23:97-111.

Nilsson, S.E.G. 1964. Receptor cell outer segment development and ultrastructure of the disk membranes in the retina of the tadpole (Rana pipiens). J. Ultrastruct. Res. 11:581-620.

Nordestgaard, B.G. & J. Rostgaard 1985. Critical-point drying versus freeze drying for scanning electron microscopy: a quantitative and qualitative study on isolated hepatocytes. *J. Microscopy.* 137:189-207.

Ockleford, C.D. 1975. Redundancy of washing in the preparation of biological specimens for transmission electron microscopy. *J. Microscopy.* 105(2):193-203.

Patten, W. 1886. Eyes of molluscs and arthropods. *Mitth. a. d. Zool. Stat. zu Neapel.* 6:42-756.

Patten, W. 1887. Eyes of molluscs and arthropods. *J. Morph.* 1:67-92.

Pelseneer, P. 1908. Les yeux branchiaux des lamellibranches. *Bull Acad. Roy Belg.* 773-779.

Pietsch, A. & W. Westheide 1985. Ultrastructural investigations of presumed photoreceptors as a means of discrimination and identification of closely related species of the genus Microphthalmus (Polychaeta, Hesionidae). *Zoomorphology.* 105:265-276.

Poli, J.X. 1795. *Testacea utrinsque Siciliae eorumque historia et anatome tabulis aeneis illustrata.* Parmae 2:107-153.

Portman, R.W., E.L. LeCluyse & W.L. Dentler 1987.

Development of microtubule capping structures in ciliated epithelial cells. J. Cell Sci. 87:85-94.

Powell, C.V.L. 1984. Fine structure of the retina of the giant scallop, Placopecten magellanicus. Proc. 42nd Ann. Meeting of EMSA. 312-313.

Prytherch, H.F. 1934. The role of copper in the setting, metamorphosis, and distribution of the American oyster, Ostrea virginica. Ecol. Monogr. 4:45-107.

Raven, CHR.P. 1966. Morphogenesis: The Analysis Of Molluscan Development. Pergamon Press. London, Oxford, N.Y.

Rawitz, B. 1888. Der Mantelrand der Acephalen. I. Teil: Ostreacea. Zeit. f. Medizin und Naturw. 22:415-556.

Rees, W.J. 1957. The living scallop. In: The Scallop (I. Cox, ed.). Shell Transport and Trading Co., London. 15-32.

Richardson, D.C., L. Jarrett & E.H. Finke 1960. Embedding in epoxy resins for ultrathin sectioning in electron microscopy. Stain Technol. 35:313-323.

Röhlich, P., B. Aros & Sz. Virágóh 1970. Fine structure of photoreceptor cells in the earthworm, Limbricus terrestris. Z. Zellforsch. 104:345-357.

Rosen, M.D., C.R. Stasek & C.O. Hermans 1978. The ultrastructure and evolutionary significance of the cerebral ocelli of Mytilus edulis, the Bay Mussel. Veliger. 21(1):10-18.

Rosen, M.D., C.R. Stasek & C.O. Hermans 1979. The ultrastructure and evolutionary significance of the ocelli in the larva of Katharina tunicata (Mollusca: Polyplacophora). Veliger. 22:173-178.

Ruppert, E.E. 1978. A review of metamorphosis of tubellarian larvae. In: Settlement And Metamorphosis Of Marine Invertebrate Larvae (F.S. Chia & M.E. Rice, eds.). Elsevier, N.Y. 65-81.

Sabatini, D.D., K. Bensch & J. Barnett 1963. The preservation of cellular ultrastructure and enzymatic activity by aldehyde fixation. J. Cell Biol. 17:19-58.

Salvini-Plawen, L.V. & E. Mayr 1977. On the evolution of photoreceptors and eyes. In: Evolutionary Biology, Vol. 10 (M.K. Hecht, W.C. Steere, B. Wallace, eds.).

Schmidt, E.O. 1882. Handbuch der Vergleichenden Anatomie.  
8. Auflage, Jena.

Schreiner, K.E. 1896. Die Augen bie Pecten und Lima.  
Bergens Museums Aarbog. 1:1-51.

Semper, C. 1877. Über Schneckenaugen vom Wirbelthiertypus.  
Arch. mikr. Anat. 14:117-124.

Sharp, B. 1884. On the visual organs in Lamellibranchiata.  
Mitth. a. d. Zool. Stat. zu Neapel. 5:447-470.

Sorokin, S.P. 1962. Centrioles and the formation of  
rudimentary cilia by fibroblasts and smooth muscle  
cells. J. Cell Sci. 15:363-377.

Sorokin, S.P. 1968. Reconstructions of centriole formation  
and ciliogenesis in mammalian lungs. J. Cell Sci.  
3:207-230.

Spagnolia, T. & L.A. Wilkens 1979. Ultrastructure of the  
lateral lobe of the scallop parietovisceral ganglion.  
Am. Zool. 19:960.

Spagnolia, T. & L.A. Wilkens 1983. Neurobiology of the

scallop. II: Structure of the parietovisceral ganglion lateral lobes in relation to afferent projections from the mantle eyes. *Mar. Behav. Physiol.* 10:23-55.

Spurr, A.R. 1969. A low-viscosity epoxy resin embedding medium for electron microscopy. *J. Ultrastruct. Res.* 26:31-43.

Stowe, S. 1980. Rapid synthesis of photoreceptor membrane and assembly of new microvilli in a crab at dusk. *Cell Tissue Res.* 211:419-440.

Stowe, S. 1981. Effects of illumination changes on rhabdom synthesis in a crab. *J. Comp. Physiol.* 142:19-25.

Stubblefield, E. & B.R. Brinkley 1966. Cilia formation in Chinese hamster fibroblasts in vitro as a response to colcemid treatment. *J. Cell Biol.* 30:645-652.

Such, J. 1969. Sur la présence de structures évoquant des ébauches ciliaires abortives dans les cellules rétinienennes du jeune embryon de Carausius morosus. *C. R. Acad. Sc. Paris.* 268:948-949.

Thornhill, R.A. 1972. The development of the labyrinth of the lamprey (Lampetra fluviatilis Linn. 1758). *Proc. R. Soc. Lond. B.* 181:175-198.

Thrum, U. 1969. General organization of sensory receptors.  
Rendiconti della Scuola Internazionale di Fisica E.  
Fermi. XLIII Corso. 44-68.

Toh, Y. & T.H. Waterman 1982. Diurnal changes in compound  
eye fine structure in the blue crab Callinectes. J.  
Ultrastruct. Res. 78:40-59.

Tonosaki, A. 1967. Fine structure of the retina in  
Haliotis discus. Z. Zellforsch. 79:469-480.

Toyoda, J-I. & R.M. Shapley 1967. The intracellularly  
recorded response in the scallop eye. Biol. Bull.  
133:490.

Uexküll, J.v. 1912. Studien über den Tonus. VI. Die  
Pilgermuschel. Zeit. f. Biol. 58:305-332.

Vanfleteren, J.R. 1982. A monophyletic line of evolution?  
Ciliary induced photoreceptor membranes. In: Visual  
Cells In Evolution (J.A. Westfall, ed.). Raven Press,  
New York. 107-136.

Vanfleteren, J.R. & A. Coomans 1976. Photoreceptor  
evolution and phylogeny. Z. zool. Syst. Evolut.-  
forsch. 14:157-169.

Venable, J.H. & R.E. Coggeshall 1965. A simplified lead citrate stain for use in electron microscopy. *J. Cell Biol.* 25:407-408.

Wachmann, E. & A. Hennig 1974. Centriolen in der Entwicklung der Retinulazellen von Megachile rotundata (F.) (Hymenoptera, Apidae). *Z. Morph. Tiere.* 77:337-344.

Waller, T.R. 1981. Functional morphology and development of veliger larvae of the European Oyster, Ostrea edulis Linné. *Smithsonian Contributions to Zoology.* 328: 1-70.

Waterman, T.H. 1975. Expectation and achievement in comparative physiology. *J. Exp. Zool.* 194:309-344.

Watson, M.L. 1958. Staining tissue sections for electron microscopy with heavy metals. II. Application of solutions containing lead and barium. *J. Biophys. Biochem. Cytol.* 4:727-730.

Wenrich, D.H. 1916. Notes on the reactions of bivalve mollusks to changes in light intensity; Image formation in Pecten. *J. Animal Behav.* 6:297-318.

White, K.M. 1937. Sense Organs. *Trans. Liverpool Biol.*

Soc. 23:421-429.

Wilkens, L.A. 1981. Neurobiology of the scallop. I:  
Starfish-mediated escape behaviours. Proc. Roy. Soc.  
Lond. B. 211:341-372.

Wilkens, L.A. & B.W. Ache 1977. Visual responses in the  
central nervous system of the scallop Pecten ziczac.  
Experientia 33:1338-1339.

Wilkens, L.A. & T. Spagnolia 1979. Projections of optic  
fibers in the parietovisceral ganglion of the scallop:  
A light microscope autoradiographic study. Am. Zool.  
19:961.

Xylander, W.E.R. 1984. A presumptive ciliary photo-  
receptor in larval Gyrocotyle urna Grube and Wagener  
(Cestoda). Zoomorphology. 104:21-25.

Yamamoto, M. & M. Yoshida 1978. Fine structure of the  
ocelli of a synaptid holothurian, Opheodesoma  
spectabilis, and the effects of light and darkness.  
Zoomorphology. 90:1-17.

Young, R.W. 1978. Visual cells, daily rhythms, and vision  
research. Vision Research. 18:573-578.

Zwaan, J. 1975. Fine structure of the developing lens.

Int. Ophthalmol. Clin. 15:39-52.

## APPENDICES

## APPENDIX A

## 11.1. Data: Scallop Characteristics

Table A-1: Parameters recorded for individual scallops

Shell Height (mm)	Shell Length (mm)	Number Of Eyes Upper	Number Of Eyes Lower	Sex
083.8	087.0	74	97	male
098.7	101.4	62	62	female
105.2	107.8	111	76	male
100.0	100.9	102	64	male
091.5	094.8	77	69	female
096.0	100.0	96	73	male
107.9	109.9	82	73	male
097.2	103.2	87	79	male
100.6	102.4	93	73	male
112.0	113.2	86	82	female
099.1	103.9	94	65	female
099.0	102.6	89	73	male
098.8	097.9	86	69	male
128.1	133.8	89	75	male
113.8	117.2	89	62	female
116.0	121.9	104	76	male
124.0	131.0	77	62	male
094.6	094.8	80	74	male
089.8	091.0	79	50	female
077.8	080.9	89	60	female
076.5	080.0	95	77	male
089.8	093.2	87	63	female
076.9	079.9	74	63	female
060.7	063.4	83	58	male
076.8	081.2	96	62	female
086.1	086.9	90	76	male
079.0	079.9	104	68	female
078.5	079.3	93	69	female
078.0	079.3	105	67	male
080.9	081.9	90	67	male
084.6	084.9	87	69	male
070.6	073.8	93	67	female
070.5	070.5	69	70	female
052.2	055.1	84	60	female
059.8	060.0	89	50	female
056.2	058.5	89	69	male
075.5	079.6	84	65	male
083.6	083.7	89	70	male
055.4	055.4	89	63	female

Shell Height (mm)	Shell Length (mm)	Number Of Eyes Upper	Number Of Eyes Lower	Sex
043.3	043.0	79	72	immature
044.0	043.1	80	61	immature
042.5	041.1	65	54	immature
047.8	047.5	77	57	immature
046.0	043.3	74	47	immature
045.8	045.7	73	50	immature
043.5	042.2	65	50	immature
047.5	047.0	77	57	immature
046.9	045.0	77	58	immature
042.3	041.9	73	59	immature
044.0	043.1	74	46	immature
043.5	041.9	82	53	immature
043.4	042.2	63	45	immature
040.6	039.3	69	52	immature
043.5	042.8	73	60	immature
044.5	043.1	86	65	immature
044.1	042.1	73	45	immature
045.9	044.1	80	57	immature
044.0	041.0	70	57	immature
043.2	041.0	82	55	immature
044.9	043.7	78	54	immature
040.8	038.9	77	59	immature
044.1	042.7	72	55	immature
076.0	079.0	98	74	female
079.0	080.0	96	67	female
084.0	086.0	95	69	male
069.0	071.0	87	68	male
077.0	078.0	100	77	male
066.0	067.0	82	65	male
067.0	070.0	89	70	female
072.0	070.0	95	67	male
078.0	077.0	96	70	female
085.0	084.0	88	72	male
079.0	075.0	85	67	female
100.0	100.0	100	78	female
096.0	096.0	99	74	female
097.0	097.0	89	63	female
096.0	100.0	97	73	female
100.0	102.0	78	72	female
077.7	083.0	93	71	female
076.3	084.3	102	78	male
124.0	131.0	83	57	female
089.4	095.8	88	65	male
087.8	098.2	90	65	female
118.8	130.0	91	54	female
117.7	128.9	85	53	female
037.1	035.2	74	58	immature
037.9	036.3	85	65	immature
047.6	046.9	80	67	immature

Shell Height (mm)	Shell Length (mm)	Number Of Eyes Upper	Number Of Eyes Lower	Sex
051.8	051.5	84	65	immature
054.8	055.4	80	64	immature
044.7	043.2	74	52	immature
040.2	039.8	64	57	immature
041.2	039.5	77	60	immature
038.8	037.5	77	64	immature
040.7	040.2	75	57	immature
042.1	041.6	84	62	immature
026.4	025.1	77	58	immature
026.4	025.7	82	60	immature
028.9	025.9	69	54	immature
021.5	020.1	69	53	immature
022.6	021.8	57	50	immature
029.0	028.6	64	57	immature
024.7	023.3	55	53	immature
018.5	017.4	53	51	immature
094.5	100.5	80	60	male

## APPENDIX B

11.2.

## Statistical Data

Table B-1: Statistics for regressions of the total number of eyes against shell height.

$P < 0.001$	$\bar{x} = 146.59$
$F = 78.60$	$d.f. = 104$
$r^2 = 0.43$	

Table B-2: Statistics for t-test for paired observations for the differences in the number of eyes between the upper and lower mantle lobes.

$P < 0.001$	$\bar{x} = 19.52$
$T = 21.33$	

Table B-3: Statistics for t-test for the differences in the total number of eyes between sexes.

$P > 0.1$		
$F = 1.31$		$d.f. = 61$
$T = -2.44$		

sex	n	$\bar{x}$	std dev	std error
F	32	153.63	13.40	2.37
M	31	161.36	11.72	2.10









